# VI. DISCUSSION OF SEVERAL EPISODES IN THE LOS ANGELES BASIN

## A. July 24-26, 1973

### 1. Background

From July 24 to July 26, 1973, a major smog episode occurred in the Los Angeles Basin. Although not the worst episode to occur in Los Angeles, this particular one was the first and only occasion that Federal offices have been closed because of smog. The episode was also particularly well documented by both aircraft and Air Resources Board (ARB) trailer measurements and was the only occasion when aircraft measurements were made on an around-the-clock basis.

The meteorological conditions during this period were typical of the early to mid-summer regime during which the worst of the smog episodes in the Los Angeles Basin have generally occurred in recent years. In particular, this episode was characterized by the "Upland Anomaly" of very high ozone concentration in the northeastern part of the basin.

Because it was both representative and well documented, this episode was chosen for special study. This chapter traces the buildup and decay of the episode and tries to put the three-dimensional distribution and transport of pollutants into perspective using the meteorology. Specific attention is paid to the mini-basin which includes Upland, Ontario, and Riverside. The Upland Anomaly (as well as the mixing layer structure), the 3-D distribution of pollutants at night, and the effect of certain point sources in the mini-basin are all discussed. The sampling began on the 25th, so that day is chosen for most of the discussion. Data from the 26th are used to illustrate specific points.

### 2. Synoptic Meteorology of the Episode

The meteorology during the episode of 24 to 26 July 1973 was typical of that leading to early summer episode conditions in the inland valleys. The water offshore was 3 to 5°F colder than normal, causing fog conditions typical of early summer, while a thermal low existed in the desert areas. On 23 July, a strong high pressure ridge started developing near the coast and, by 24 July, it was well developed.

During this episode, subsidence associated with the high pressure area lowered and strengthened the marine inversion and created a cap of hot air over the Los Angeles Basin. In places, a double inversion actually occurred, with a marine inversion below an independent subsidence inversion. In addition, on the 24th, the ridge created higher pressure to the north and east of the basin and tended to retard the sea breeze. This high pressure ridge and the inland thermal low are shown on the weather map for 25 July in Fig. VI-1.

A crude indication of the occurrence of this subsidence condition, and thus of the likelihood of keeping pollutants trapped near the surface under an inversion, is the temperature at 850 mb (approximately 5000 ft). When this temperature is greater than 20 °C (60 °F), the surface temperature must get to about 95 °F before the inversion can be broken and pollutants ventilated. Table VI-1 was assembled using data from soundings at L. A. Airport.

TABLE VI-1

TEMPERATURES AT 850 mb FROM
23 JULY 1973 TO 26 JULY 1973

| Date and Time | | Temperature |
|---|---|---|
| 23rd | 5:30 a.m. PST | 20 °C |
| | 11:30 a.m. | 21 °C |
| 24th | 5:30 | 23 °C |
| | 11:30 | 25 °C |
| 25th | 5:30 | 27 °C |
| | 11:30 | 27 °C |
| 26th | 5:30 | 27 °C |
| | 11:30 | 23 °C |

From this table, it is easy to see that 24 and 25 July were likely to be bad smog days, but that midday on 26 July, the situation should have improved. This was exactly the case; on the 24th and 25th, hourly average ozone values exceeding 0.6 ppm were

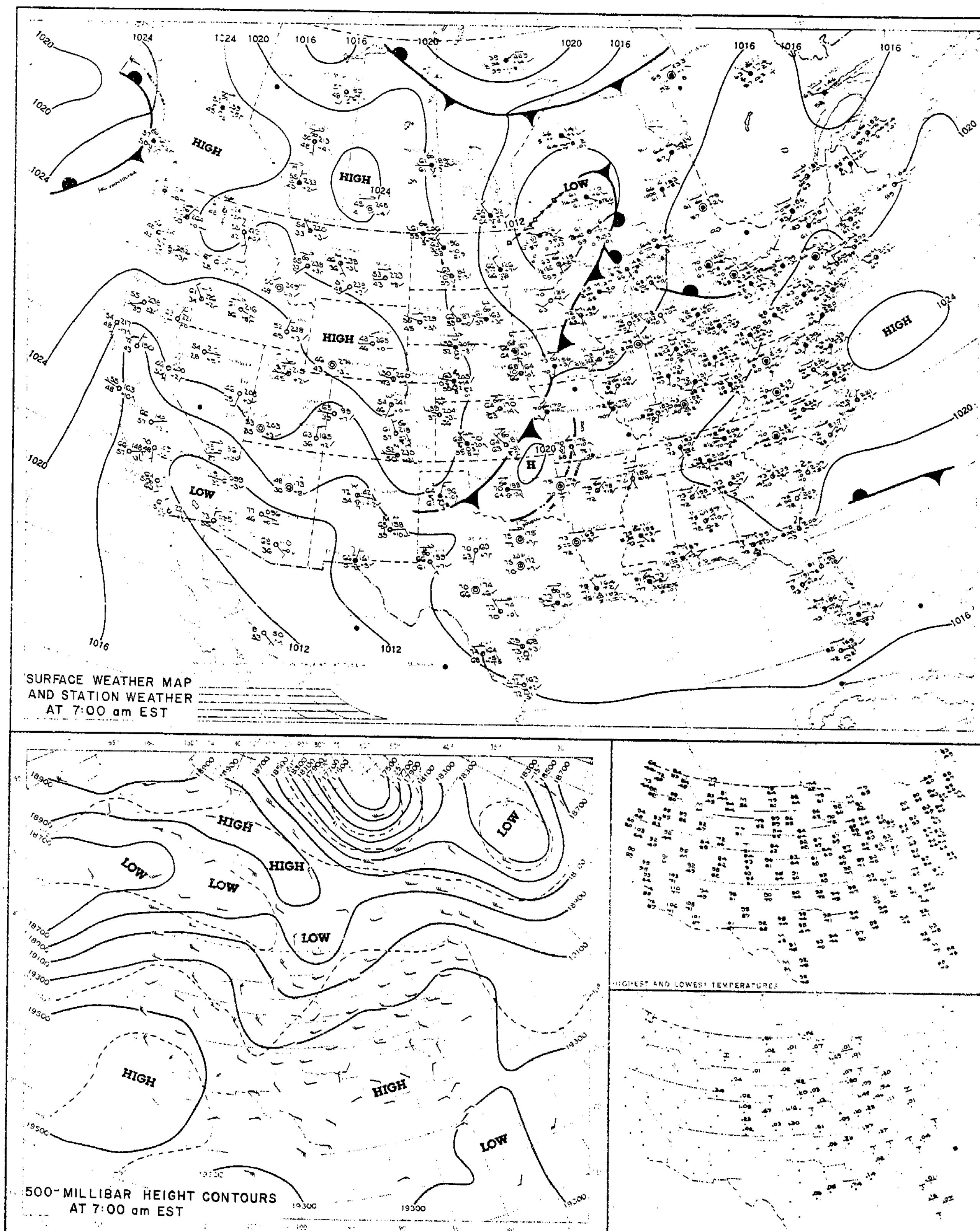


Fig. VI-1. WEATHER MAP FOR JULY 25, 1973 recorded in the basin and air stagnation advisories were called, while on the 26th, the highest value was 0.5 ppm and conditions improved rapidly in the afternoon. This high pressure ridging along the coast and corresponding high temperatures aloft are typical of July weather. For 10 years between 1960 and 1973, the 850 mb temperature in southern California exceeded 20°C in July an average of 25 days.

The high pressure ridge moved slightly north on the 25th allowing the sea breeze to build up, but maintaining the subsidence inversion. On the 26th, the ridge weakened and moved farther north. Surface temperatures had risen to over 100°F in the inland valleys during the subsidence condition and, when the temperature aloft decreased, the inversion was broken at inland points and pollutants were ventilated upward. On the 24th and 25th, the winds aloft were generally light and variable, but by midday on the 26th, the flow aloft became organized and westerly, thus carrying off the pollutants ventilated through the inversion.

### 3. Flow Patterns and Meteorology for July 25, 1973

This day began with widespread fog over most of the coastal plain in the early morning hours extending inland as far as Pomona and Chino by 0700 PDT. Visibilities were down to zero in fog at some coastal localities, but increased to 2-1/2 to 3 miles in haze and smoke in the San Gabriel and San Bernardino Valleys and as high as 15 miles in the San Fernando Valley where relatively clean drainage flows from the mountains to the north had cleansed the valley. Air movement during these early morning hours consisted of a weak, disorganized sea breeze in the coastal areas and a disorganized easterly flow inland. By 0900 PDT, the coastal fog was scattered and lifting, but absent altogether in the inland valleys. Most inland areas were still reporting haze and smoke except Van Nuys which reported 7 miles visibility. A well organized sea breeze did not start to develop until about 1100 PDT. By early afternoon, the sea breeze had approached a semi-steady state situation, penetrating well inland to Redlands and Riverside. The streamlines changed little until after 1900 PDT, although the velocities varied slightly. The streamlines for 1600 PDT are shown in Fig. VI-2. Note that the flow pattern transports air across the southern coastal plain northward into the San Gabriel Valley (EMT, AZU, etc.) and then eastward to Upland (CAB) and San Bernardino (SBD). At the same time, air is transported across Orange County (AN, SNA) through Santa Ana Canyon (COR) and into the Chino-Riverside area (CNO, RAL). This is

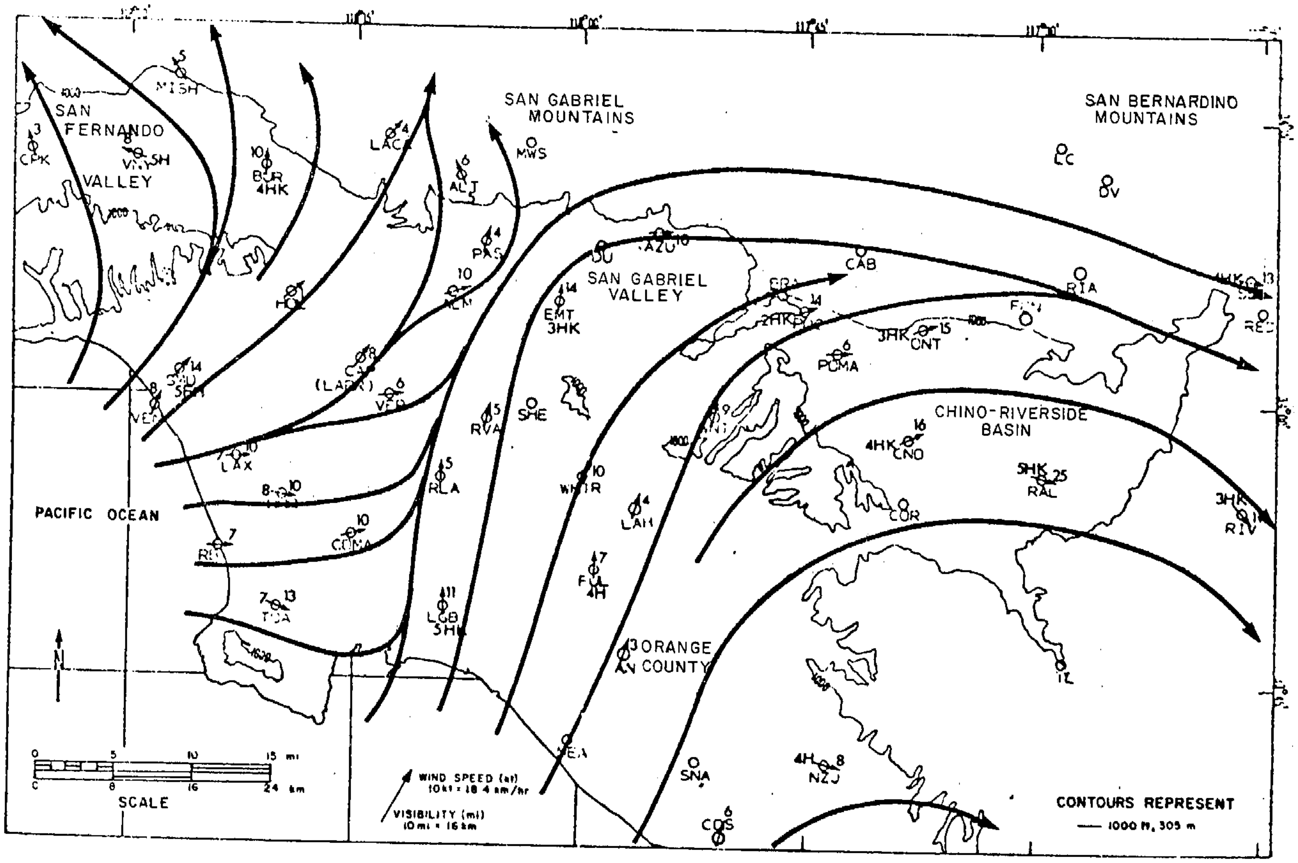


Fig. VI-2. SURFACE WIND STREAMLINES - 1600 PDT, JULY 25, 1973 basically the flow pattern within the surface mixing layer. Above the mixing layer, the winds were light and variable until mid-afternoon.

Winds aloft on July 25, 1973 were measured at four stationary sites. Pilot balloons (pibals) were released hourly at Chino (CNO), in the eastern basin, and at Elysian Park, midway between Hollywood (HOL) and the Los Angeles Railroad Yard (LARR) in the western basin. In addition, pilot balloons were released at 1233 PDT from Los Angeles International Airport (LAX), and at 1335 and 1654 PDT from El Monte Airport (EMT).

Figures VI-3 and VI-4 show trajectories, computed from these wind observations, for the air arriving over Upland (CAB) at 1600 PDT and Redlands (RED) at 1800 PDT. The extreme northerly and southerly winds within the mixed layer (from pibal observations) were used to construct an envelope of possible trajectories, and the mean wind within the mixed layer was used to construct a characteristic trajectory.

On July 25th, the California Air Resources Board station at Upland (CAB) reported an average ozone concentration of 60 pphm for the hour beginning 1600 PDT, the highest such concentration recorded in the Los Angeles Basin that year. Figure VI-5 shows that surface concentrations were generally high in the northern part of the eastern basin at that time. The trajectories shown in Figs. VI-3 and VI-4 indicate that much of the air over Upland at the time of peak ozone at that location was onshore before the sea breeze started, probably having accumulated pollutants since the night before, while much of the air over Redlands at the end of the afternoon had come onshore with the start of the sea breeze. The air arriving over Upland at 1600 PDT had the longest residence time in the western basin of any air arriving over Upland that day, which may account for the timing of the ozone maximum there.

The streamlines and trajectories indicate that polluted western basin air was advected into the eastern basin during the afternoon of July 25. This conclusion is corroborated by the afternoon gradients in surface ozone concentration, which clearly show the advance of cleaner air from the coast with the onset of the sea breeze and the displacement of the more ozone-laden air eastward. The hourly average surface ozone concentrations from 1600 to 1700 PDT (Fig. VI-5) provide a snapshot of this effect, showing a strong gradient between La Habra (LAH) and downtown Los Angeles (CAP), which had already been flushed with marine air, and Azusa (AZU) and Upland (CAB), which had not.

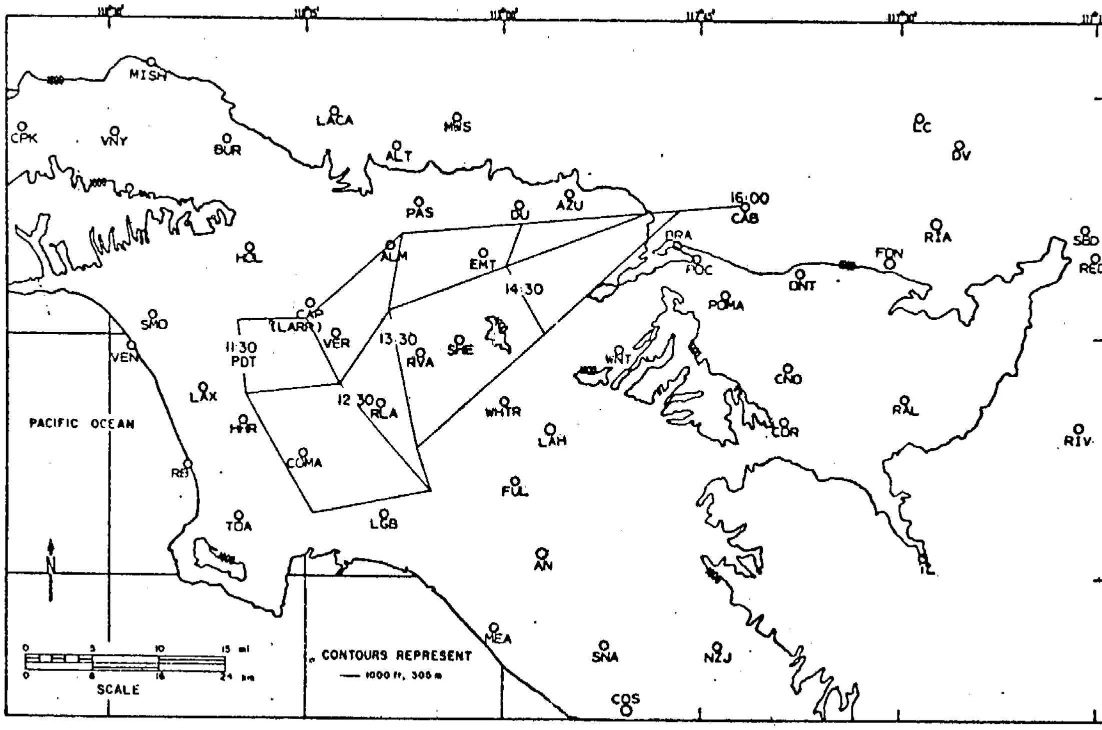


Fig. VI-3. TRAJECTORY ENVELOPE FOR AIR ARRIVING AT CABLE AIRPORT (UPLAND) 1600 PDT, JULY 25, 1973

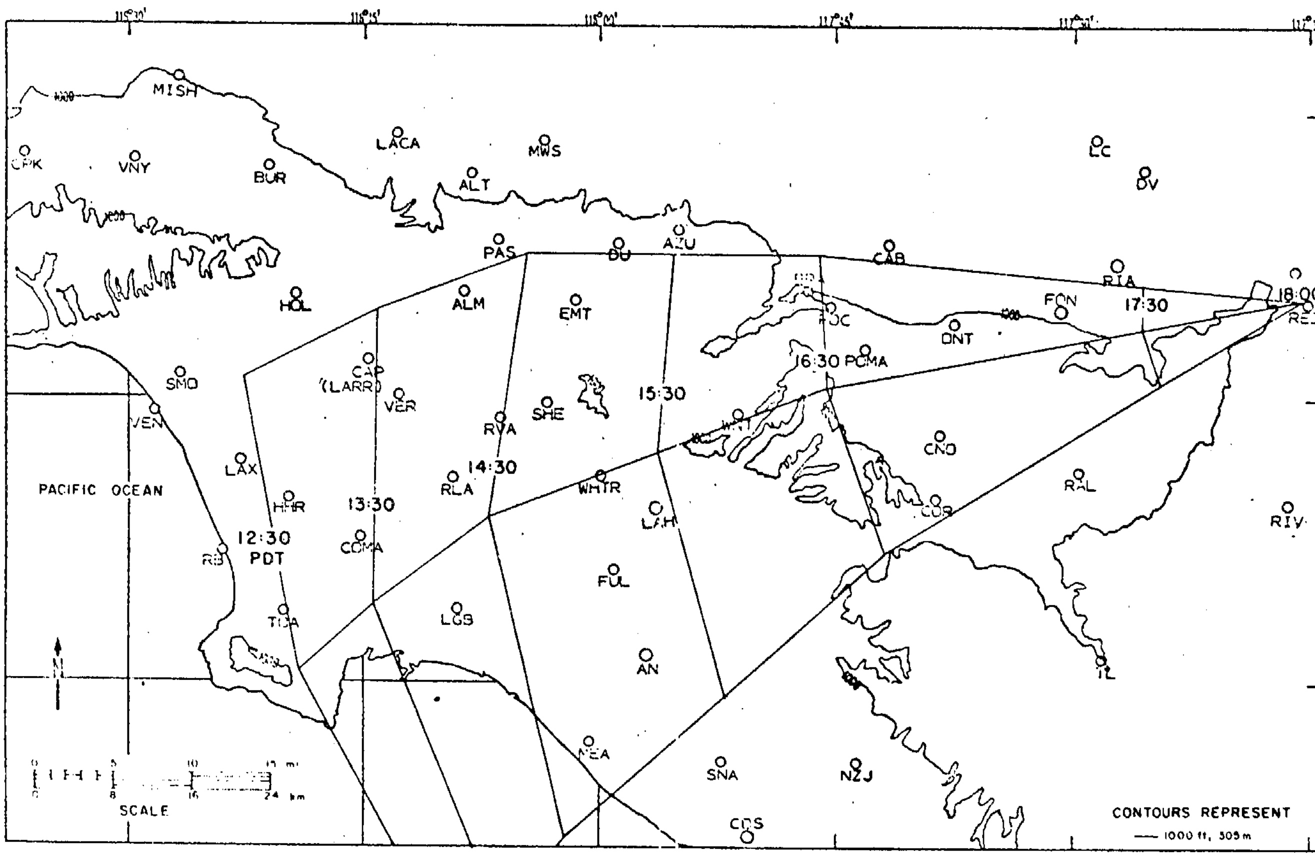


Fig. VI-4. TRAJECTORY ENVELOPE FOR AIR ARRIVING OVER REDLANDS AT 1800 PDT, JULY 25, 1973

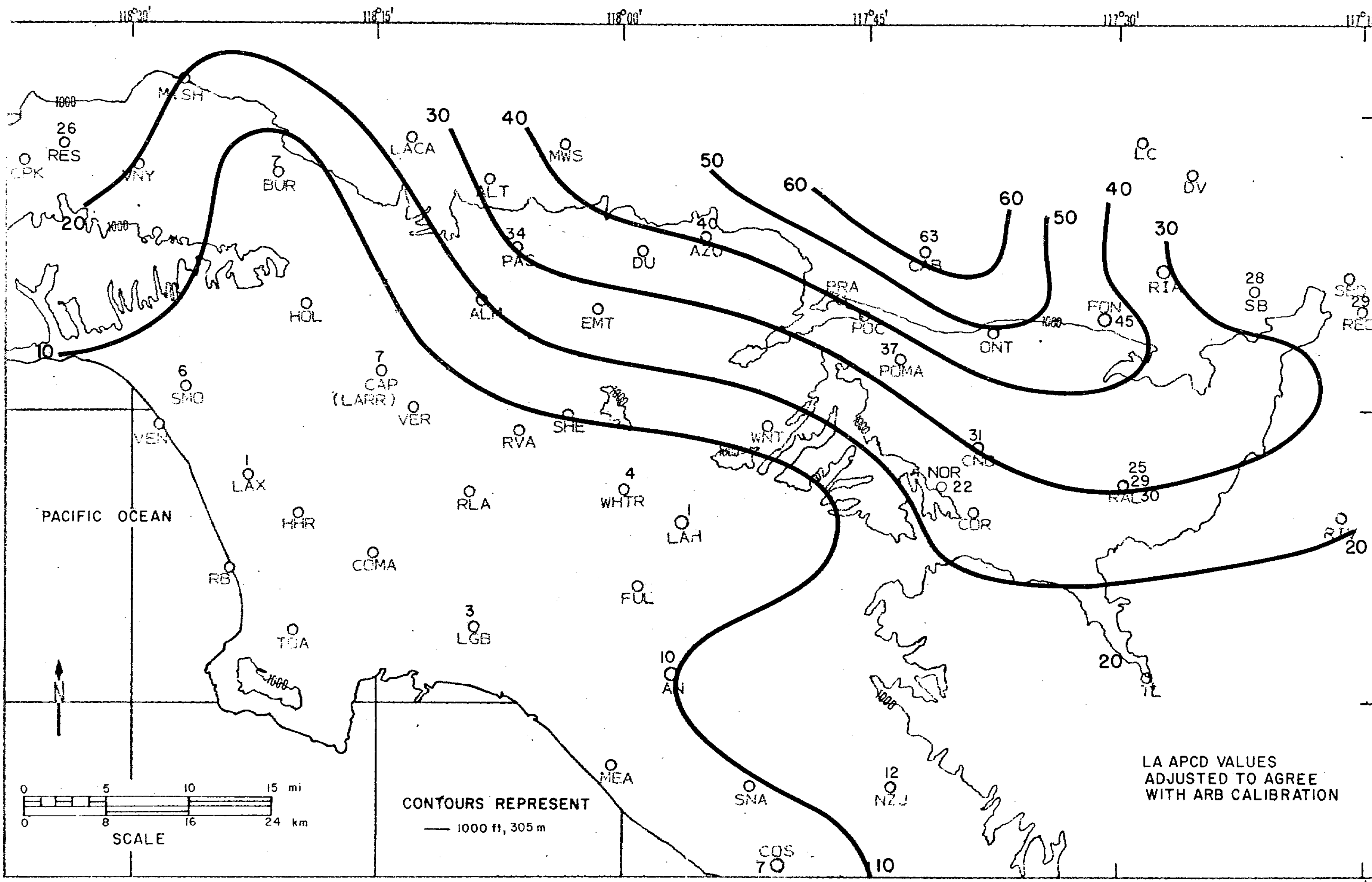


Fig. VI-5. SURFACE OZONE CONCENTRATIONS (pphm), 1600-1700 PDT, JULY 25, 1973

Figure VI-6 shows the approximate times at which the sea breeze began to flush various locations in the basin during the afternoon. These times were determined from California Air Resources Board and local Air Pollution Control Districts (APCD) ozone data according to an objective criterion: the approximate time of arrival of the sea breeze is calculated as M:00 PDT, where M is the first integer i such that $X_{i+1} \leq 1/2\ X_i$, $X_i$ being the average ozone concentration during the hour beginning at i:00 PDT. Comparison of Fig. VI-6 with the trajectories to Upland and Redlands in Figs. VI-3 and VI-4 shows that these trajectories depict air moving just ahead of the advancing cleaner sea air. From 1600 to 1900 PDT, the marine front moved about 45 miles inland at an average speed of about 15 miles per hour, in good agreement with observed wind speeds.

### 4. Mixing Layer Structure for July 25, 1973

In the morning before solar heating became important, the mixing layer over the basin was about 1000 ft or less above ground level (AGL). Mixing was limited by a radiation inversion caused by the cooling of the ground during the night. Pollutants emitted near the surface were trapped within this layer. The subsidence inversion remained on top of the radiation inversion at about 3000 ft above sea level (msl).

Fig. VI-7 is a vertical profile taken over Brackett Airport (BRA) on the 25th at 8:42 PDT. The night time radiation inversion was still quite strong, and fresh pollutants were trapped within a mixing layer which extends up to about 1600 ft msl. Fresh emissions are indicated by the high concentrations of condensation nuclei (X) and CO (C) under the inversion. The high $b_{scat}$ values near the surface are indicative of the thick haze left in the basin as the fog burned off. The ozone values show a deficit under the radiation inversion, pointing out that ozone is destroyed by fresh emissions of NO.

Above the radiation inversion, a sharp increase in ozone occurs. This high level of ozone is accompanied by high $b_{scat}$ levels, yet lower condensation nuclei and CO levels. This combination suggests an aged air mass left over from the day before and separated from the surface mixing layer. This layer aloft was trapped between the radiation inversion and the subsidence inversion, which starts at about 2800 ft msl, and pollutants were not carried off during the night due to the light wind conditions aloft. By midday, surface heating had destroyed the radiation inversion in the eastern portion of the

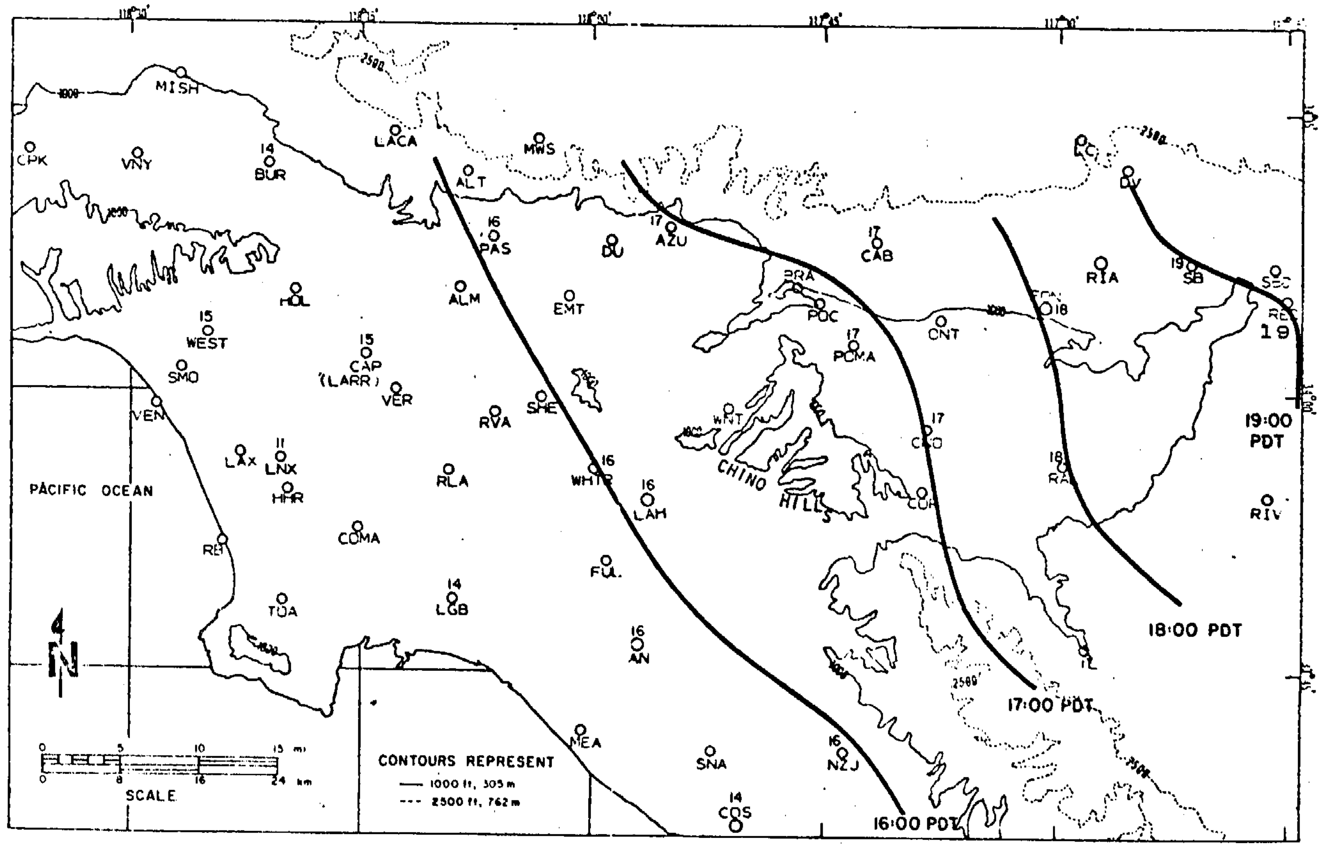


Fig. VI-6. APPROXIMATE TIME (PDT) OF ARRIVAL OF SEA BREEZE FRONT, JULY 25, 1973 (Objective criterion based on ground level ozone concentrations.)

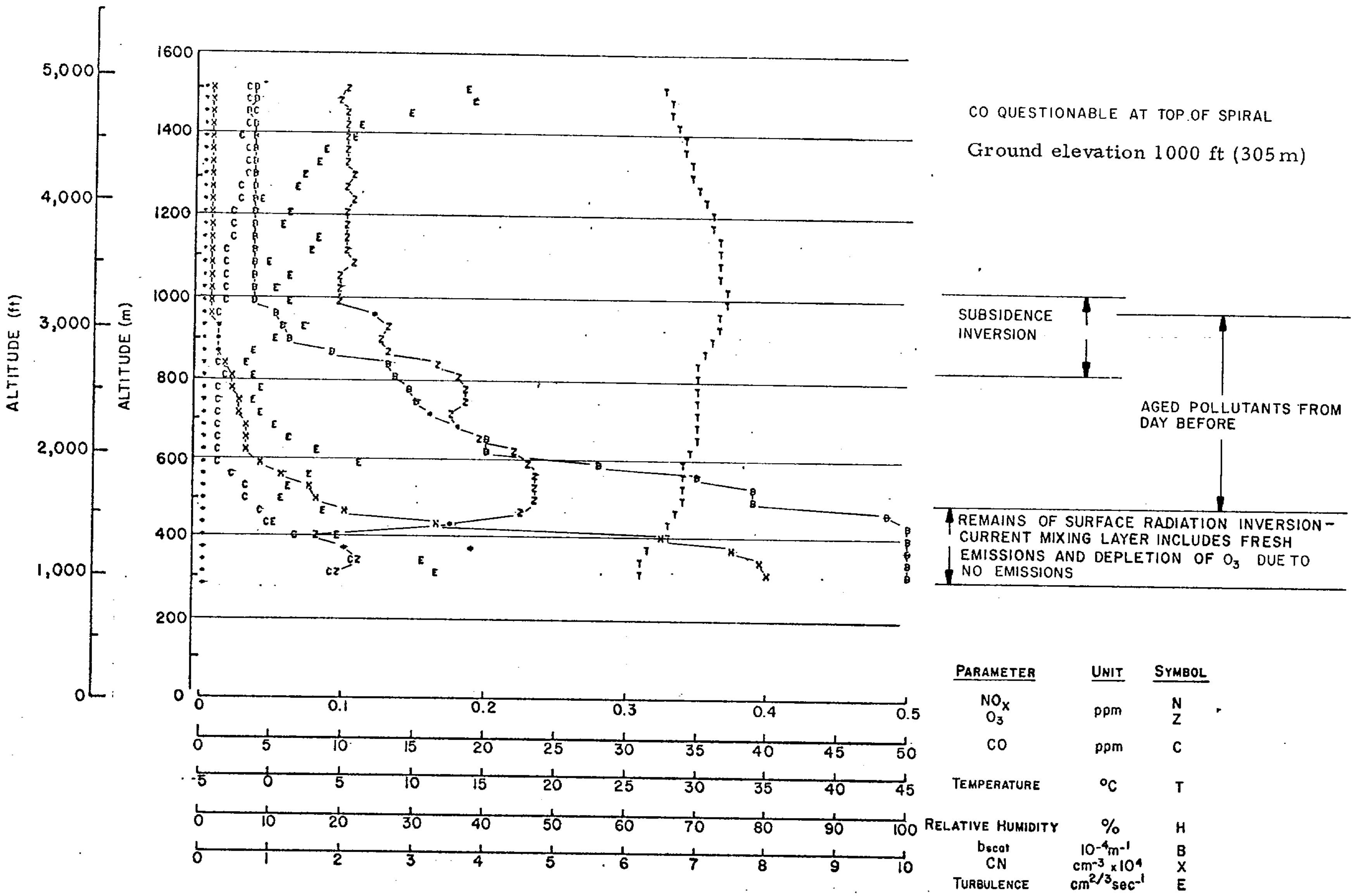


Fig. VI-7. VERTICAL PROFILE OVER BRACKETT (BRA) 0843 PDT JULY 25, 1973 basin, and the mixing layer extended up to the subsidence inversion, allowing the pollutants that had been trapped aloft to mix throughout the layer.

Fig. VI-8 shows a midday vertical cross-sectional contour map of $b_{scat}$ for the northern part of the basin from the coast at Santa Monica (SMO) to Redlands (RED). The contours (isopleths) are lines of equal $b_{scat}$. Superimposed on the contour plot are the winds aloft vectors at points and times closest to the points shown on the map. The numbers listed over the various locations are actual $b_{scat}$ numbers obtained from the spirals.

Throughout the day, the subsidence inversion covered the whole basin at about 3000 feet msl, while either a marine or radiation inversion existed at a lower level. By midday, a marine inversion sloped upward from about 1000 feet msl near the coast until it merged with the subsidence inversion roughly 25 miles inland. The structure of this double inversion is also shown in Fig. VI-8.

During the night and morning hours, the surface flow in the basin was either stagnant or had a slight offshore component, allowing the buildup of pollutants within the surface layer. In Fig. VI-8, the highest concentrations are seen within the source region in the western basin. Although some of the $b_{scat}$ in this figure is due to humidity effects, much of it results from emissions accumulated in a relatively stagnant air mass. At the time represented in Fig. VI-8, the sea breeze had just recently started and clean air had not yet come onshore to flush out the basin.

Figure VI-9 gives a slightly different perspective on the midday mixing layer structure. It is a mixing layer height contour map which shows that fresh emissions were confined to a relatively thin layer over the whole basin and that the venting which normally occurs in the eastern half of the basin was prevented by the subsidence. The mixing layer is higher over high terrain, but the thickness above ground is about the same over most of the basin. The tongue of lower mixing height in the Corona (COR) area is indicative of the fact that the terrain is lower in that area than farther north or east.

Later in the afternoon, as shown in Fig. VI-10, the sea breeze had ventilated much of the surface layer in the western basin, replacing air which had had a long residence time over land with cleaner air with a short time onshore. The sea breeze "front" in Fig. VI-10 is between El Monte (EMT) and Brackett (BRA). The air just ahead of the "front" had accumulated emissions over the western

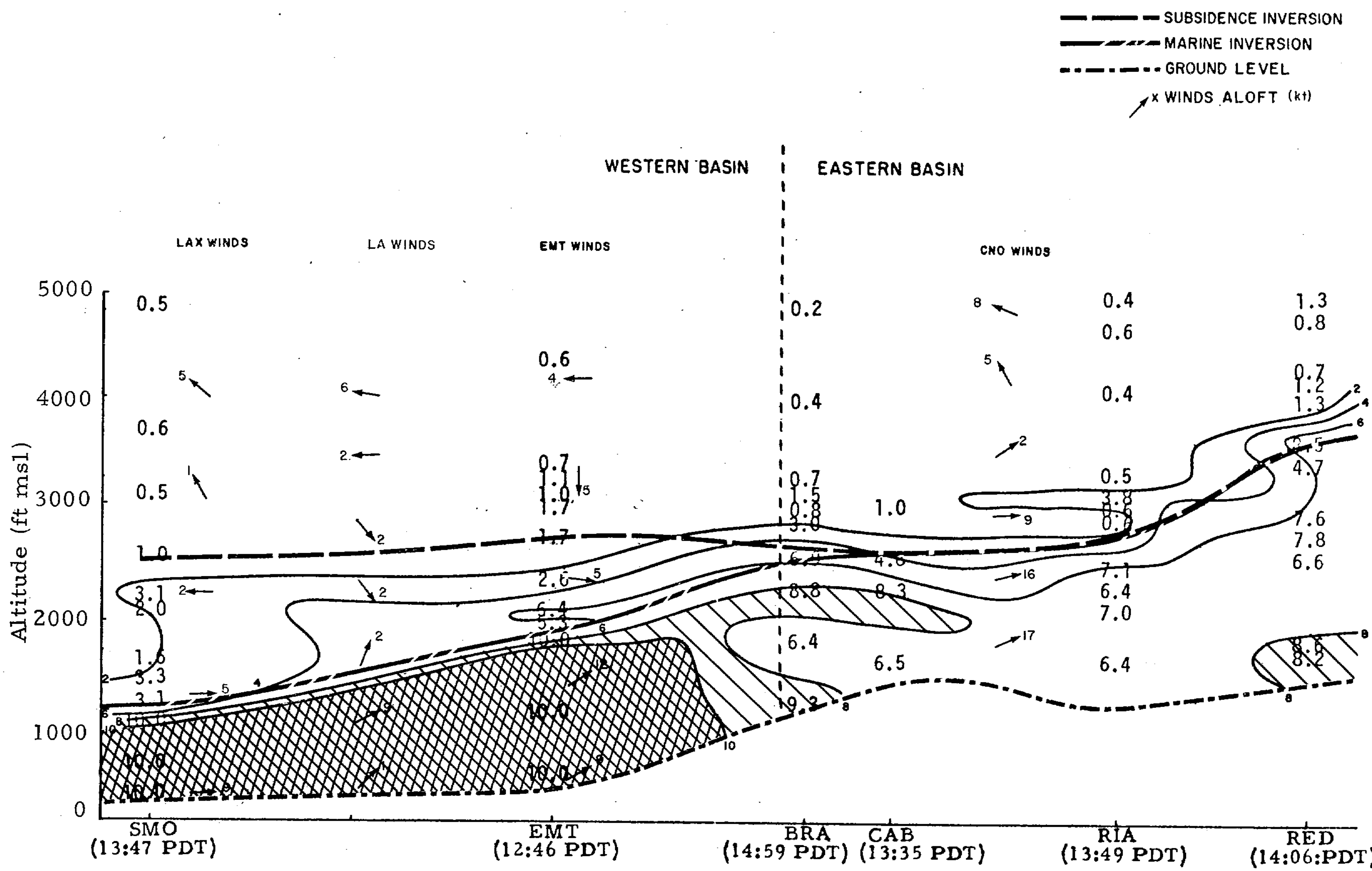


Fig. VI-8. VERTICAL CROSS-SECTION OF $b_{scat}$ FOR MIDDAY, JULY 25, 1973
(Units are $10^{-4}$ $m^{-1}$.)

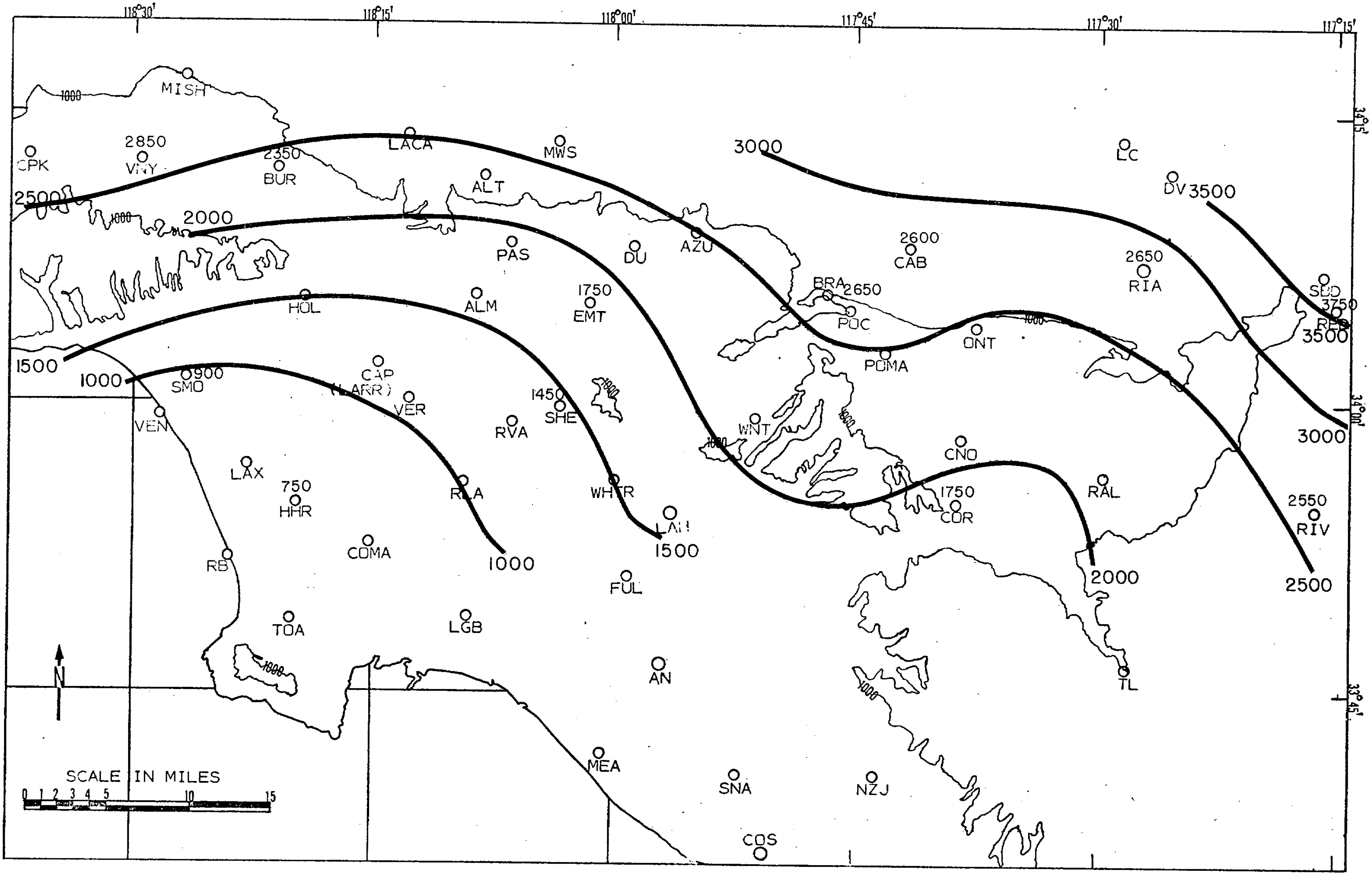


Fig. VI-9. MIXING HEIGHTS (ft msl) MIDDAY (11-1300 PST), 25 JULY 1973

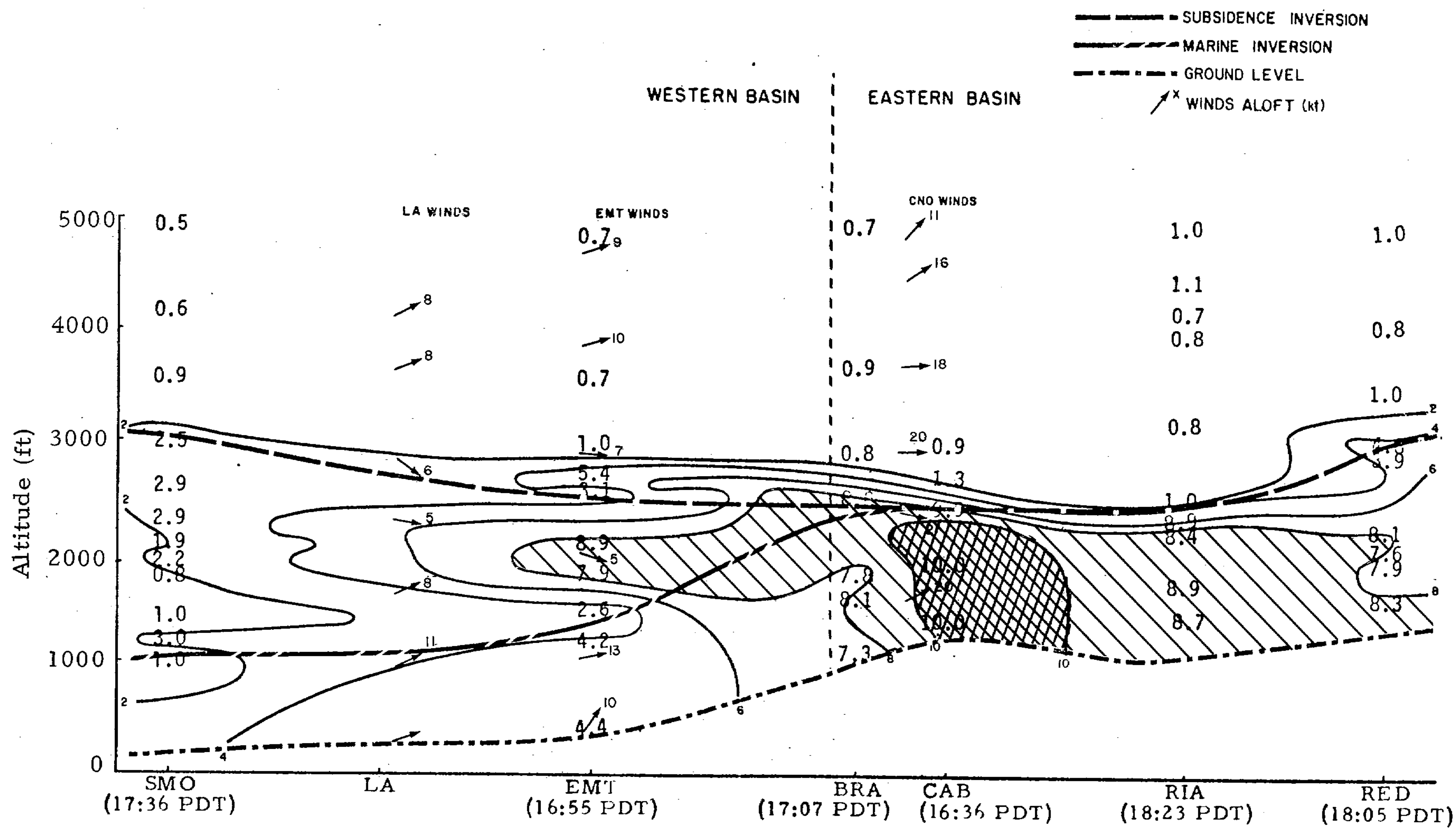


Fig. VI-10. VERTICAL CROSS-SECTION OF $b_{scat}$ FOR AFTERNOON OF JULY 25, 1973

(Units are $10^{-4}$ $m^{-1}$.)

basin earlier in the day and possibly during the night before and had the longest residence time over strong source areas of any air in the basin. Note that the highest concentrations in Fig. VI-10 are over Upland (CAB) at the time which corresponds to the peak ozone reading at Upland (and in the basin) for the day.

In both Figs. VI-8 and VI-10, upper layers are seen between the two inversions in the western basin. Pollutant concentrations remain high in these layers all day, but the aircraft sounding and pibal data indicate that these layers are decoupled from the air below. The air in the upper layers is well aged and relatively stagnant compared to surface air. These layers may be caused by upslope flow along some of the nearby hills, by lifting or undercutting of polluted air by the sea breeze, or by other means.

The difference between the air in front of and behind the sea breeze front is seen in Figs. VI-11 and VI-12. Figure VI-11 is a vertical profile over El Monte after the passage of the front. A surface mixing layer is well defined by the temperature, turbulence, and pollutant profiles extending up to about 1400 feet msl. Within this layer, the $b_{scat}$ and ozone values have dropped down from their peaks for the day. The condensation nuclei values are still high, however, indicating continuing fresh emissions. The air between about 1400 feet and 2000 feet msl is moderately well aged, but still has a moderate condensation nuclei population, possibly indicating that this air was previously part of the surface mixing layer, but was recently undercut by the advancing sea breeze. The remainder of the layer aloft could be a remnant of the layer existing earlier in the midday soundings.

Figure VI-12 is a vertical profile at Upland (CAB) before the passage of the front. The mixing layer is well defined and pollutant concentrations are high within the layer. The ozone concentration exceeds 0.5 ppm. The air within the mixing layer at Upland is similar to that just above the sea breeze in Fig. VI-11. This profile represents the period of peak ozone concentration at Upland.

### 5. Ozone Distribution and the Upland Anomaly

It is apparent from the previous discussion that this episode was characterized by very high ozone levels in the northeastern part of the basin. The ozone concentrations well exceeded 0.5 ppm at Upland (CAB) on both the 24th and 25th. Figure VI-13 is a contour map of the surface level ozone concentration for 1300 PDT on

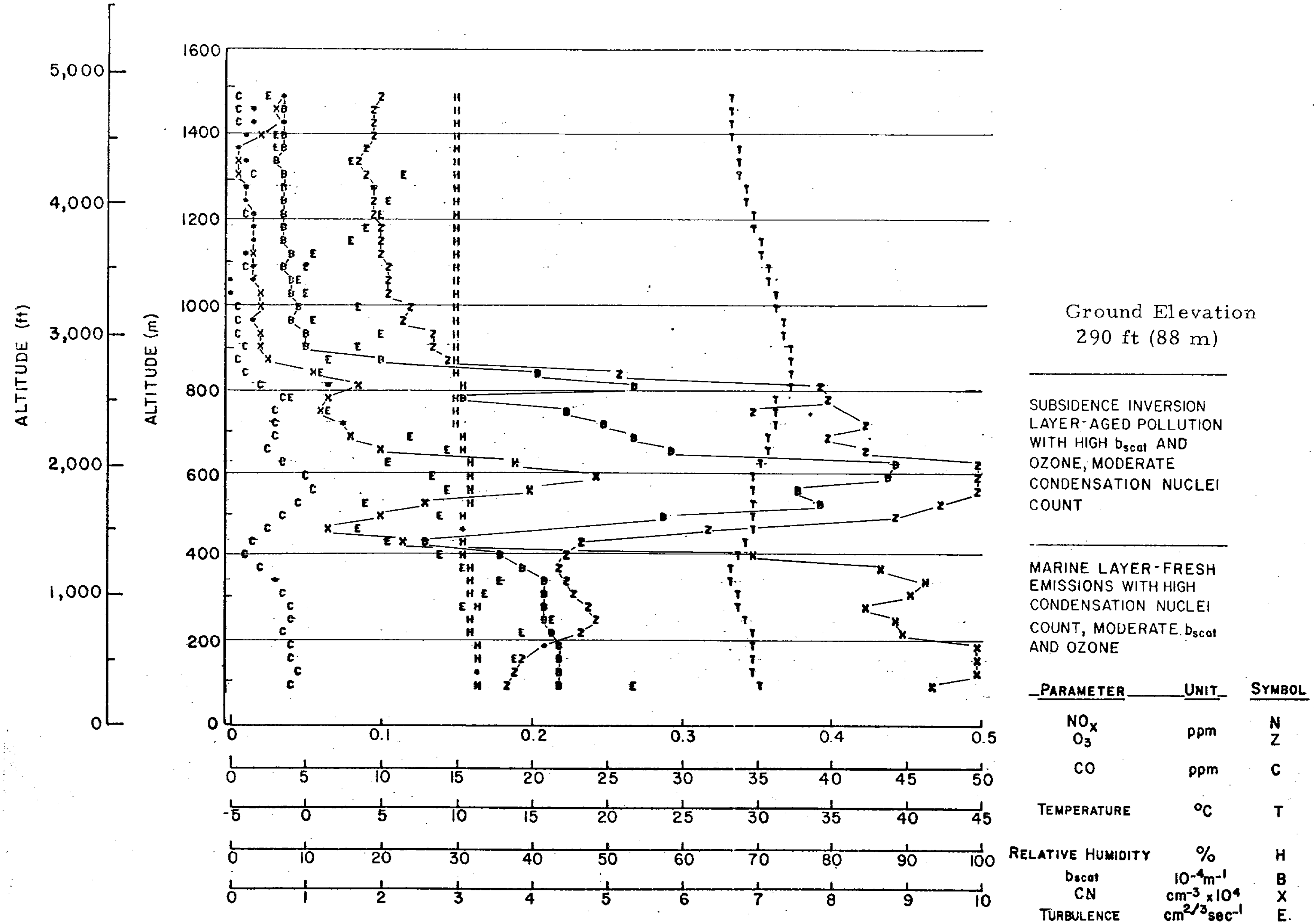


Fig. VI-11. VERTICAL PROFILE OVER EL MONTE (EMT) JULY 25, 1973, 1655 PDT, AFTER PASSAGE OF SEA BREEZE FRONT

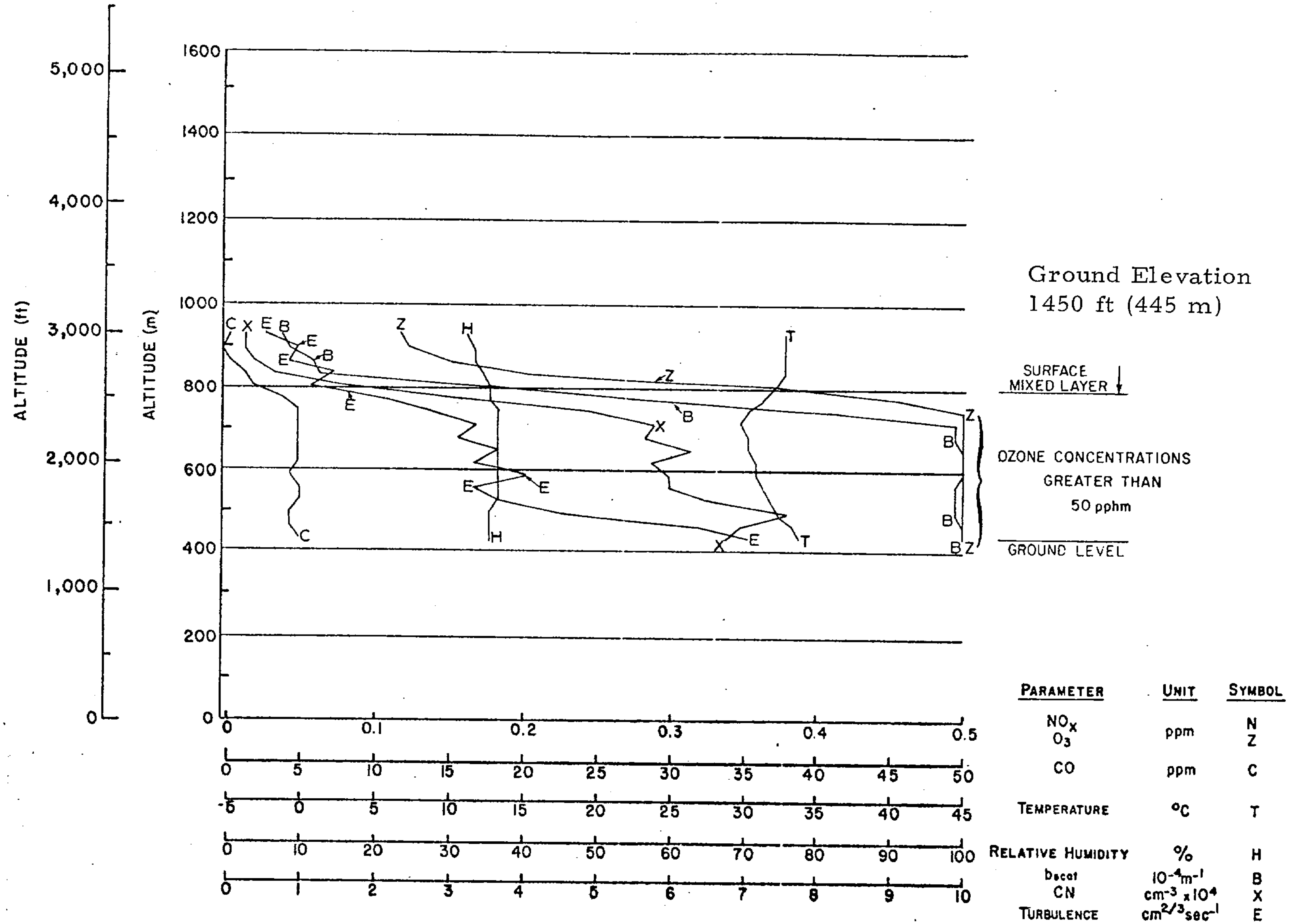


Fig. VI-12. VERTICAL PROFILE OVER CABLE (CAB) JULY 25, 1973, 1636 PDT

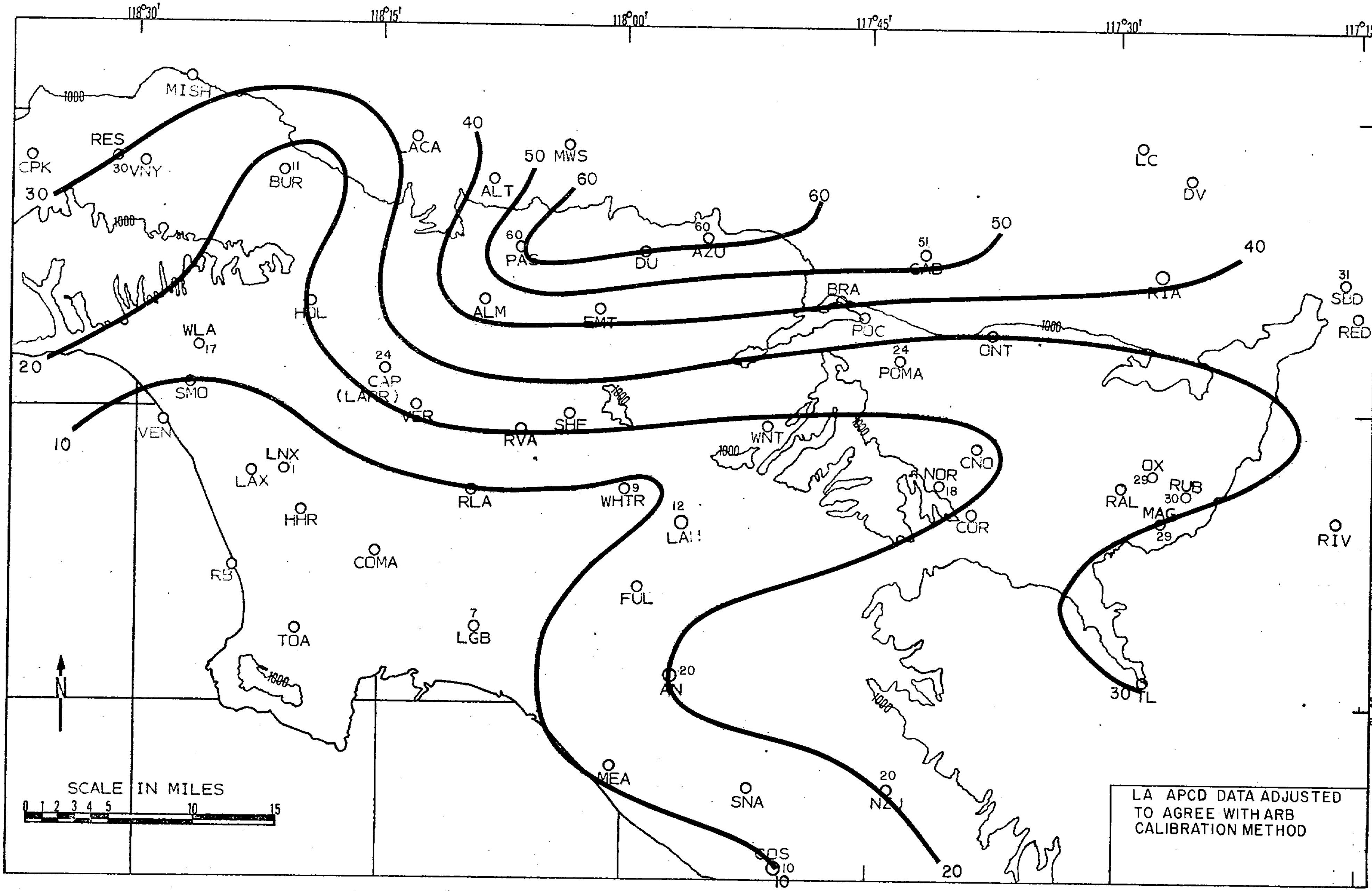


Fig. VI-13. SURFACE OZONE CONCENTRATIONS (pphm) 1300 PDT, JULY 25, 1973 the 25th.* The areas of highest concentration of ozone are the foothill areas in the northern portion of the basin. These areas share several features in common which may account for their high concentrations:

1. At midday, the air they have received has had a long residence time over heavy source areas and has not yet been influenced by the fresh onshore flow of marine air.

2. The air masses reaching them have been irradiated for several hours and were not recently shielded by fog.

3. The mixing layer in these areas has entrained ozone containing air from the aged layers aloft, thus increasing the pollutant burden in the mixing layer.

4. The foothill areas generally have a lower source strength of NO than the more heavily industrialized upwind areas from which they are receiving their air, thus ozone in the surface layer is not scavenged as effectively as at upwind locations.

This combination of features points out that the areas of highest ozone concentration are those receiving heavily polluted air which is most aged in a photochemical sense. Other areas in the basin appear to be receiving air which is "younger" (less sunlight or more recent NO emissions) or less polluted to start with.

The importance of "aging" and lack of fresh NO emissions for the generation of ozone is pointed out again in Fig. VI-14. This figure presents an isopleth map for the midday peak ozone value above the mixing layer. The data were taken from the vertical profiles. The area of highest concentration in this case is the area above the coastal plain where pollutants are trapped above the mixing layer and below the subsidence inversion. This layer is also seen in the vertical cross-section of Fig. VI-8. Due to the limited amount of data involved, the map should be taken only as an indication and not used for detailed interpretation, but it does show that the ozone values aloft are considerably higher than at the surface in the same area.

---

* Unless otherwise noted, surface ozone maps in this report are adjusted for the difference between ARB and LAAPCD calibration procedures. All LAAPCD ozone values are multiplied by 1.4.

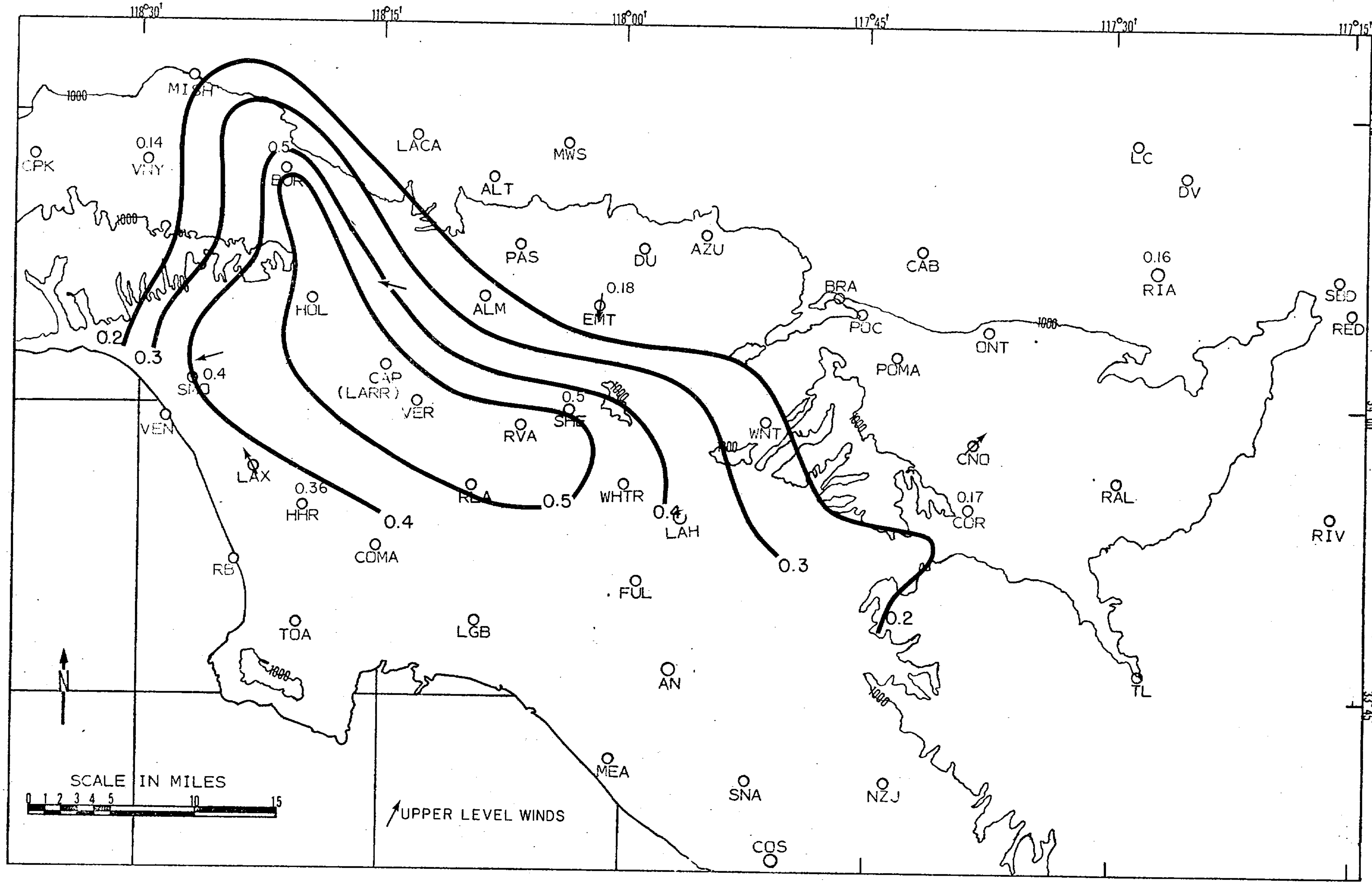


Fig. VI-14. PEAK $O_3$ ABOVE MIXING LAYER (ppm) 25 JULY 1973, MIDDAY

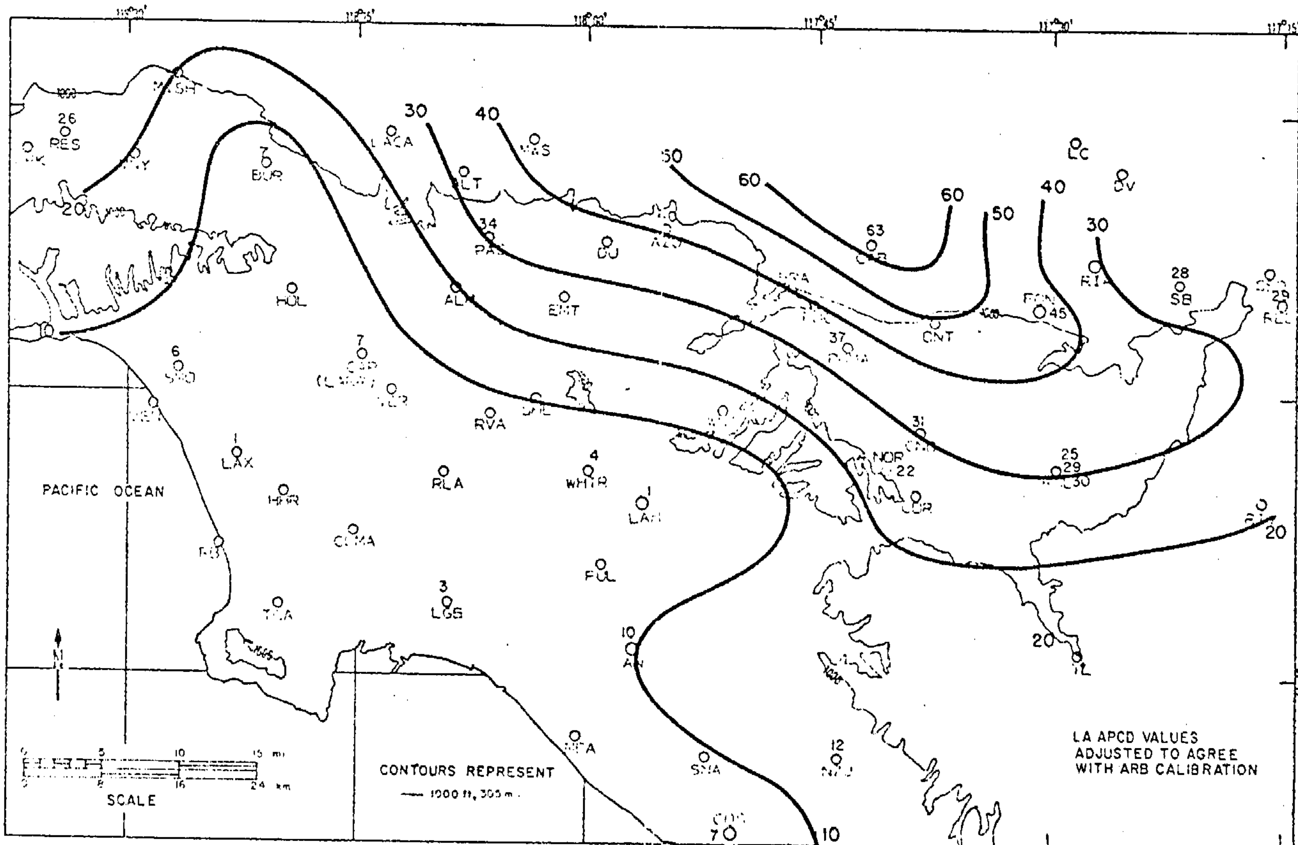


Fig. VI-15. SURFACE OZONE CONCENTRATIONS (pphm), 1600-1700 PDT, JULY 25, 1973

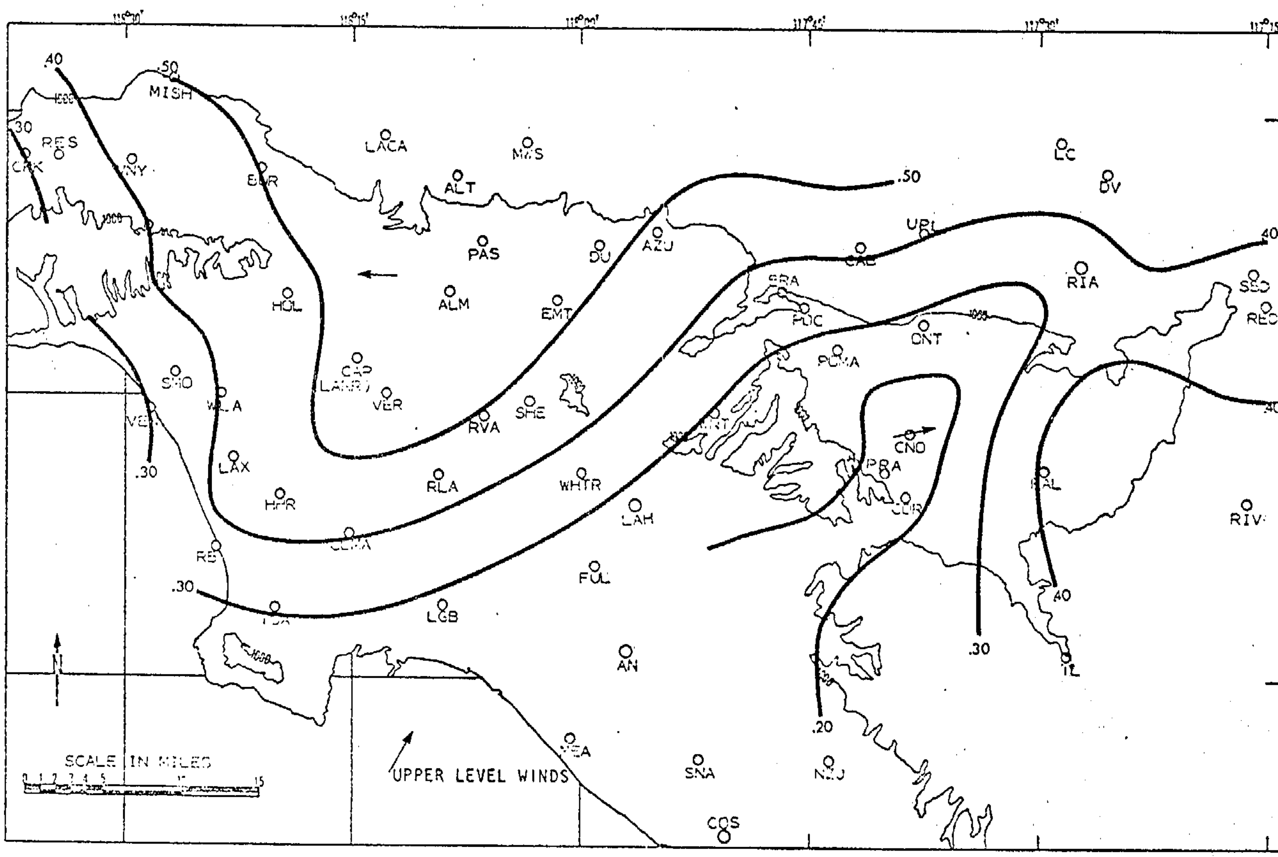


Fig. VI-16. PEAK $O_3$ ABOVE MIXING LAYER (ppm), 25 JULY 1973, AFTERNOON

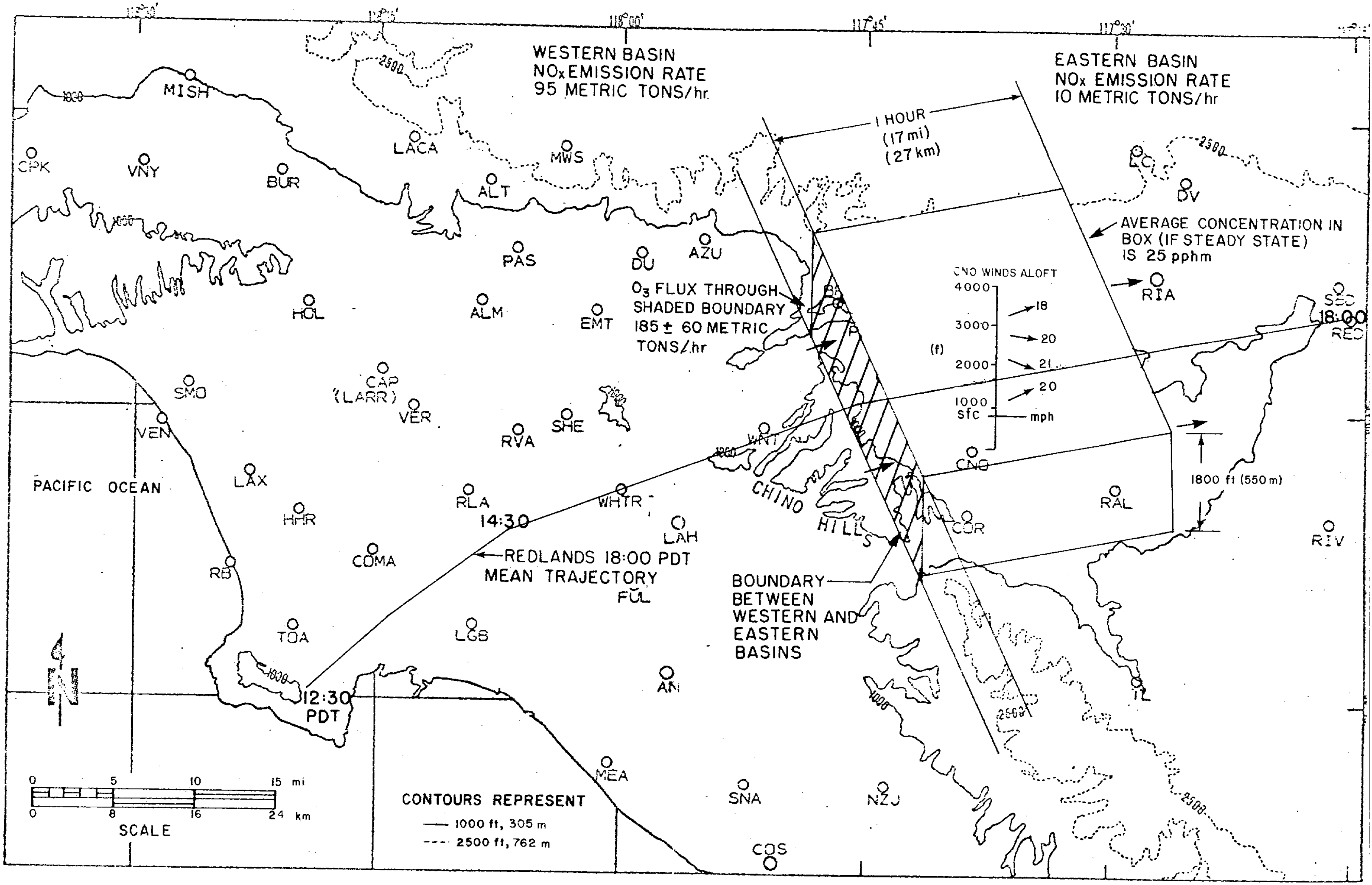


Fig. VI-17. ESTIMATED OZONE FLUX FROM WESTERN TO EASTERN BASIN, JULY 25, 1973 1700 PDT distance covered in one hour by the moving air. In a steady-state situation in the absence of diffusion or diffluent winds, the box would thus contain about 185 metric tons of ozone, corresponding to a uniform concentration of about 25 pphm. For comparison, the average late afternoon concentrations of ozone within the surface mixed layer at Riverside (RAL), Redlands (RED), Rialto (RIA), and Ontario (ONT) were, respectively, 36, 24, 25, and 13 pphm. (Data were taken from aircraft soundings.) The flux was calculated for about 1700 PDT since soundings were available for roughly that time, but 1700 PDT was also roughly the time of arrival of the sea breeze front. Crude flux calculations for about 2 hours earlier indicated slightly greater flux and a correspondingly higher average concentration in the box.

In the absence of photochemistry, one ton (as $NO_2$) of freshly emitted $NO_x$ (mostly NO) could scavenge about one ton of ozone under conditions of good mixing. The daily emissions of $NO_x$ in the entire eastern basin are estimated to be only about 120 metric tons. Roth et al. (1974) found that, in the western basin, about 16 percent of a weekday's total car mileage was driven between 1600 and 1800 PDT. If this 8 percent per hour figure is used to scale all $NO_x$ emissions to hourly rates (for around 1700 PDT), one obtains an estimate of 10 metric tons per hour for the $NO_x$ emission rate in the eastern basin. This is inadequate to scavenge more than a small fraction of the advected ozone.

The estimate of the ozone flux and the corresponding average concentration in the eastern basin "box" were based on the following considerations:

1. A quasi-steady state prevailed for at least one hour at the boundary between the basins. This assumption was quite good at the boundary, even though this was not the case over the whole western basin as the progress of the sea breeze in Fig. VI-6 shows. Pollutants which had accumulated in the western basin for many hours were flushed out into the eastern basin by the sea breeze starting about midday. For this reason, pollutant fluxes out of the western basin are not directly comparable to pollutant emissions within the western basin. The western basin was "emptied" more rapidly than it was "filled," giving rise to fluxes which were large in comparison with emission rates.

2. Using metric units for convenience of calculation, afternoon soundings at Brackett (BRA) (Fig. VI-18) and Corona (COR) (Fig. VI-19) showed a capping subsidence inversion at about 860 m msl. Ground elevations east of the Chino Hills slope from roughly 310 m msl at Brackett to 165 m msl at Corona; the Chino Hills themselves range 400-500 m msl, and the width of the pass between the western and eastern basins is 25-35 km. The area across which the flux was calculated was taken as 25 km x (860 m - 310 m) $\simeq 1.4 \times 10^7$ $m^2$.

3. The 1700 PDT winds aloft at Chino (CNO) were above 32 km per hour throughout the mixed layer and the 1700 PDT surface winds at Chino, La Verne College (POC), and Ontario (ONT) were all 27 km per hour. All wind directions in this area were near westerly. The rate at which air was transported into the eastern basin was taken to be:

$$1.4 \times 10^7 \text{ m}^2 \times 27 \text{ km/hr} \simeq 3.8 \times 10^{11} \text{ m}^3\text{/hr}.$$

The average ozone concentrations measured between 310 and 860 m msl on the 1700 PDT Brackett and Corona soundings were, respectively, 33.5 pphm = 660 $\mu g/m^3$ and 16.8 pphm = 330 $\mu g/m^3$. These were slightly lower than the corresponding values for the 1500 PDT soundings. The distribution of ozone concentrations at the surface indicates that concentrations between Brackett and Corona were generally intermediate in value. The rate at which ozone was advected into the eastern basin was estimated to lie between $3.8 \times 10^{11}$ $m^3/hr \times 600$ $\mu g/hr \simeq 250$ metric tons/hr and $3.8 \times 10^{11}$ $m^3/hr \times 330$ $\mu g/hr \simeq 125$ metric tons/hr.

Using this crude technique, it is clear that much of the ozone loading in the eastern basin on the afternoon of July 25 can be accounted for by advection from the western basin. In light of the preceding analyses, it is probable that a significant portion of the 24 pphm of ozone within the mixed layer arriving at Redlands at about 1800 PDT had its origin in the western basin. Redlands is approximately 65 miles from the area south of Los Angeles where the trajectory originated; thus it is reasonably certain that large source areas such as Los Angeles and Orange Counties can and do export a significant amount of ozone and ozone precursors to distant surrounding areas. This is not to say that the eastern basin does not contribute to its own ozone concentrations. Ozone values exceeding

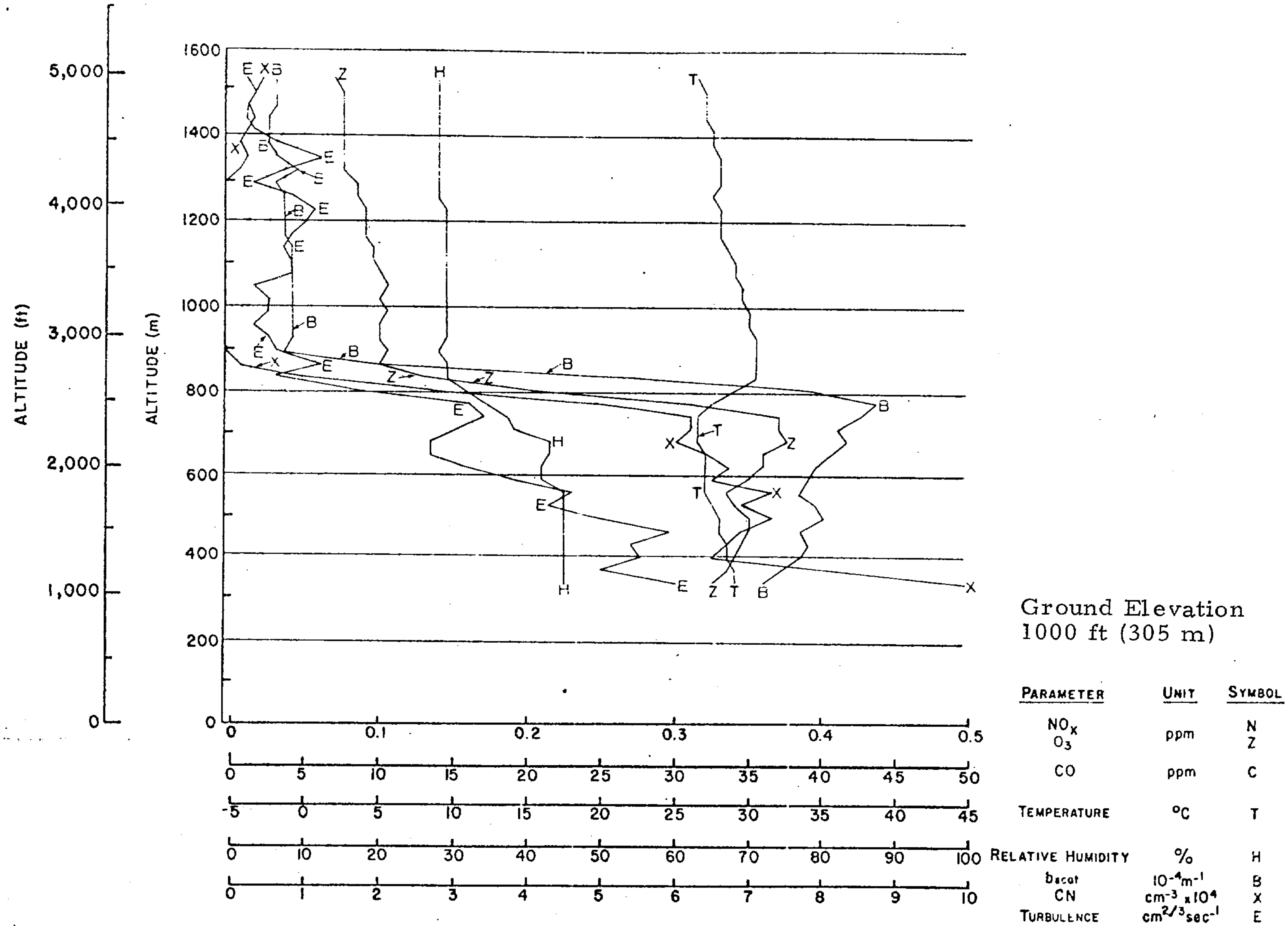


Fig. VI-18. VERTICAL SOUNDING AT BRACKETT (BRA) JULY 25, 1973, 1707 PDT

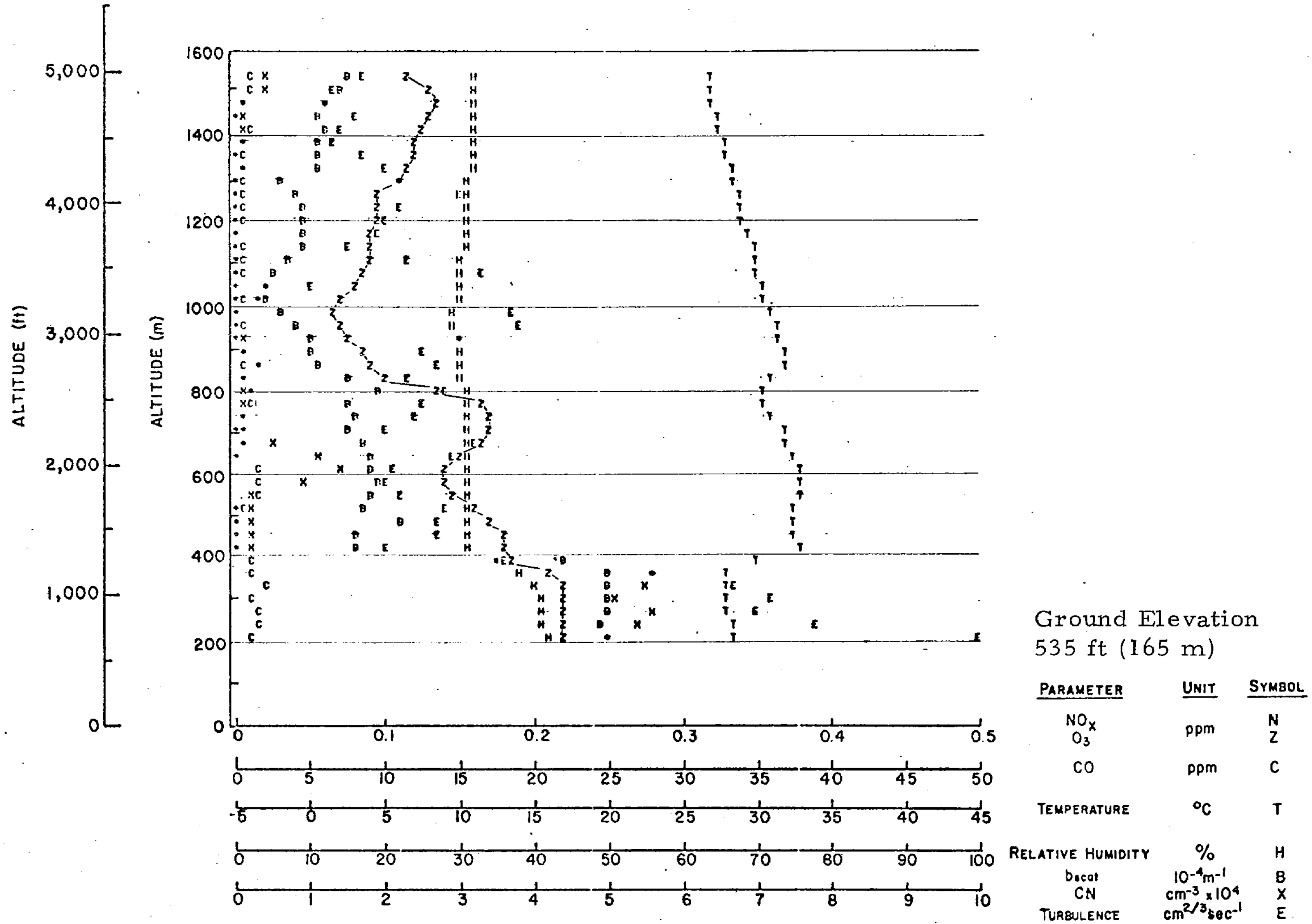


Fig. VI-19. VERTICAL PROFILE OVER CORONA (COR) JULY 25, 1973, 1724 PDT the federal standard also occur occasionally in the morning before the onset of the sea breeze.

July 25, 1973 was used in this analysis since a considerable amount of data was available for that day, but similar evidence can be provided for numerous days in the Los Angeles Basin.

### 6. End of the Episode - Basin Ventilation on July 26

July 26th started similarly to the 25th, with fog in the coastal areas and a late developing sea breeze. The high pressure ridge, however, was moving northward and weakening. By mid-morning the temperature aloft had dropped substantially (see Table VI-1), weakening and raising the subsidence inversion, thus allowing deeper mixing and lowering surface concentrations of pollutants. By 1300 PDT, the winds aloft had become organized and westerly at nine knots or greater from the surface to 7000 feet. Thus, pollutants which remained aloft from previous days or which were vented up the mountain slopes during the morning were finally swept away.

To show the ventilation processes in the eastern portion of the basin, the scattering coefficient data ($b_{scat}$) were integrated from the surface to 5000 feet for each time and location in the eastern basin. The result of the integration is an optical depth for each location and time. The average of the optical depth from the whole eastern basin was then found and plotted as a function of time in Fig. VI-20. Since $b_{scat}$ is roughly correlated with aerosol mass in the 0.1 to 1.0 $\mu$m size range, this average optical depth is a crude indication of the total aerosol mass in the eastern basin. Figure VI-20 nicely shows the gradual buildup of mass from the morning of the 25th to the morning of the 26th and then indicates the sharp drop as the winds aloft picked up, the inversion weakened, and the basin ventilated.

Another indication of this ventilation is seen in the vertical cross-sectional plots of $b_{scat}$ for the three daytime flights on the 26th (Fig. VI-21). The morning cross-section and soundings show independent layers existing up to 5000 feet. The morning soundings indicate that the subsidence had weakened, but that the atmosphere was still stable to the 5000 foot level. The winds were light and variable, so these upper layers were not ventilated. Most of the $b_{scat}$, however, was confined to layers below 2500 feet. A distinct dense layer is also apparent between about 2000 feet msl and 2500 feet msl. (This layer will be discussed in more detail later.)

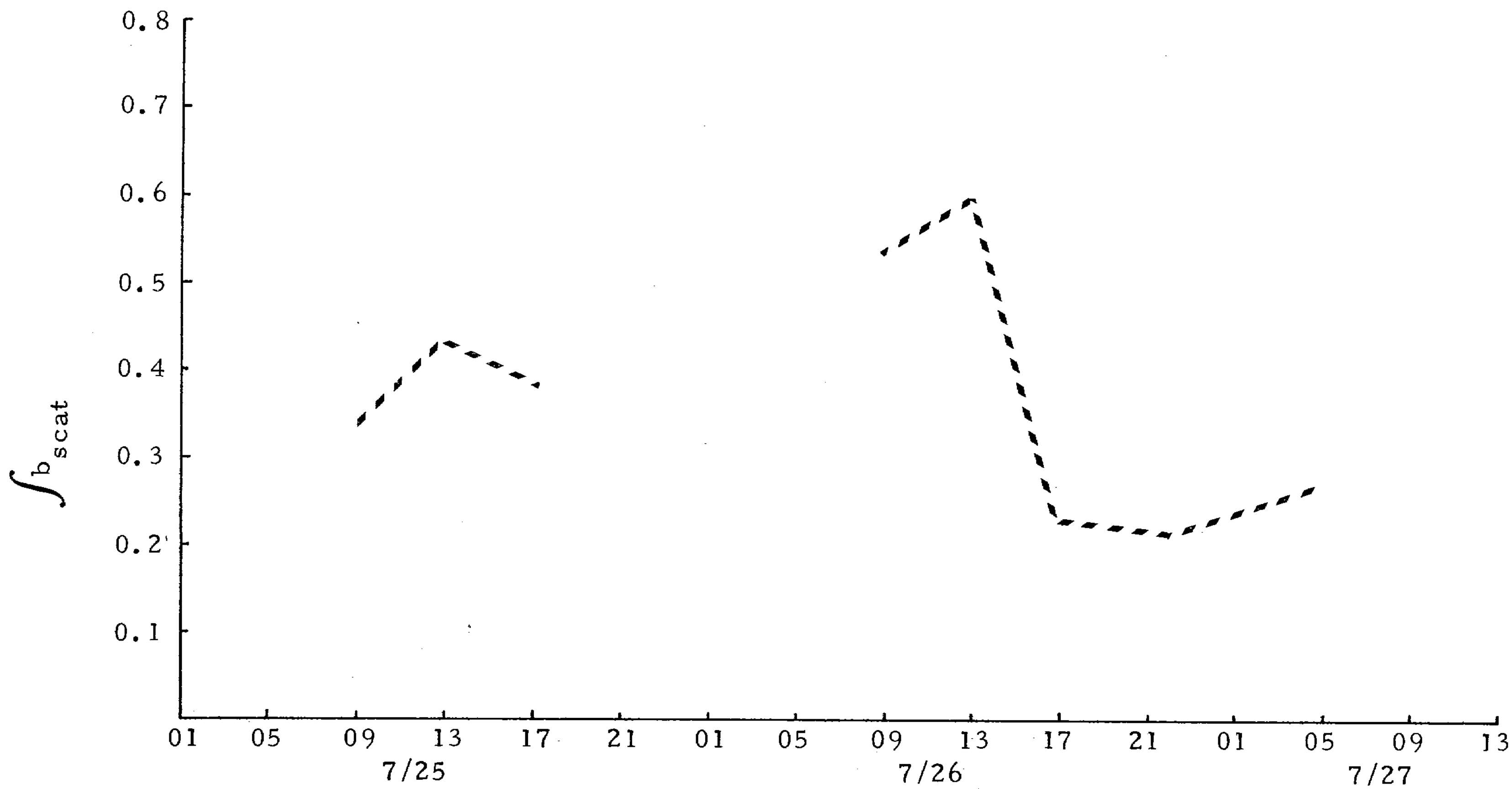


Fig. VI-20. VALUES OF THE AVERAGE OF $\int b_{scat}\,dz$ FROM SURFACE TO 5000 FT OVER THE RIVERSIDE ROUTE

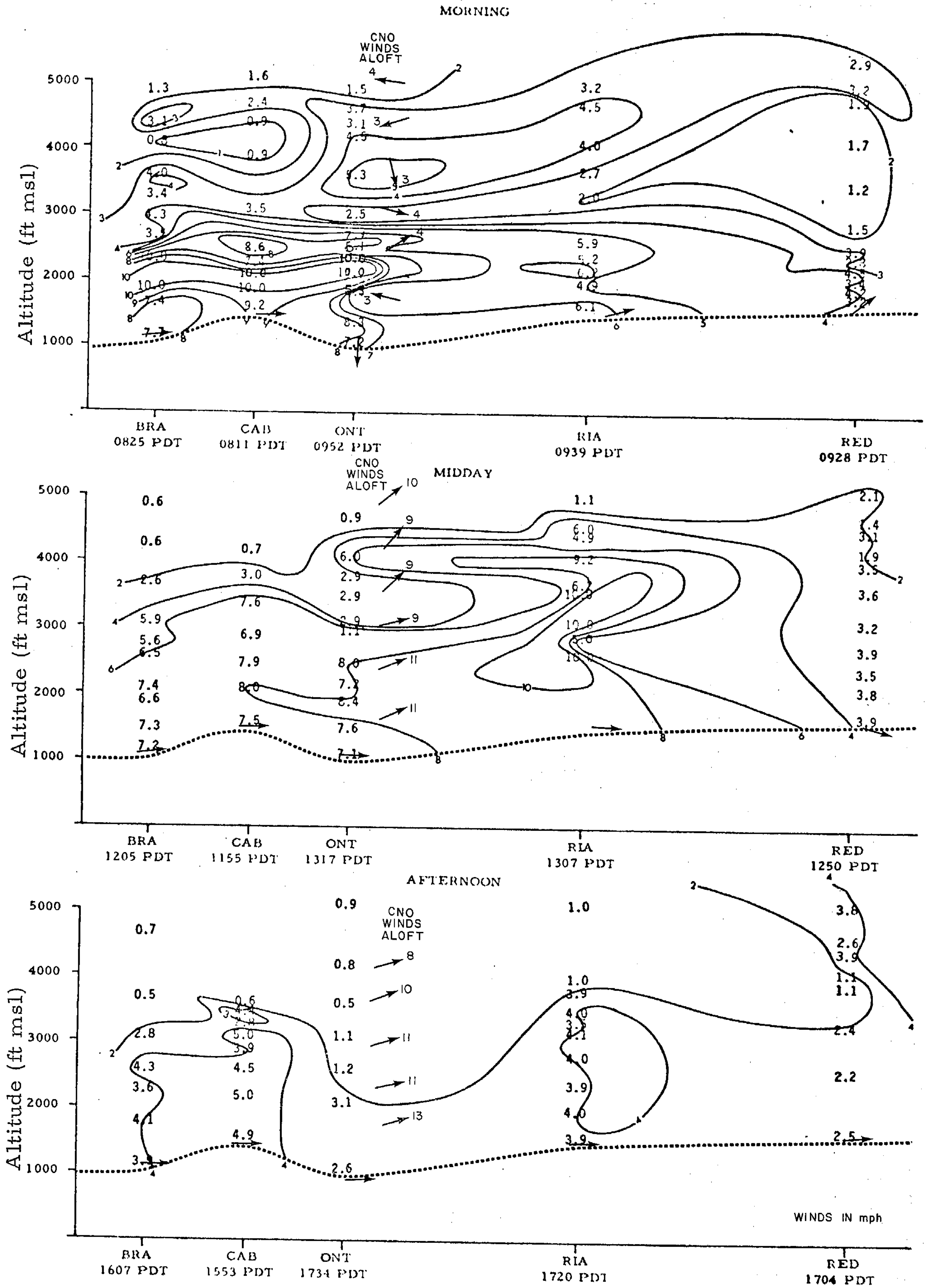


Fig. VI-21. VERTICAL CROSS-SECTIONS OF $b_{scat}$, 26 July 1973

By midday, surface heating had caused mixing of the various layers from the surface to the top of the stable layer. The independent layers existing earlier had merged and the dense layer at 2000 feet was ventilated to the surface as well as upward. The winds aloft became organized and the basin started to ventilate to the east.

The afternoon cross-section shows a considerably decreased particulate burden. By this time, the inversions had disappeared and mixing was limited only by some isothermal layers. In the eastern portion of the basin at Redlands, the atmosphere was neutral to over 8000 feet msl and pollutants were ventilating upward and being carried off by the winds aloft. This is the normal state on non-episode, non-subsidence days during the summer.

### 7. Characteristics of the Layers - Day and Night

It was pointed out earlier that in the morning cross-section shown in Fig. VI-21, several distinct and independent layers aloft existed. Figure VI-22 is the vertical profile taken at Ontario at 9:52 PDT which corresponds to the morning cross-section. This figure points out the necessity of measuring several parameters simultaneously in order to be able to interpret the three-dimensional structure. Using temperature alone, it would be almost impossible to determine the surface mixing depth, but by using a combination of parameters, one can assign a mixing height of about 1500 feet msl. Below that level, the NO, $b_{scat}$, CO, and condensation nuclei increase while the ozone drops slightly. These all indicate entrainment of relatively fresh emissions. In addition, the turbulence increases dramatically below this point, indicating good mixing.

Between about 1900 feet and 2500 feet msl, another layer is apparent. This layer was seen covering much of the eastern basin in Fig. VI-21. Looking at the combination of parameters in the layer, it is reasonable to conclude that this layer is the result of injection of a plume into the stable region above the surface mixing layer by a large elevated or buoyant point source. The high values of $b_{scat}$, $NO_x$, CO, and especially condensation nuclei, and the sharp deficit of ozone suggest fresh emissions, yet this layer is separated from the surface and would be slow to receive pollutants from the surface by diffusion. This same layer is seen on many of the other soundings in the area. It also appears in the soundings taken on the night of the 26th and appears to originate in the area of the steel mill and power generation complex in Fontana (between Ontario and Rialto (RIA) on the cross-sections).

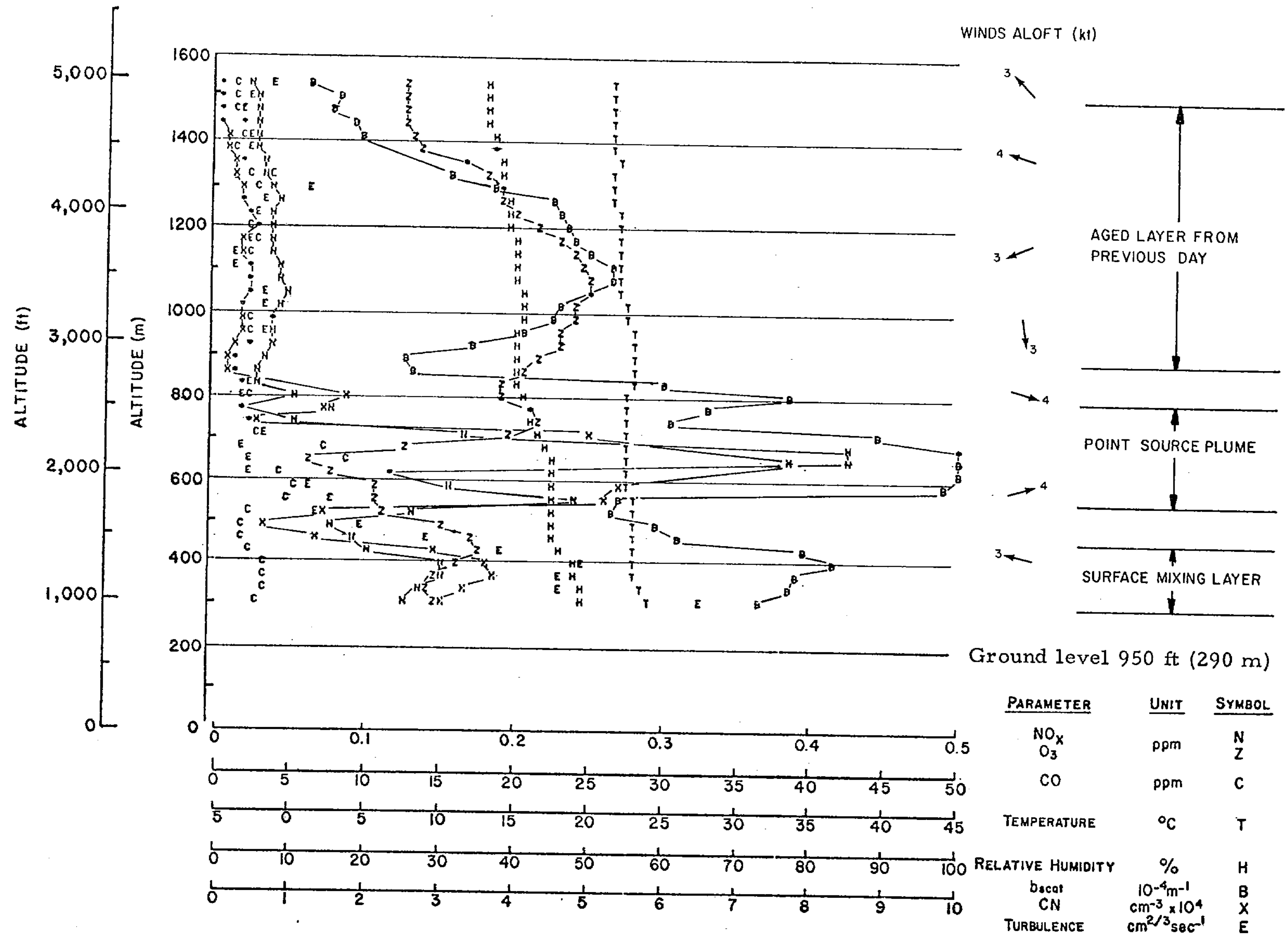


Fig. VI-22. VERTICAL PROFILE OVER ONTARIO (ONT) 0953 PDT July 26, 1973

Another layer exists between about 2900 feet and 4500 feet msl. This layer clearly consists of aged pollutants and is well separated from the ground. We have seen from our data that, in general, for a well aged air mass, $b_{scat}$ and ozone are usually well correlated, indicating that both are secondary products. Primary emissions such as $NO_x$, and especially condensation nuclei, are usually well depleted by reactions and coagulation, respectively. Thus, this upper layer is well aged and has probably remained from the previous day.

In an air mass which contains both primary and aged pollutants, almost any combination is possible. If fresh NO emissions are present, however, the ozone is usually depleted. Aerosol-caused $b_{scat}$, on the other hand, is stable once formed. $b_{scat}$ can also be due to primary emissions such as in the plume shown above or from field burning, etc., but these sources are becoming rarer due to more stringent emission controls.

On the night of the 26th, the atmosphere again became stable to at least 5000 feet and the winds aloft died down. Figure VI-20 indicates a slow buildup of $b_{scat}$ during the night over the eastern basin. This can be due to humidity effects or to fresh emissions. A combination of both is possible. Figure VI-23 shows the vertical cross-sectional plots of $b_{scat}$ during the night. It is clear from the plots that the eastern portion of the basin contributes to its own pollutant burden, at least during the night. Both the $b_{scat}$ and $NO_x$ burdens (not shown) increased over the eastern basin during the late night when winds were generally light and transport minimal. Much of the burden was in the raised layer at about 2000 feet, assumed to be due to the sources in Fontana. In the morning, this upper layer should have been ventilated to the surface as the mixing layer deepened and entrained it.

Although the eastern basin is not a strong source area, the burden accumulated during the night may be photochemically reactive and contribute to the morning ozone concentration when the sun comes up. In general, later in the day, as the sea breeze picks up, the pollutant burden in the eastern basin is probably due largely to transport in from other areas.

Finally, Fig. VI-24 is a vertical profile taken at Rialto shortly before sunrise. As in Fig. VI-22, a surface mixing layer, a plume aloft, and aged pollutants above that are visible. This figure is important in that it points out the stability of ozone in an aged air mass. The ozone in the layers aloft has existed all night at

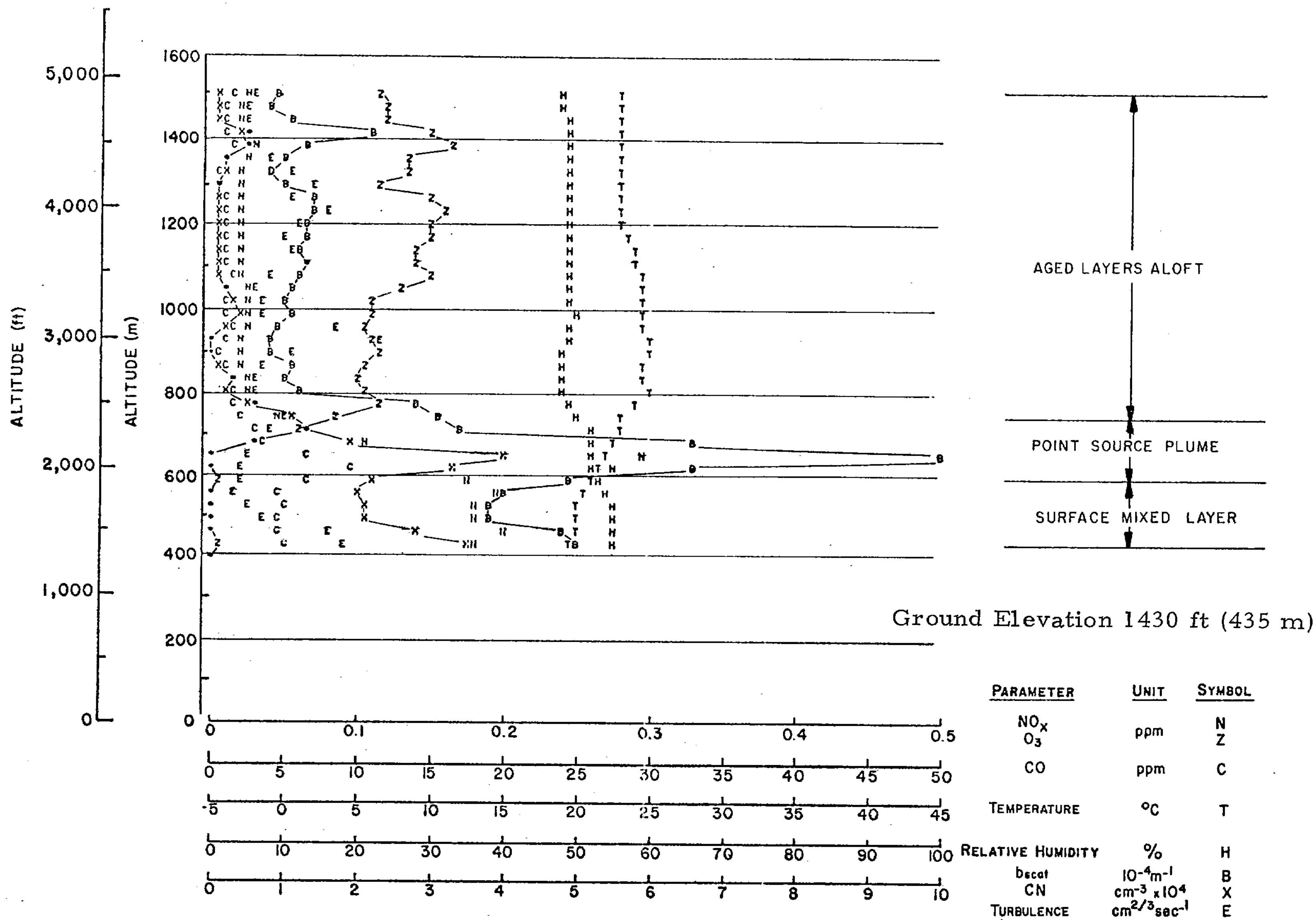


| PARAMETER | UNIT | SYMBOL |
|---|---|---|
| $NO_x$ | ppm | N |
| $O_3$ | ppm | Z |
| CO | ppm | C |
| TEMPERATURE | °C | T |
| RELATIVE HUMIDITY | % | H |
| $b_{scat}$ | $10^{-4}m^{-1}$ | B |
| CN | $cm^{-3} \times 10^4$ | X |
| TURBULENCE | $cm^{2/3}sec^{-1}$ | E |

Fig. VI-24. VERTICAL PROFILE OVER RIALTO (RIA) 0535 PDT JULY 27, 1973

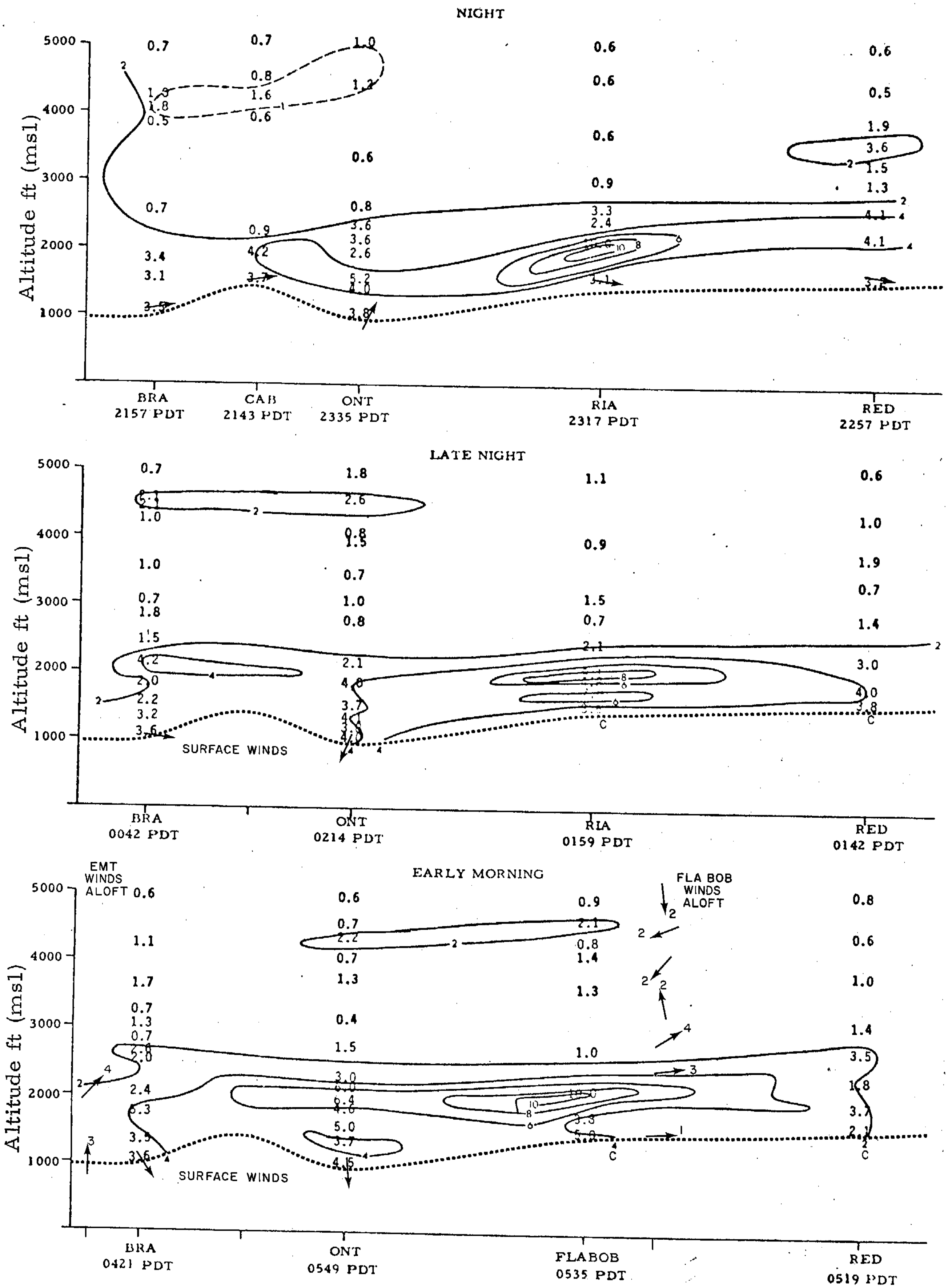


Fig. VI-23. VERTICAL CROSS-SECTION OF $b_{scat}$, 26-27 JULY 1973 concentrations greater than 0.16 ppm, in the absence of fresh emissions to scavenge it. All other soundings during the night also showed these high ozone values. Within the surface mixing layer or in the plume, however, the ozone was almost totally depleted by fresh emissions, indicating that low ozone values do not necessarily imply clean air.

### B. September 20, 1972

The day was warm and sunny under a mild Santa Ana condition. Few, if any, low clouds were present along the coast in the early morning. Maximum temperatures were in the mid-90's in the inland areas such as Ontario, Riverside, and the San Fernando Valley. Relative humidities in the early morning (7:00 a.m. PDT) were in the mid-90's along the coastal areas, in the mid-80's in the interior regions (Ontario-Riverside), but in the mid-70's at Burbank, the latter as an effect of a weak flow from the desert areas. Areas of low visibility formed along the coastal regions from LAX to Long Beach and near Ontario around 9:00 a.m. PDT. By noon, the low visibilities had spread southeastward into Fullerton and to Orange County Airport. This area of poor visibility moved into the Corona-Riverside area by middle and late afternoon. Visibility in the Ontario area improved to above six miles after noon, and visibilities in the San Fernando and western San Gabriel Valleys remained above 10 miles throughout the day.

Figure VI-25 shows the streamline pattern for 1000 PDT for September 20. Much of the characteristic, nocturnal, offshore flow persists as late as 1000 PDT. Slight beginnings of the sea breeze flow appear along the immediate coast at Venice (VEN) and Redondo Beach (RB) as well as at Long Beach (LGB). All of the wind velocities at this time are relatively low. Figure VI-26 shows computed surface wind trajectories beginning at 0700 PDT from several different locations in the basin. In particular, parcels from the Long Beach and south Los Angeles areas move northeastward and thence eastward during the day, while parcels originating in central Los Angeles are indicated to move into the San Fernando Valley.

Mixing layer heights determined from the morning soundings were plotted in Fig. VI-27 and contours of mixing layer heights were drawn. As plotted, heights refer to altitudes above sea level. In general, the top of the mixing layer was relatively flat in the morning flights with lowest values in the Fullerton (FUL) and Long Beach (LGB) areas.

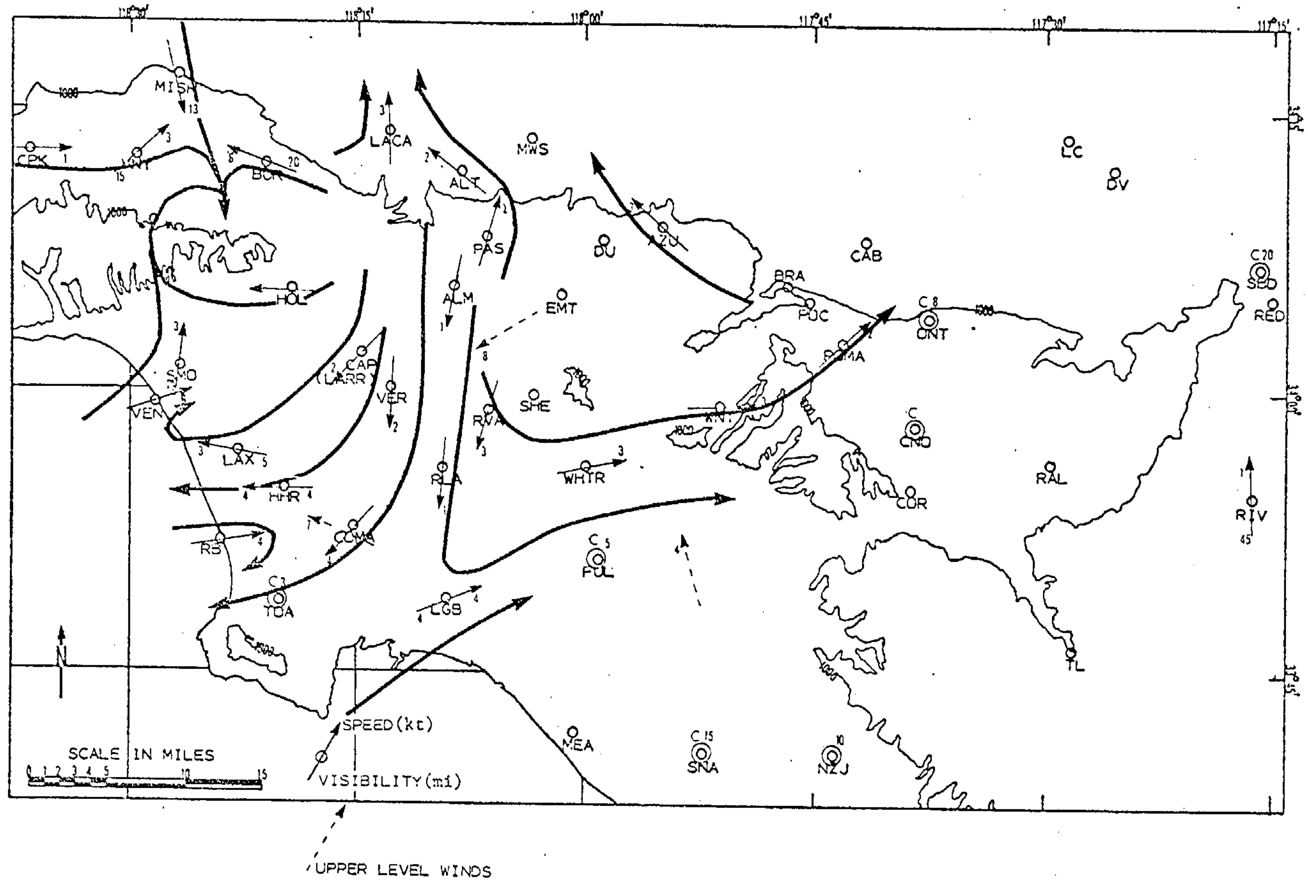


Fig. VI-25. STREAMLINE ANALYSIS - 1000 PDT, SEPTEMBER 20, 1972

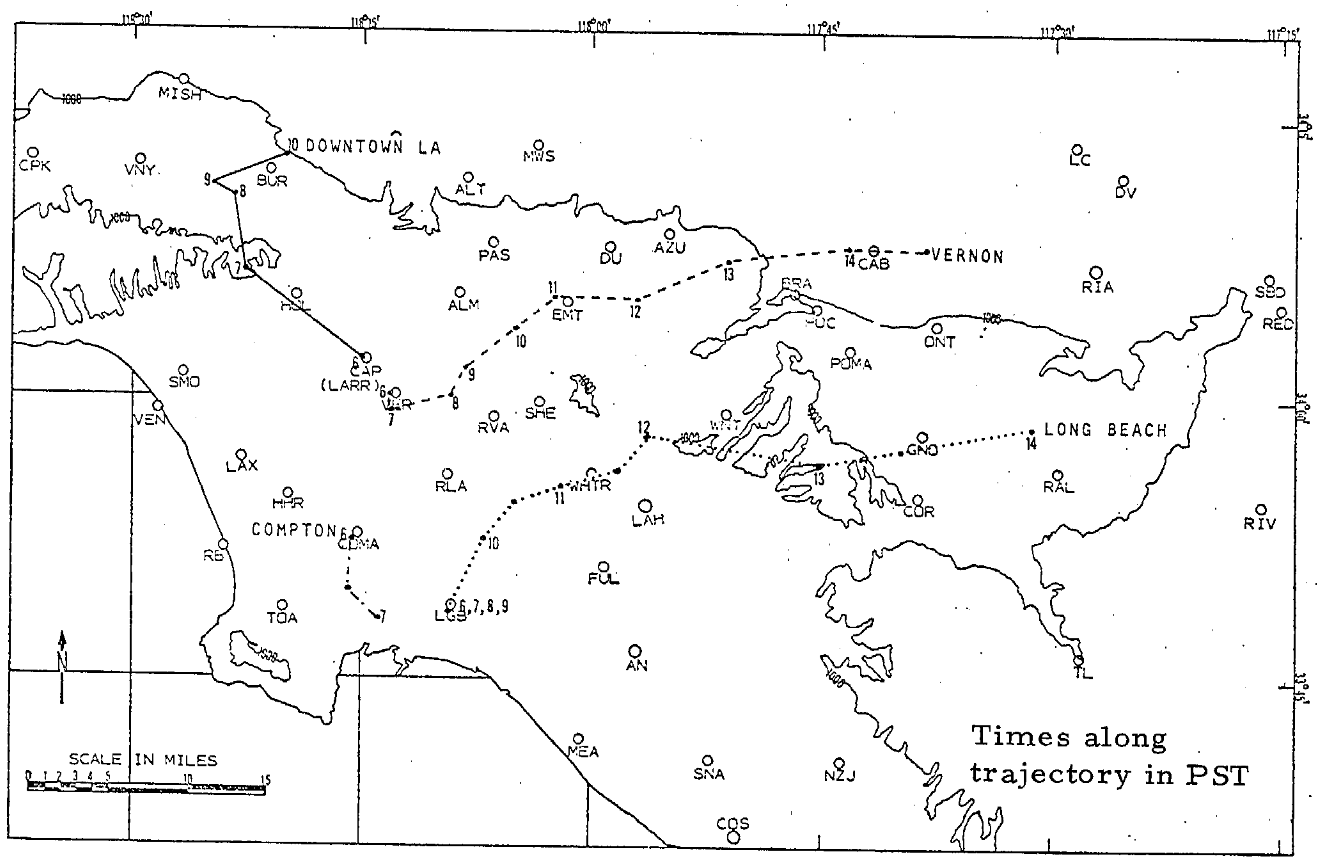


Fig. VI-26. SURFACE WIND TRAJECTORIES - BEGINNING 0600 PST (0700 PDT) SEPTEMBER 20, 1972

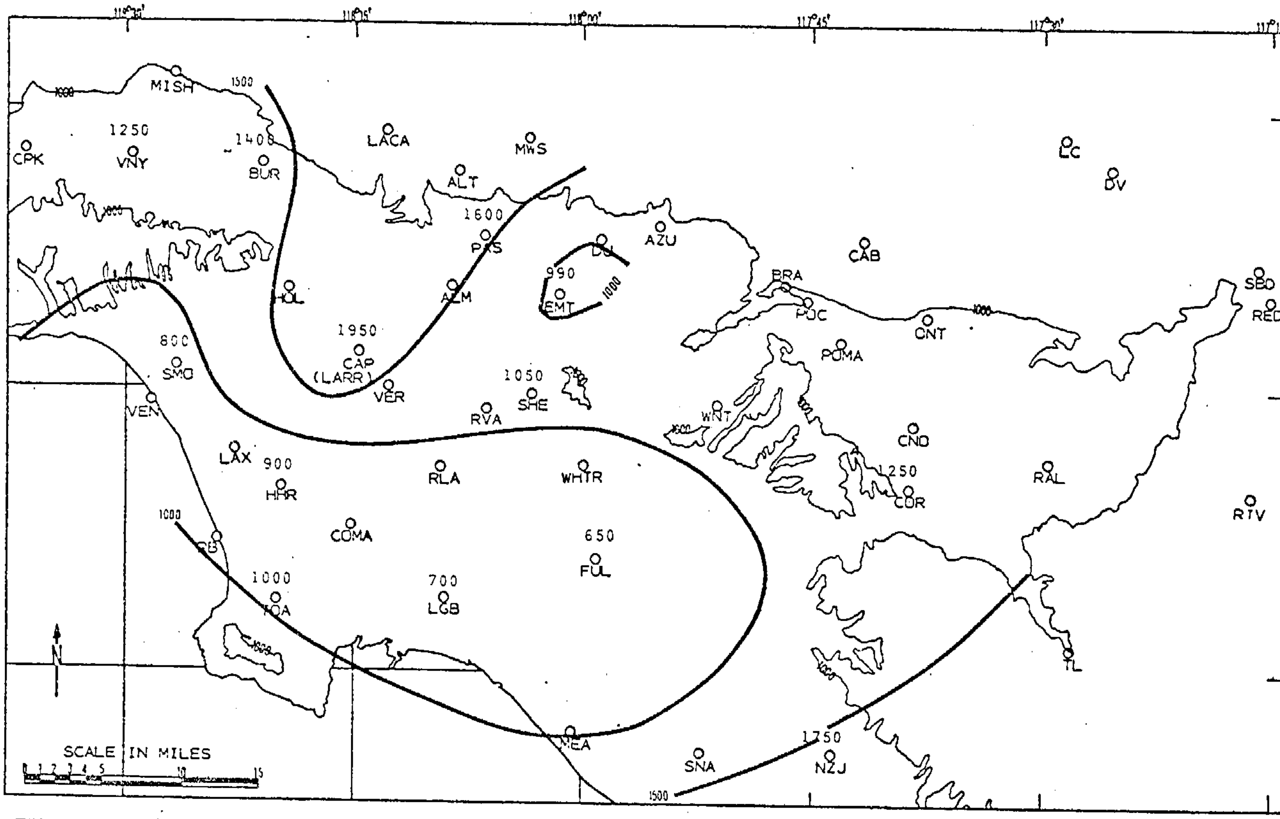


Fig. VI-27. MIXING LAYER HEIGHTS - MORNING, SEPTEMBER 20, 1972

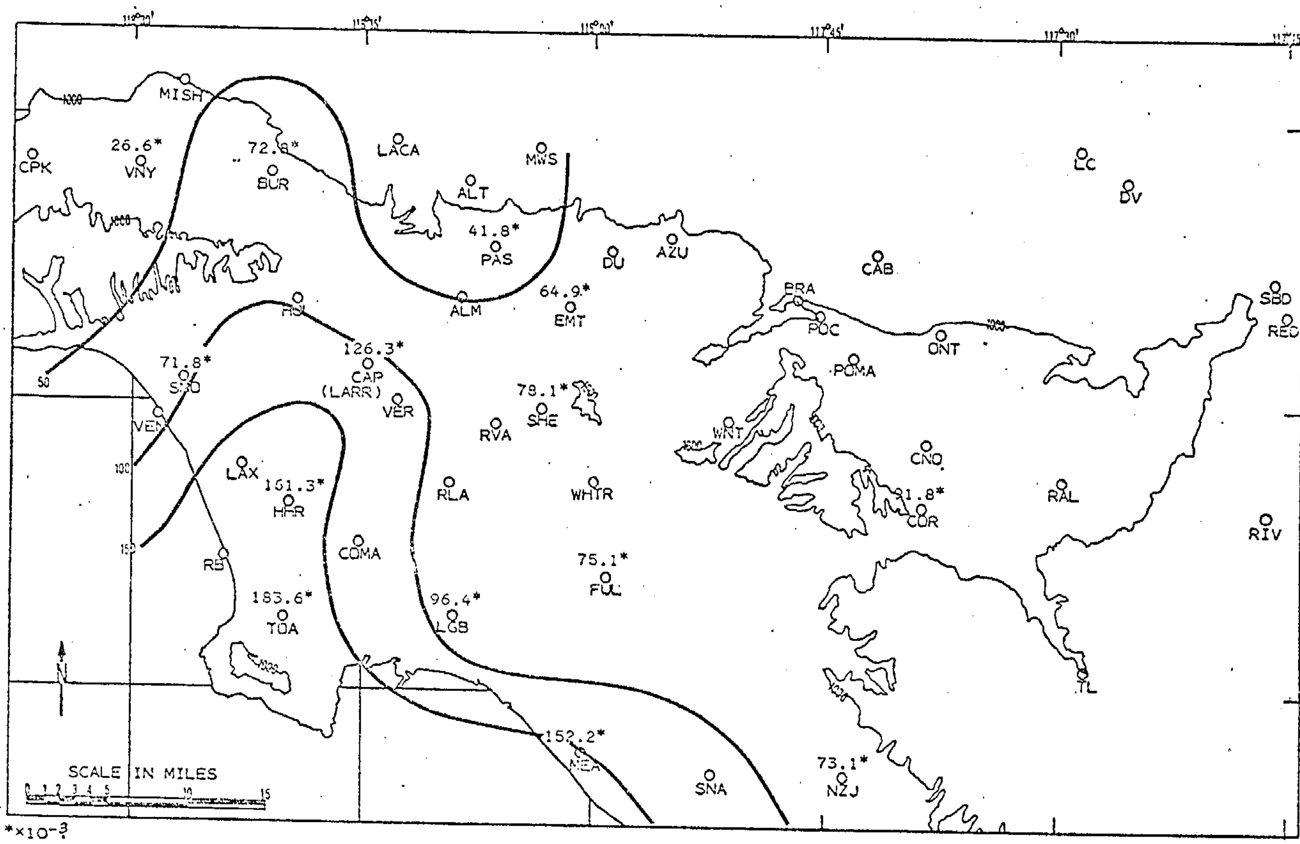


Fig. VI-28. $b_{scat}$ INTEGRATION - MORNING, SEPTEMBER 20, 1972

Values of $b_{scat}$ were integrated throughout the mixing layer for each available sounding and contours of these integrated values are shown for the morning flights in Fig. VI-28. Largest $b_{scat}$ values occur along the coastal sections from LAX through Torrance (TOA) to Meadowlark (MEA).

Values of CO for each sounding were examined, and peak values within the mixing layer at each available location were plotted for the morning flights in Fig. VI-29. The CO values show the strong influence of the heavy traffic along the coastal sections in a pattern similar to the $b_{scat}$ values. Large CO values also appear at Burbank (BUR) as a result of morning traffic in the San Fernando Valley.

By 1300 PDT (Fig. VI-30), a characteristic sea breeze flow pattern had been established, with one branch passing northwestward into the San Fernando Valley while the main flow pattern moved northeastward and then eastward along the slopes of the San Gabriel Mountains. Figure VI-31 shows this flow pattern in terms of the surface wind trajectories beginning at 1300 PDT from several locations.

Compared to the morning mixing layer heights, the mixing layer had increased markedly in depth by midday in the inland areas (Fig. VI-32). This was primarily the result of strong surface heating. The Ontario temperature, for example, increased from 71° to 88°F from morning to midday. Along the immediate coast, the mixing layer heights were not substantially changed.

Integrations of $b_{scat}$ at midday (Fig. VI-33) show a remarkable maximum in the vicinity of Fullerton (FUL) and extending over a substantial portion of the South Coast area. Surface wind trajectories indicate that the early morning source of this air at midday was from the area around Long Beach (LGB) or slightly to the west.

Peak values of CO and oxidant (Figs. VI-34 and VI-35) show a maximum in the same general area, although the CO peak is not as pronounced and the oxidant maximum is shifted somewhat to the north of the $b_{scat}$ maximum (probably due to scavenging in the strong source areas). The CO values at midday show a substantial decrease from the morning observations. In contrast, both oxidant and $b_{scat}$ values are considerably higher at midday than for the morning flights. It is also of interest to note that the large CO values shown in the San Fernando Valley during the morning flights are not reflected in high oxidant or $b_{scat}$ values by midday.

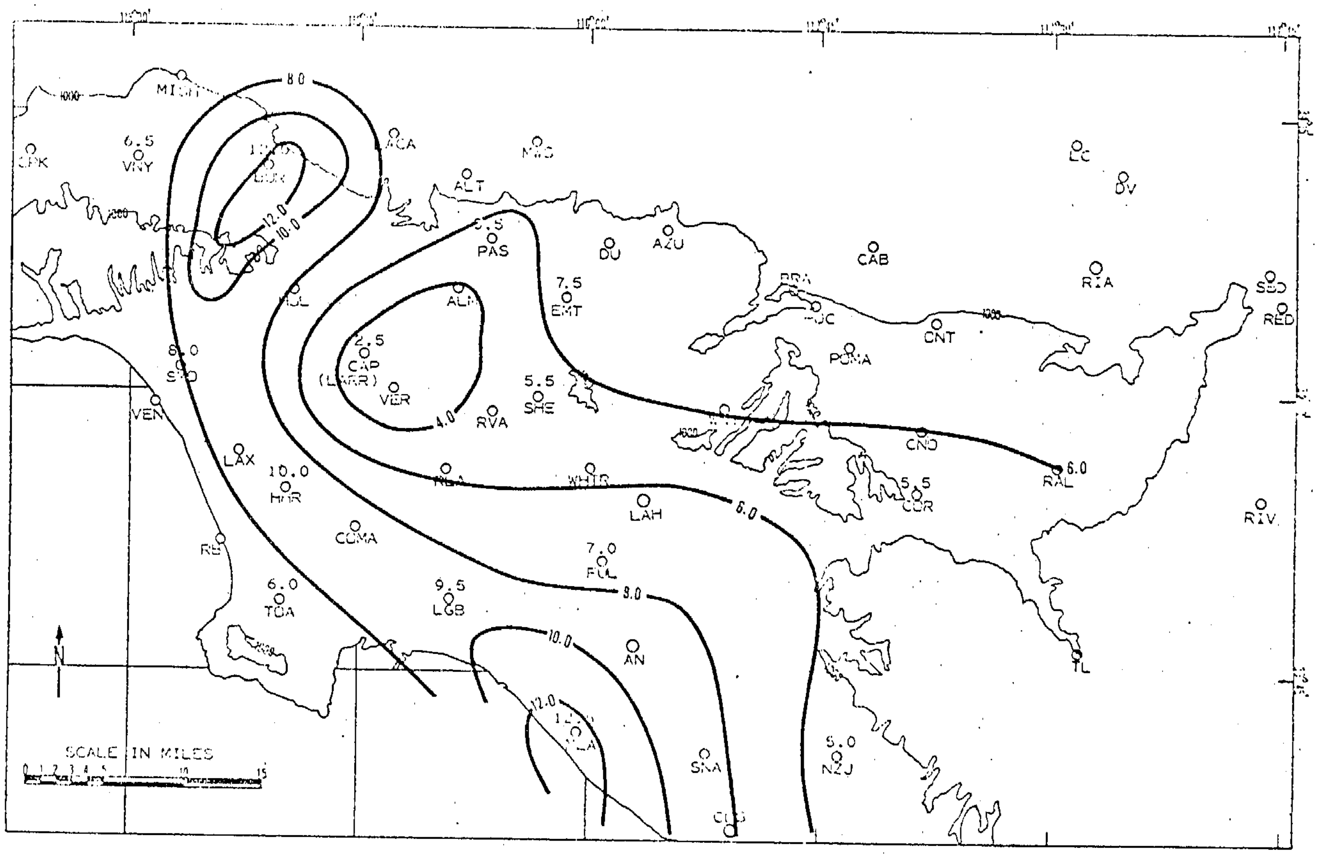

Fig. VI-29. PEAK CARBON MONOXIDE CONCENTRATIONS (ppm) WITHIN MIXING LAYER - MORNING, SEPTEMBER 20, 1972

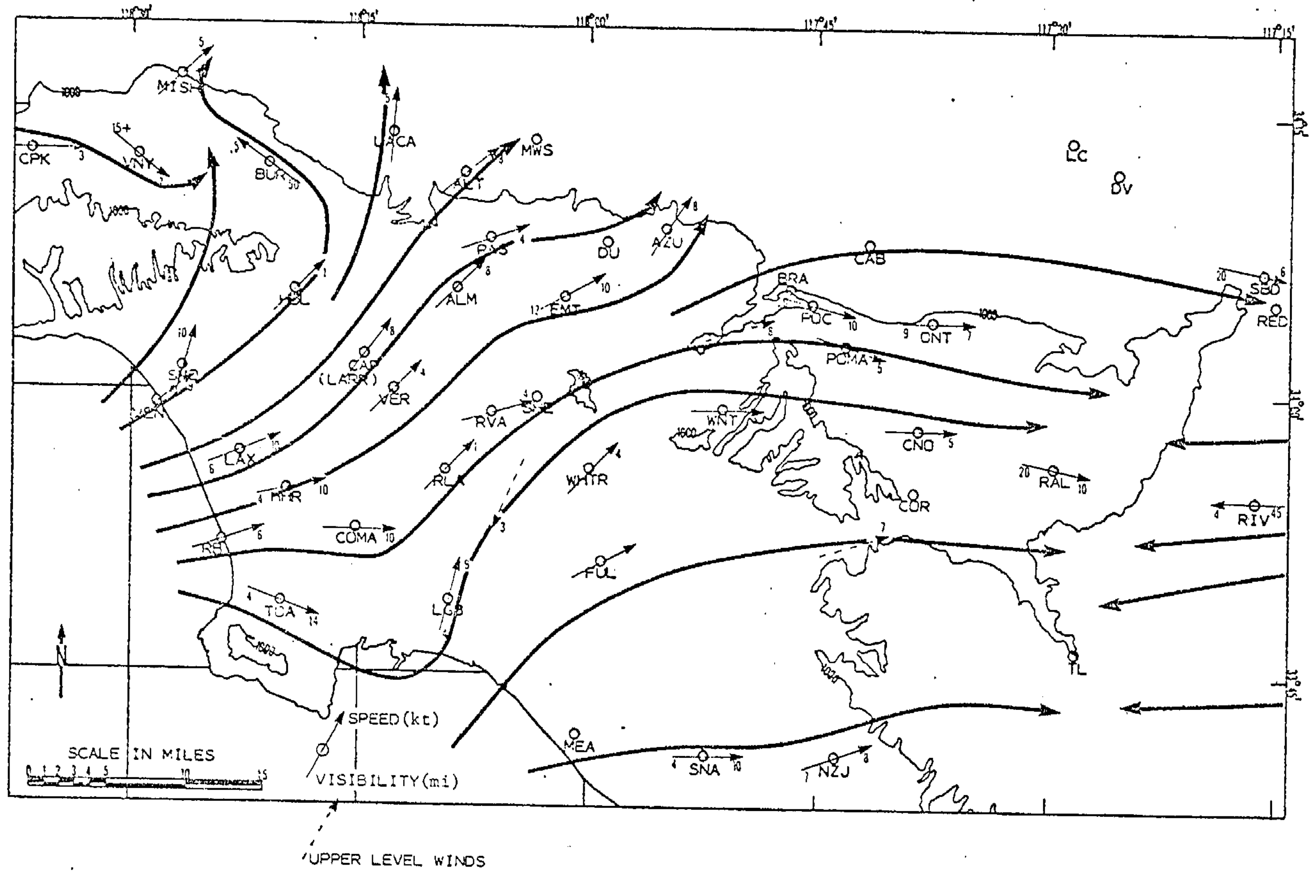


Fig. VI-30. STREAMLINE ANALYSIS - 1300 PDT, SEPTEMBER 20, 1972

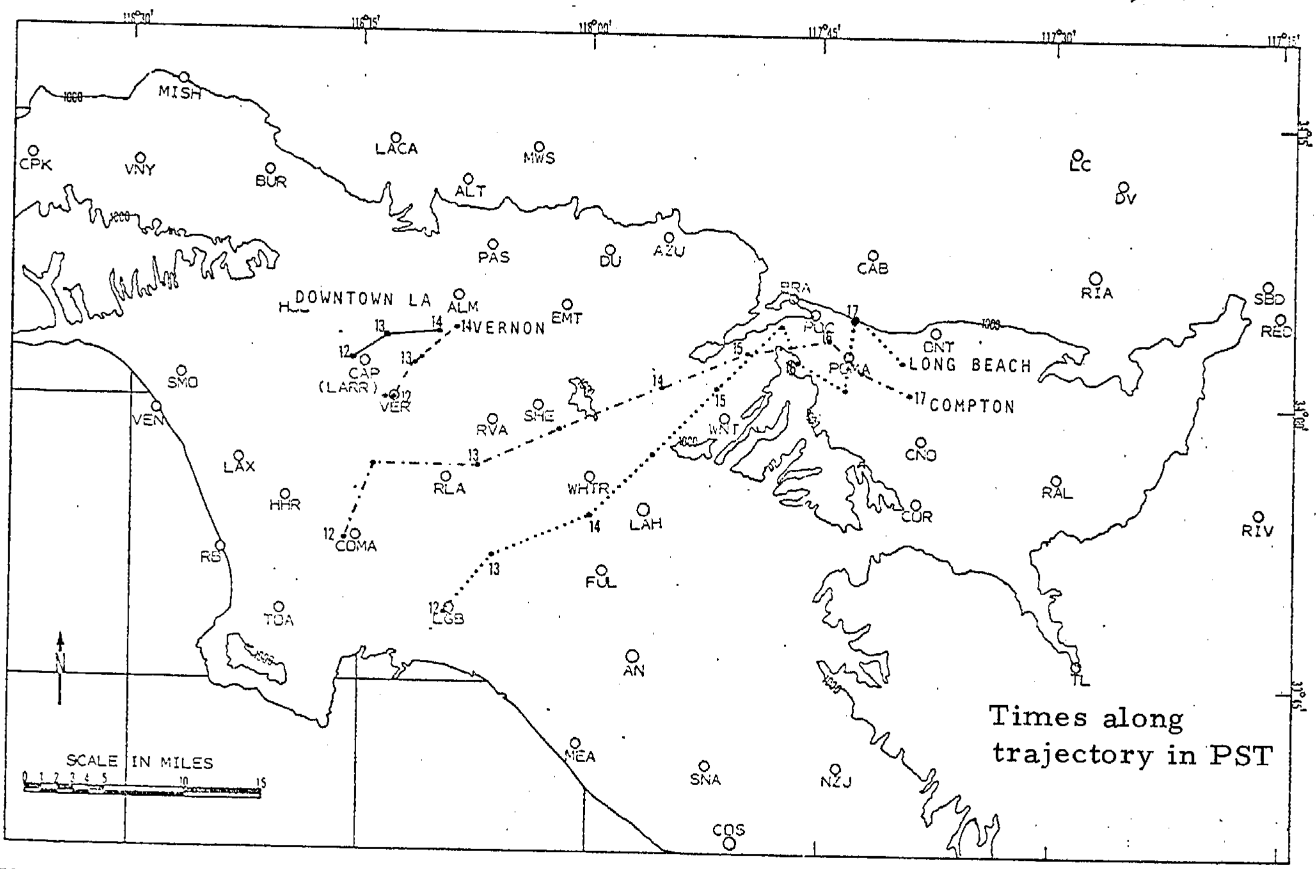


Fig. VI-31. SURFACE WIND TRAJECTORIES - BEGINNING 1200 PST (1300 PDT), SEPTEMBER 20, 1972

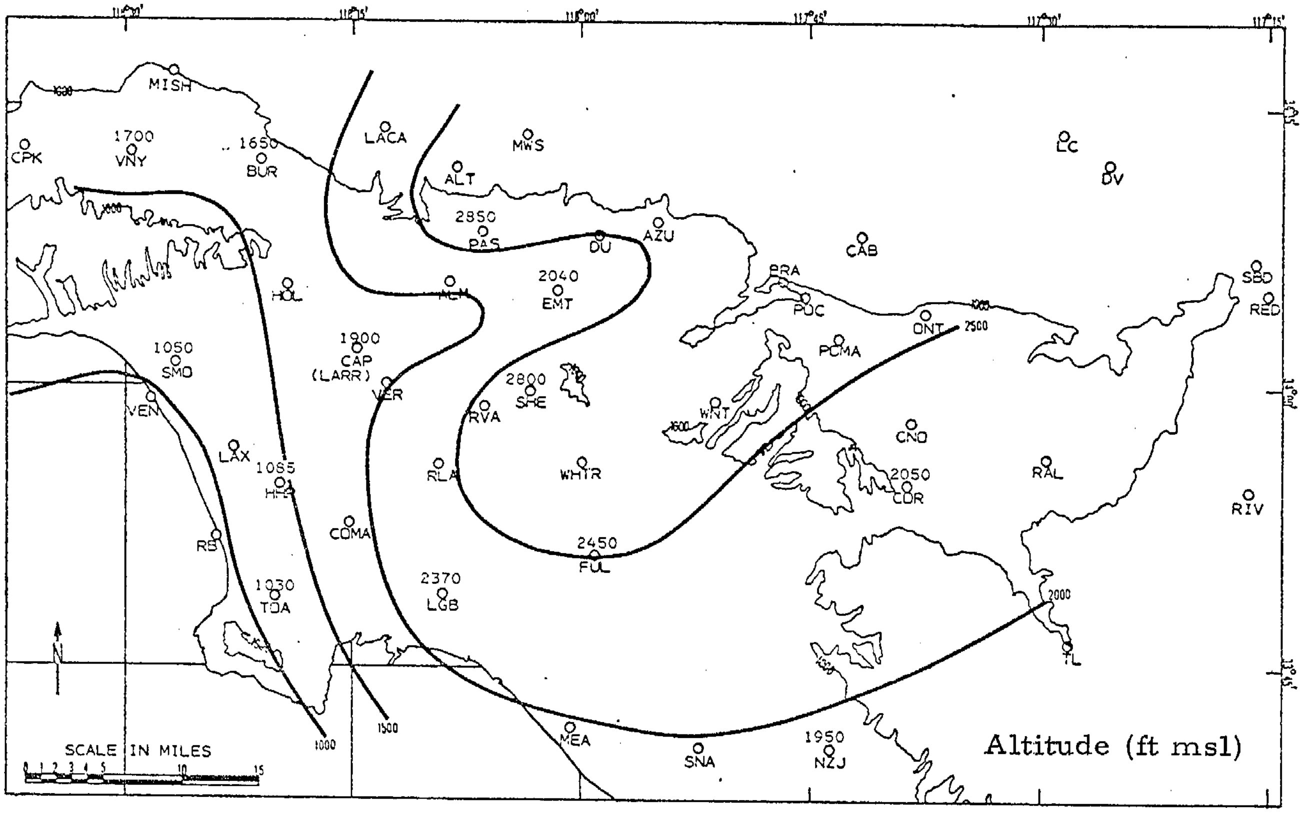


Fig. VI-32. MIXING LAYER HEIGHTS - MIDDAY, SEPTEMBER 20, 1972

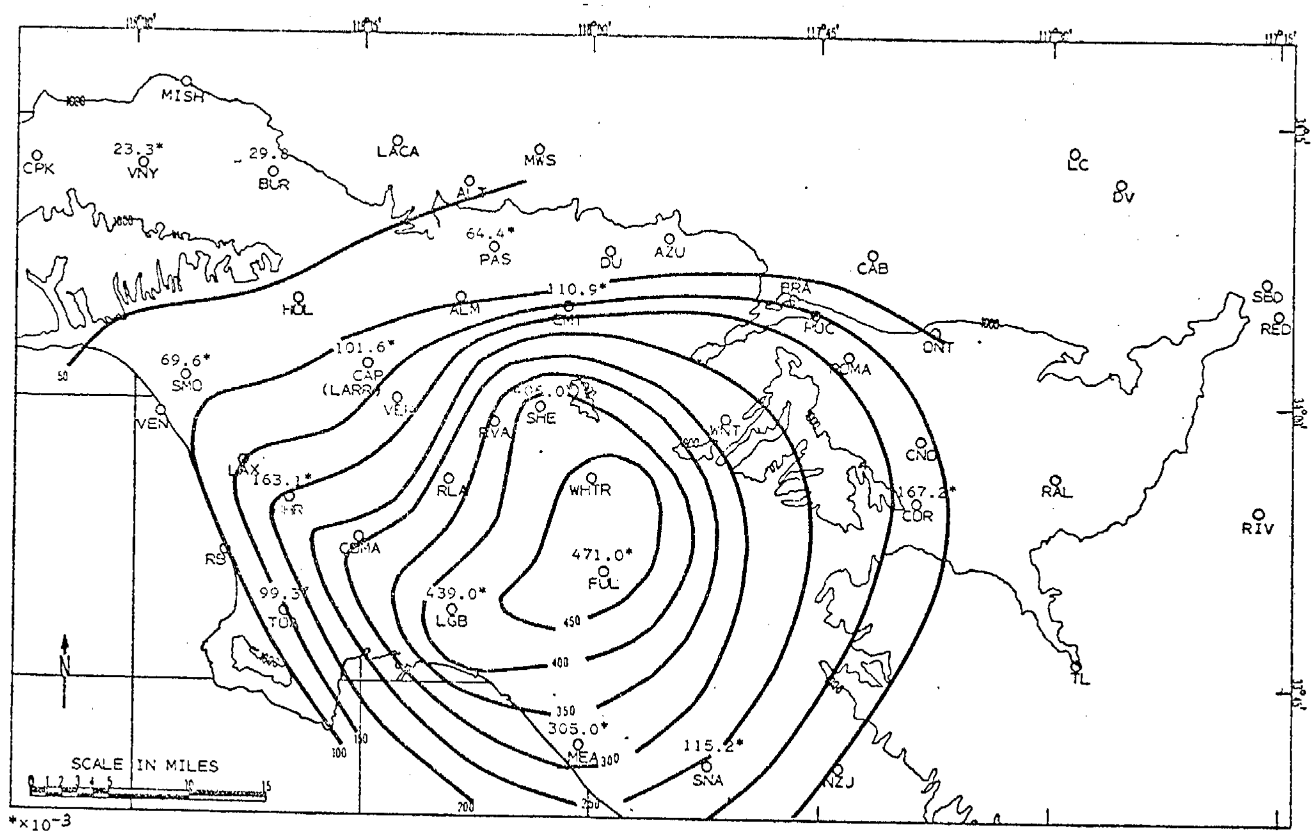


Fig. VI-33. $b_{scat}$ INTEGRATION - MIDDAY, SEPTEMBER 20, 1972

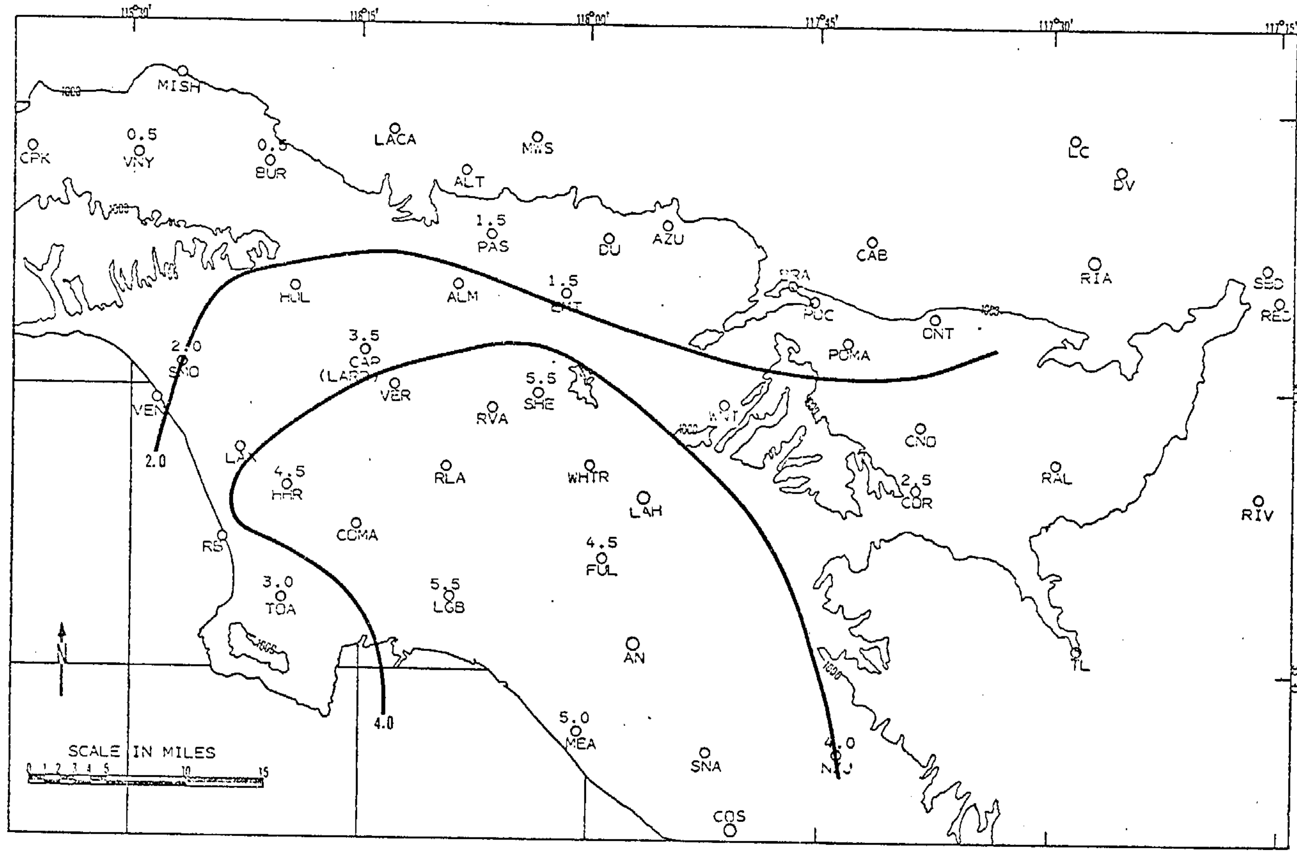


Fig. VI-34. PEAK CARBON MONOXIDE CONCENTRATIONS (ppm) WITHIN MIXING LAYER - MIDDAY, SEPTEMBER 20, 1972

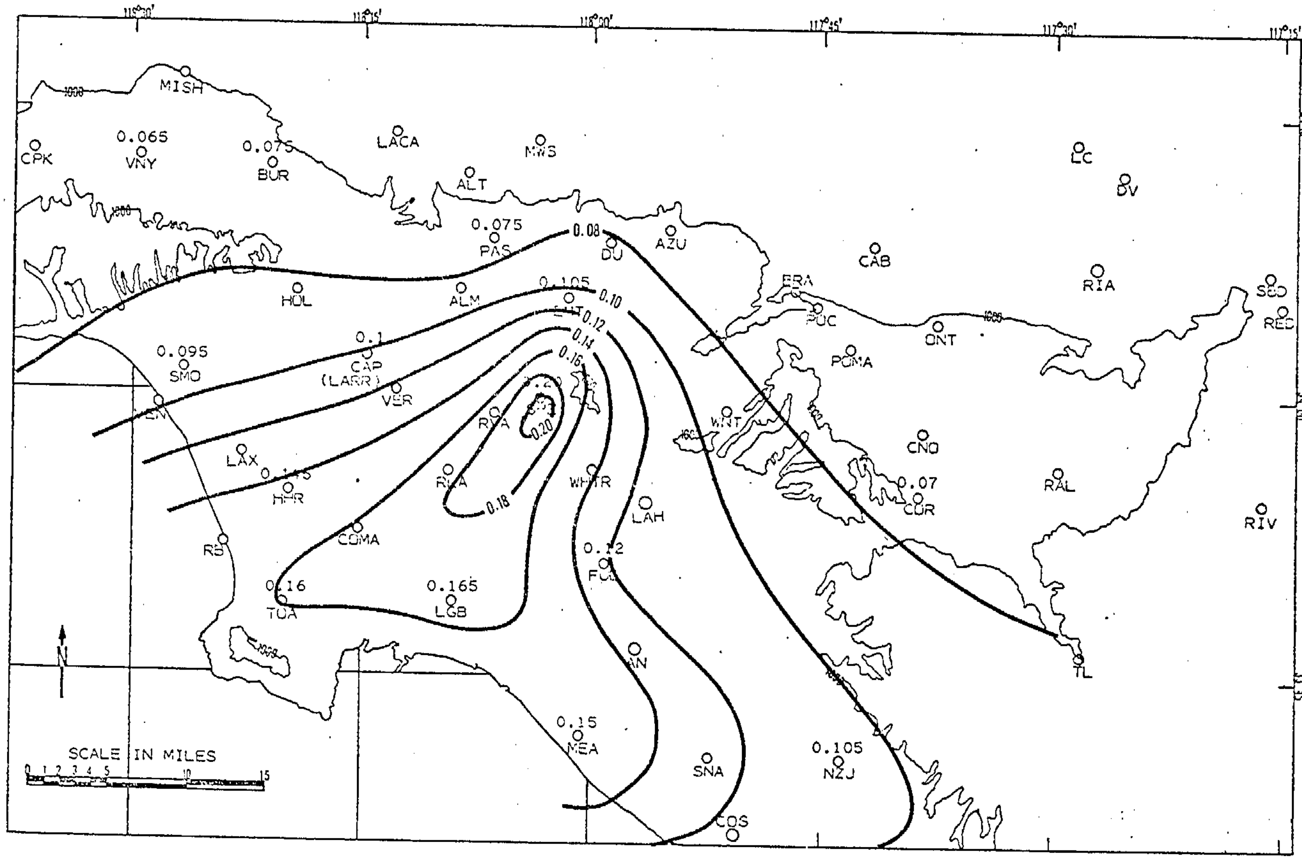


Fig. VI-35. PEAK OZONE CONCENTRATIONS (ppm) WITHIN MIXING LAYER - MIDDAY, SEPTEMBER 20, 1972

It is suggested that the large increase in $b_{scat}$ and oxidant values from morning to midday is indicative of strong photochemical activity in the South Coast area. CO serves as one indicator of the availability of primary source material (automotive exhausts) for the photochemical processes. The lack of photochemical indications in the San Fernando Valley suggests that other source components may also be important. One suggestion which fits the September 20 data has been that high humidity values might be required to make the photochemical process more effective. The occurrence of the large $b_{scat}$ maximum near Fullerton (FUL), in spite of a much more uniform area distribution of CO, could be used to support the humidity argument since the air at Fullerton at midday was in the relatively humid area near Long Beach (LGB) in the morning.

Streamline flow patterns at 1600 PDT (Fig. VI-36) show a continuation of the sea breeze pattern, but with a characteristic trend toward more westerly winds as the afternoon progresses.

Mixing layer heights (Fig. VI-37) show marked increases sloping upward toward the inland areas. Primarily, this results from the strong heating inland where temperatures reached the low 90's in contrast to the upper 70's along the coast. Considerable structure was present in the mixing layer heights with relatively low values at El Monte and high values over the central Los Angeles area.

Integrated $b_{scat}$ values (Fig. VI-38) show the transport of the pollutant material from Fullerton (FUL) to Corona (COR) by late afternoon. Large $b_{scat}$ values at Corona occur in spite of the large mixing layer height (4270 feet) which is shown in Fig. VI-37. This is indicative of a deep column of pollution which is in the process of escaping upwards and indicates one of the mechanisms for the loss of material from the basin. It is of interest to note that the maximum integrated $b_{scat}$ values at Fullerton (midday) and Corona (afternoon) are quite similar in spite of the large vertical dilution which has taken place.

Contours of CO peak values (Fig. VI-39) are relatively flat during the afternoon indicating the effects of mixing and the diverse nature of the CO sources. Oxidant values, however (Fig. VI-40), peak strongly in the Corona area in correspondence with the $b_{scat}$ contours. A comparison of the Fullerton (midday) and Corona (afternoon) soundings indicates that the $b_{scat}$ values decreased with time (dilution), while the oxidant values increased.

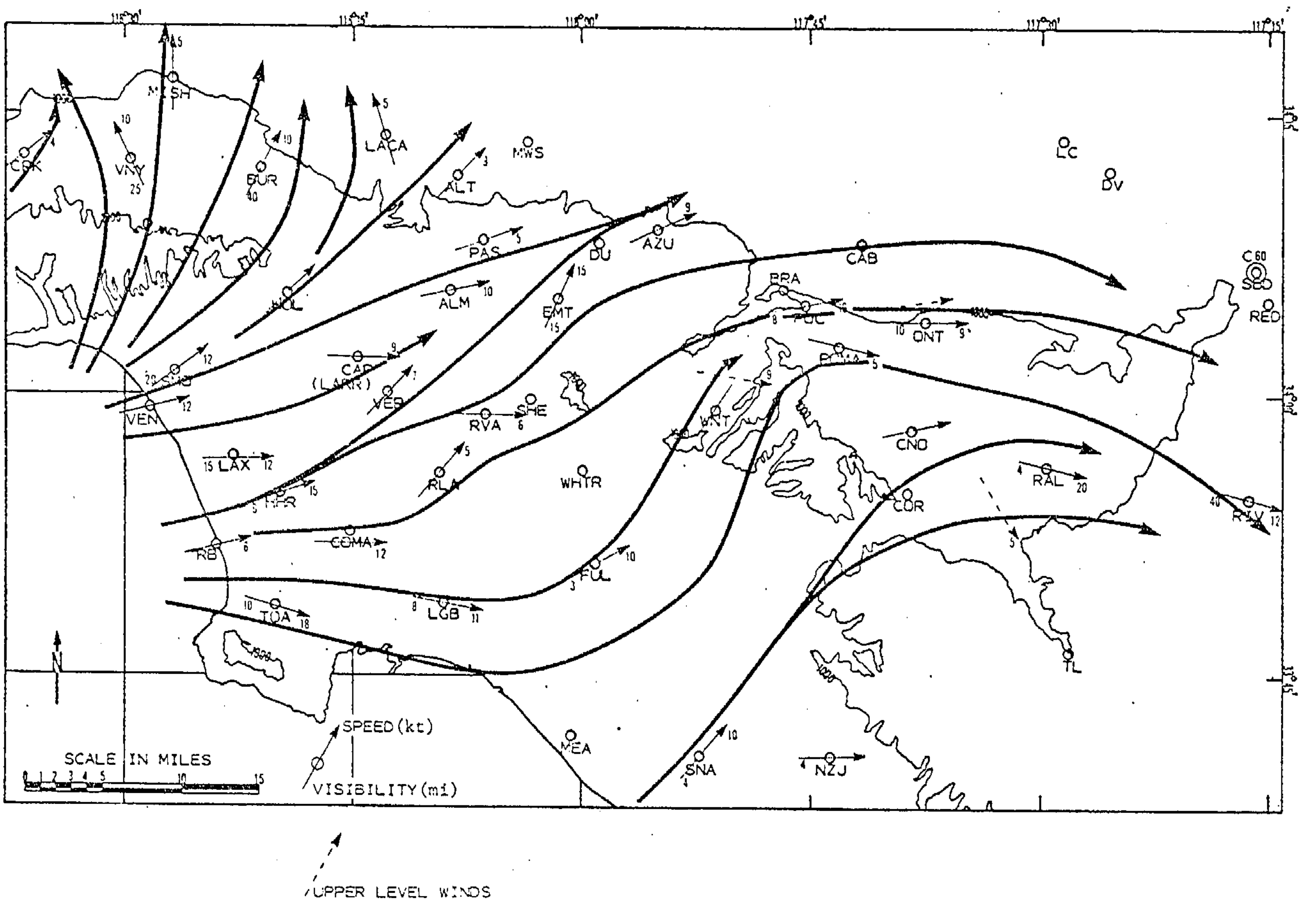


Fig. VI-36. STREAMLINE ANALYSIS - 1600 PDT, SEPTEMBER 20, 1972

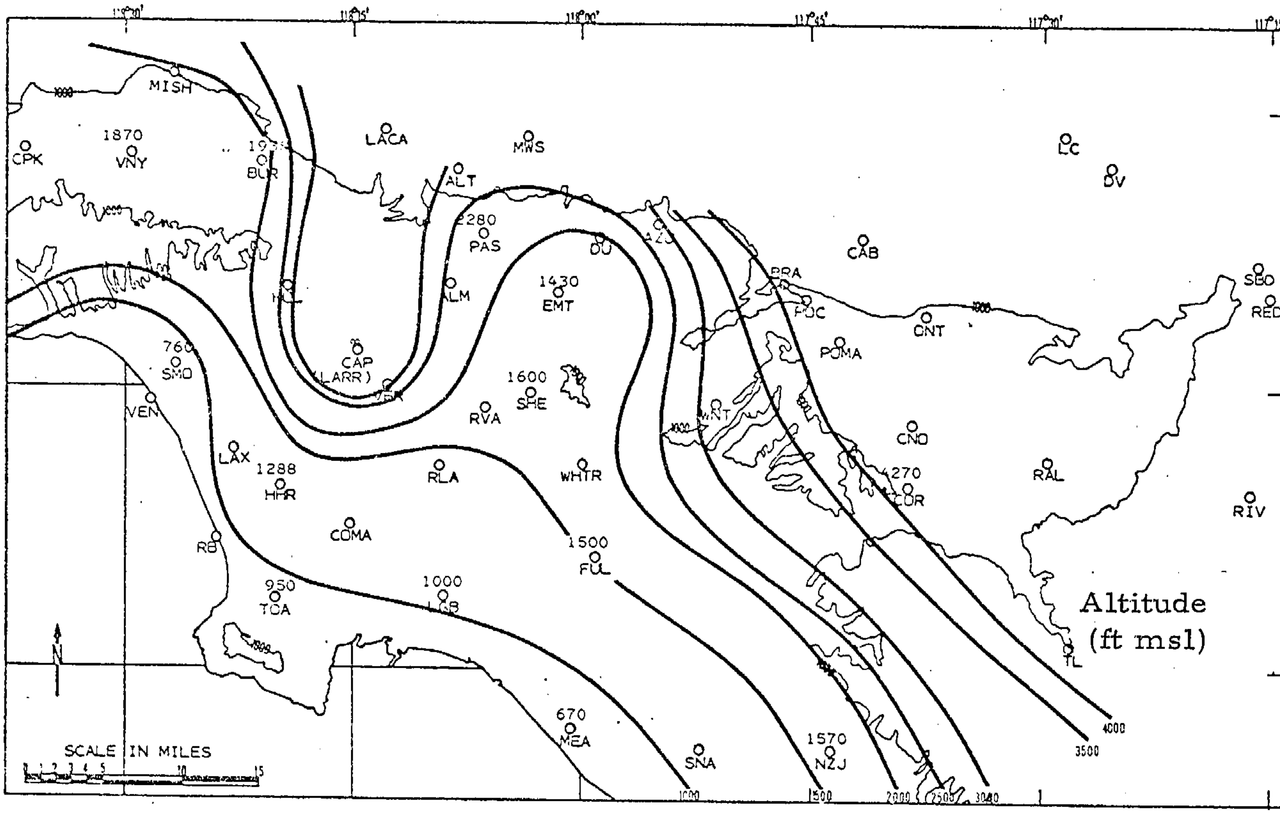


Fig. VI-37. MIXING LAYER HEIGHTS - AFTERNOON, SEPTEMBER 20, 1972

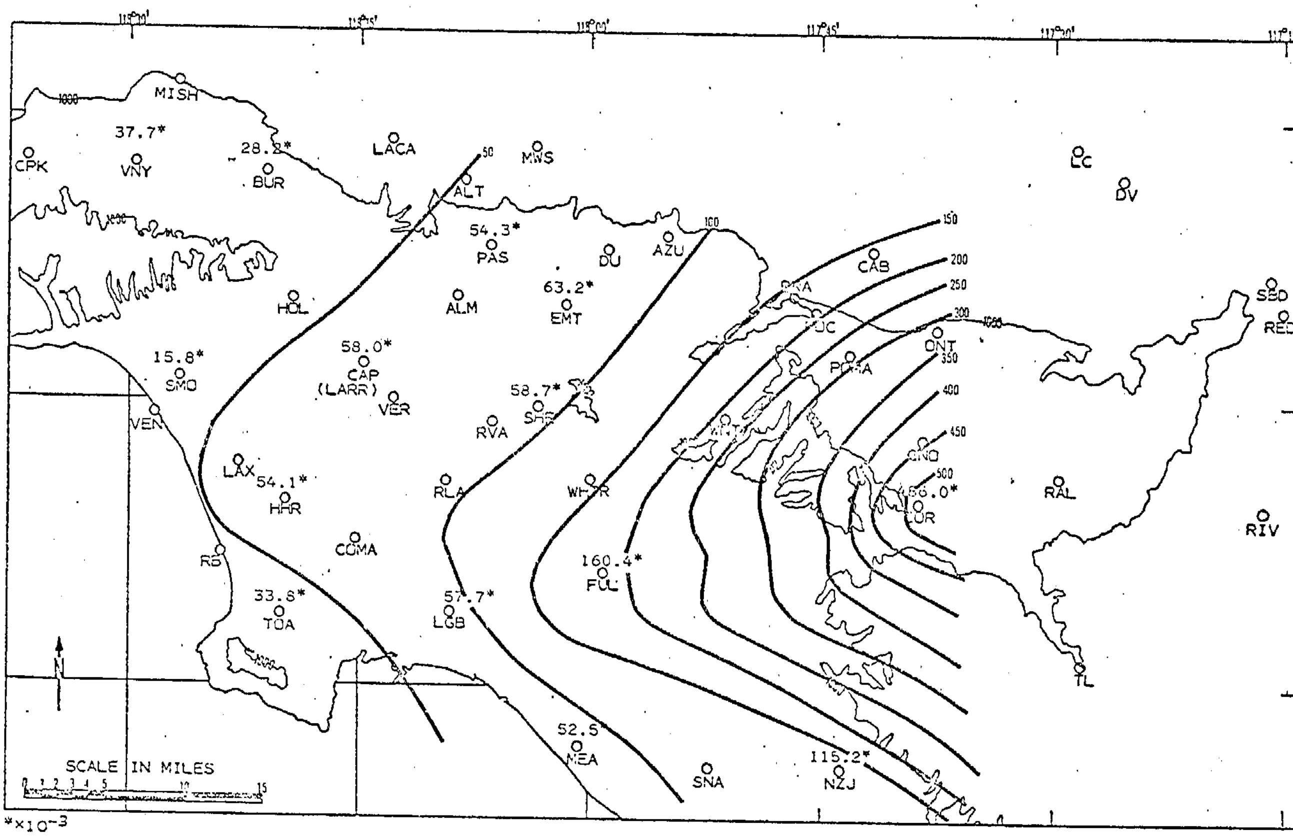


Fig. VI-38. $b_{scat}$ INTEGRATIONS - AFTERNOON, SEPTEMBER 20, 1972

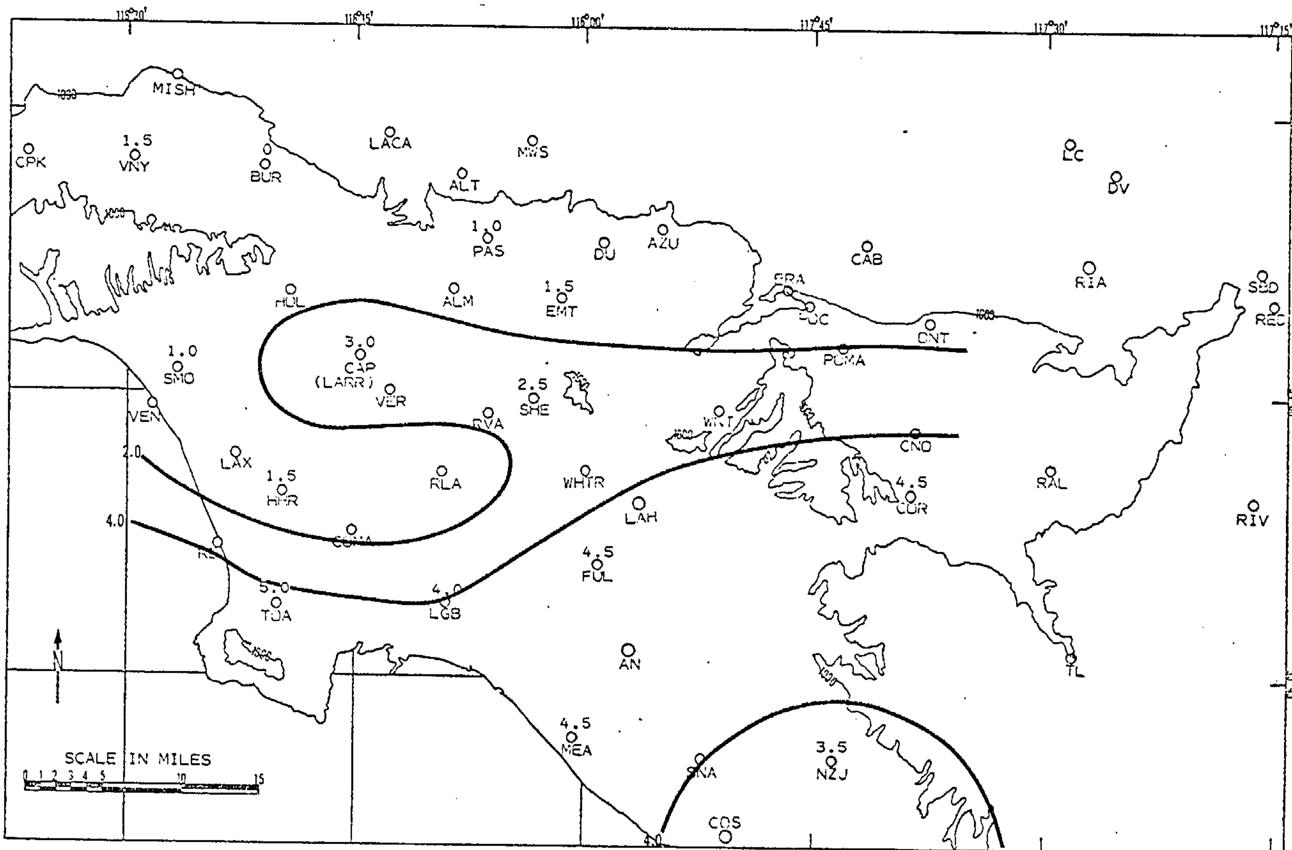


Fig. VI-39. PEAK CARBON MONOXIDE CONCENTRATIONS (ppm) WITHIN MIXING LAYER - AFTERNOON, SEPTEMBER 20, 1972

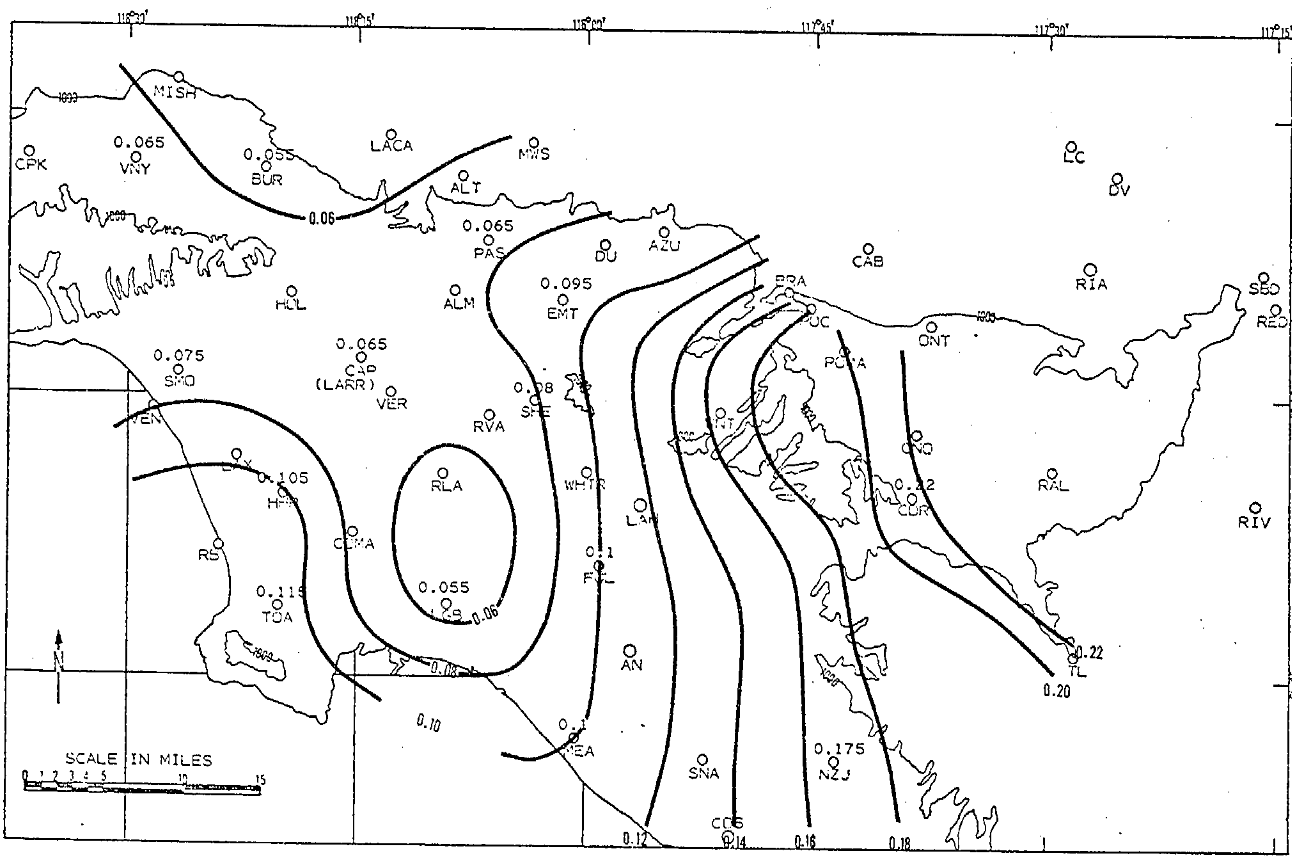


Fig. VI-40. PEAK OZONE CONCENTRATIONS (ppm) WITHIN MIXING LAYER - AFTERNOON, SEPTEMBER 20, 1972

Figure VI-41 shows vertical cross-sections of $b_{scat}$ for the morning, midday, and afternoon flights. The vertical sections were constructed along the mean wind direction and extend from Torrance (TOA) through Fullerton (FUL) to Corona (COR). The cross-sections show the substantial increase in $b_{scat}$ values and in mixing layer heights from morning to midday, together with a transport of material inland to the Fullerton area. By late afternoon, the pollutant material has been carried upward to over 5000 feet to levels where it can be advected away from the basin by higher level winds.

## C. October 24, 1972

Extensive fog and low clouds covered most of the Los Angeles Basin during the early morning. The morning flight patterns were thus restricted to the eastern sections of the basin. Maximum temperatures in the inland areas reached only to the low 80's during the afternoon as a result of the low clouds and ensuing haze. Visibilities were reduced throughout the basin during the entire day. Relative humidities were in the range of 90-100 percent during the early morning except in the San Bernardino-Riverside area where humidities were in the low 30's.

The streamline flow pattern for 1000 PDT is shown in Fig. VI-42. The wind flow is seen to be light and variable in direction, but with a tendency toward easterly winds in the eastern sections and the beginning of the sea breeze along the coast. Trajectories beginning at 0700 PDT are shown in Fig. VI-43. From the southern portions of the Los Angeles area, the trajectories indicate parcels moving northeastward during the day toward the El Monte-Azusa area before turning more eastward.

Morning mixing layer heights for the eastern portion of the basin are shown in Fig. VI-44. The elevation of the top of the mixing layer tends to slope upward from the basin toward the north and east where the ground elevations are somewhat higher and there is more opportunity for surface heating to begin increasing the mixing layer depth. At the time of the flight, for example, San Bernardino was approximately 3°F warmer than Ontario. The top of the heavily polluted layer over the Pomona-Ontario area was approximately 3000 feet msl at the time of the morning flight, but mixing from the ground upward was apparently restricted to the mixing layers shown in Fig. VI-44.

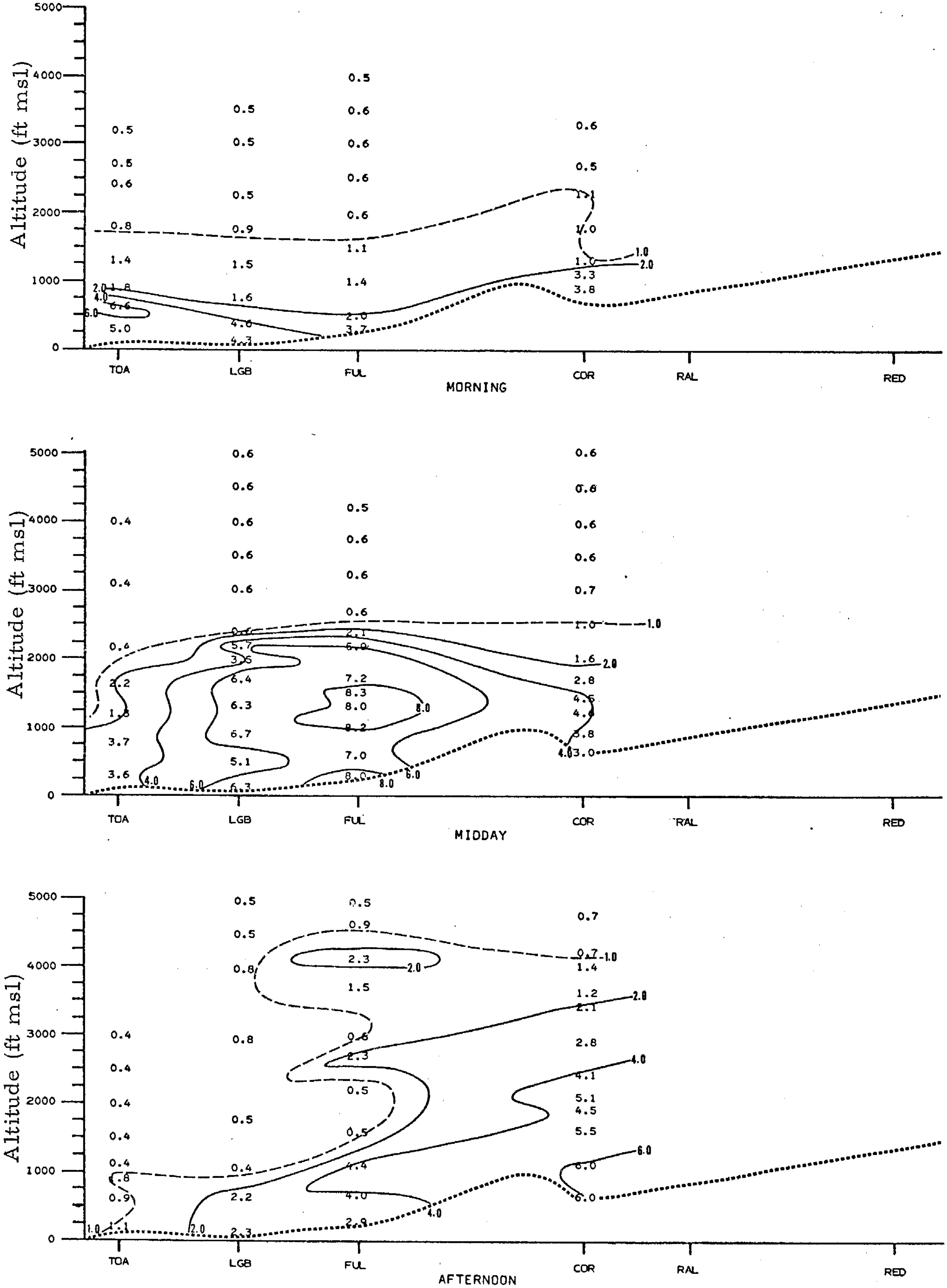


Fig. VI-41. VERTICAL CROSS-SECTION OF $b_{scat}$ - MORNING, MIDDAY, AFTERNOON, SEPTEMBER 20, 1972

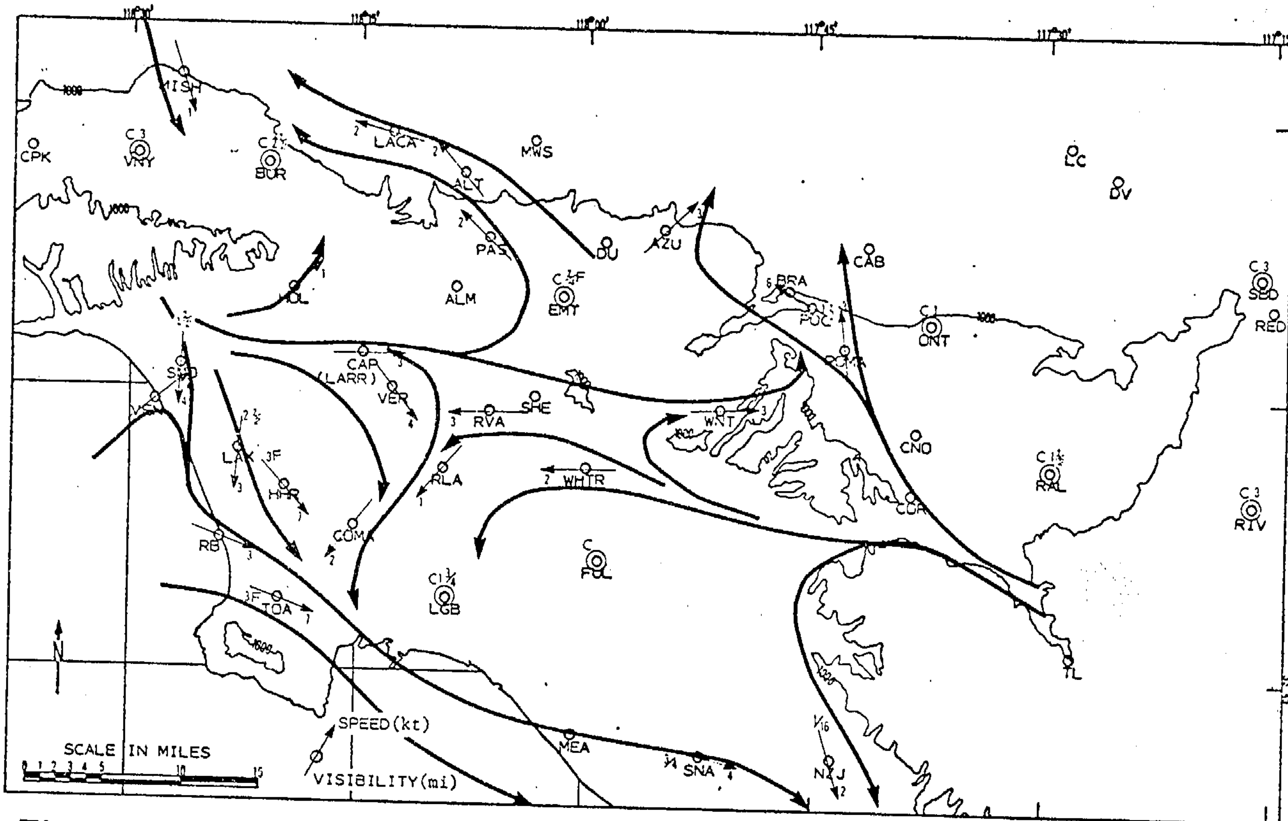


Fig. VI-42. STREAMLINE ANALYSIS - 1000 PDT, OCTOBER 24, 1972

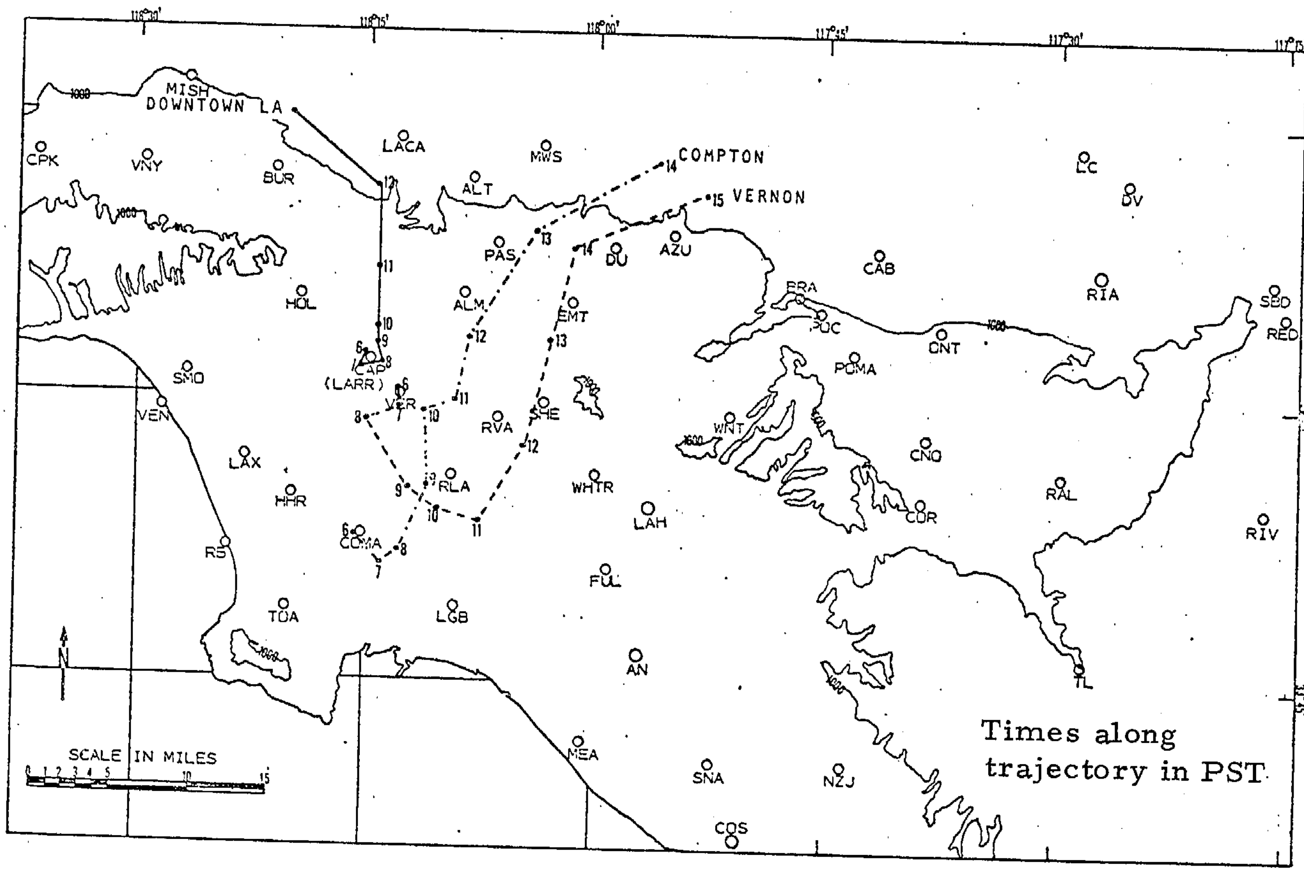


Fig. VI-43. SURFACE WIND TRAJECTORIES - BEGINNING 0600 PST (0700 PDT), OCTOBER 24, 1972

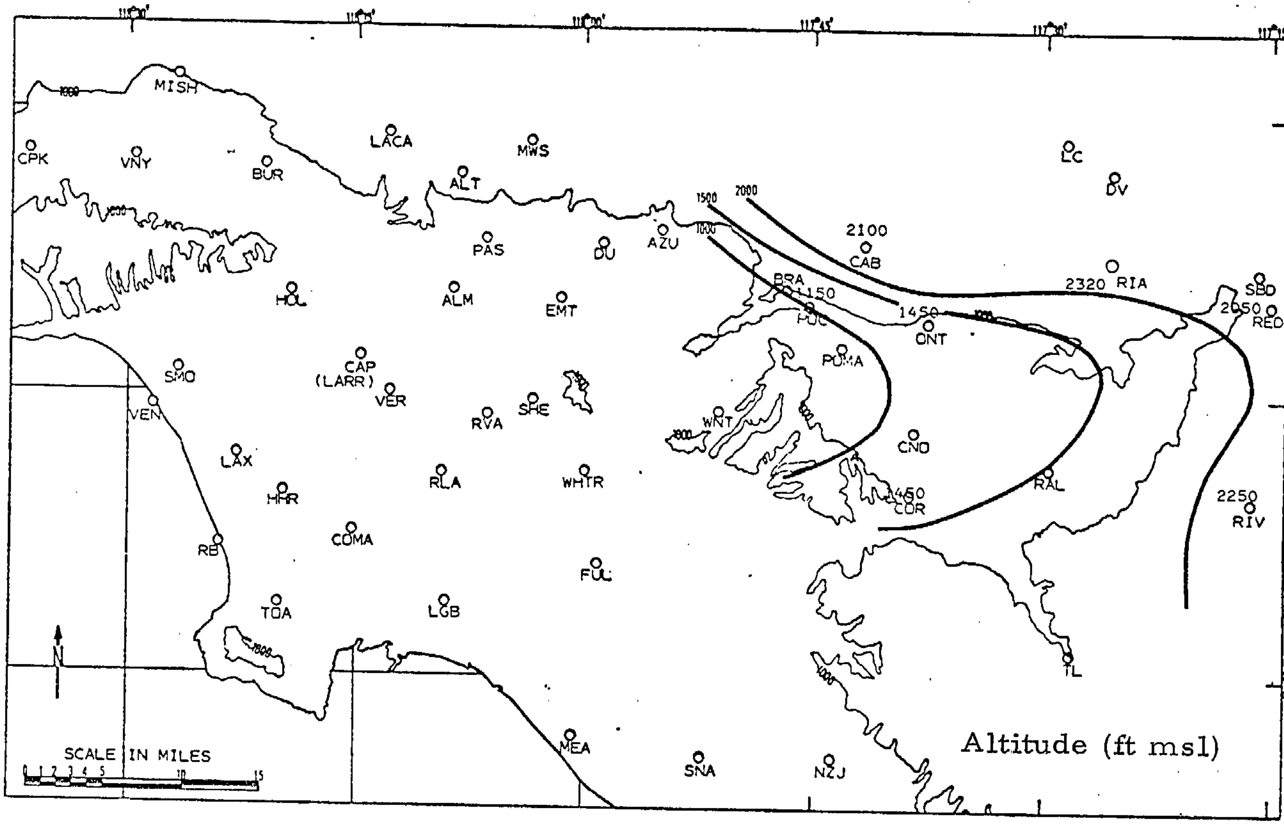


Fig. VI-44. MIXING LAYER HEIGHTS - MORNING, OCTOBER 24, 1972

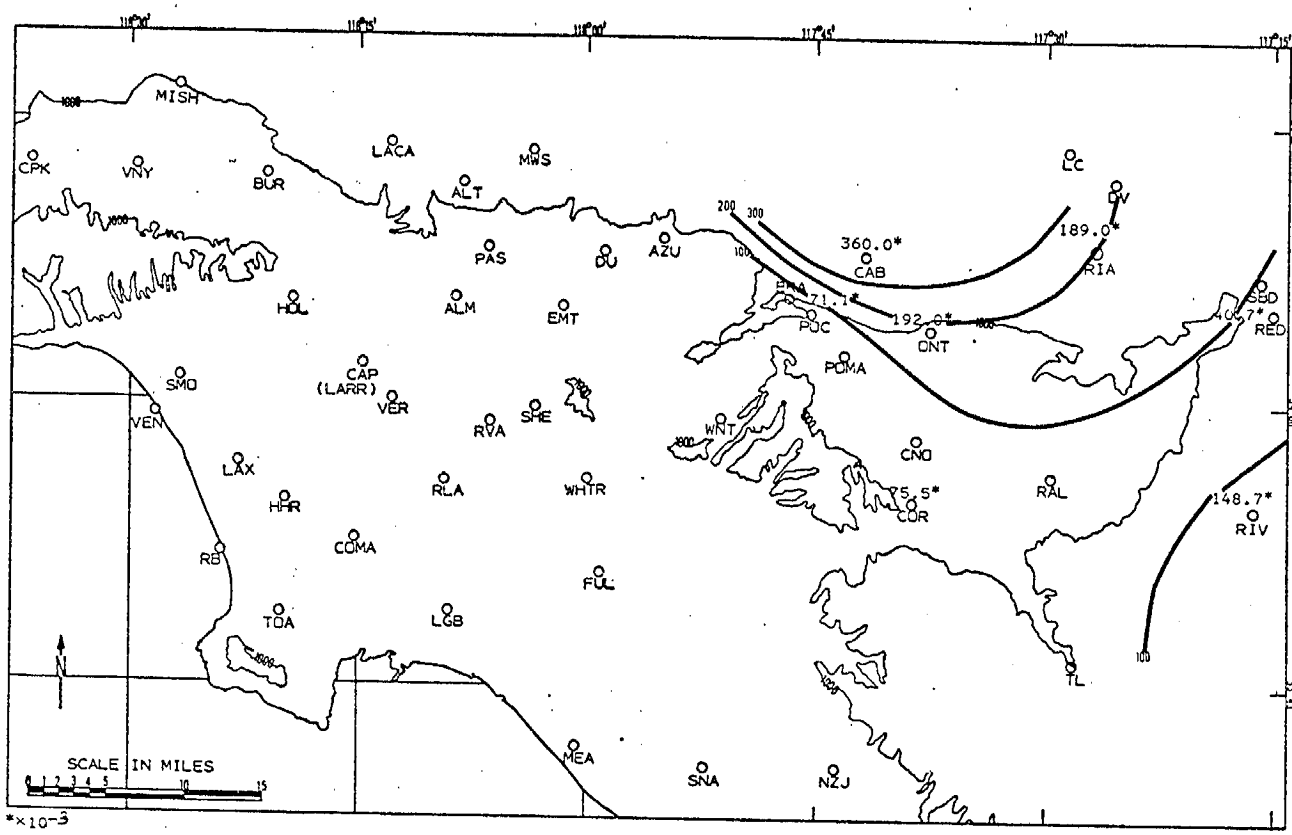


Fig. VI-45. $b_{scat}$ INTEGRATIONS - MORNING, OCTOBER 24, 1972

Integrated $b_{scat}$ contours shown in Fig. VI-45 primarily reflect the depth of the mixing layer, i.e., how much of the total polluted layer (including layers aloft) was involved in the mixing layer at the time of the sounding. Contours of $b_{scat}$ also slope upward toward the north on this basis.

Figures VI-46 and VI-47 show the CO and oxidant peak values within the mixing layer from each of the available soundings. CO concentrations were relatively uniform in the area, but oxidant values were largest in the Rialto (RIA)-Riverside (RIV)-San Bernardino (SBD) region where the solar radiation was better able to penetrate to ground levels.

Figure VI-48 shows the streamline pattern for 1300 PDT on October 24. A typical sea breeze pattern existed with a southwesterly sea breeze along the South Coast and a more westerly flow in the area of Venice (VEN) to Redondo Beach (RDB). One branch of this flow turned northwestward through the San Fernando Valley while the other branch turned eastward to parallel the San Gabriel Mountains. Surface wind trajectories in Fig. VI-49 indicate that air parcels leaving the Los Angeles-Long Beach area consistently moved northeastward toward Pasadena (PAS) and Azusa (AZU).

Mixing layer heights shown in Fig. VI-50 for midday show the effects of inland heating. San Bernardino (SBD) continued to be about 3° to 4°F warmer than Ontario (ONT) or Riverside (RIV) and, consequently, shows greater mixing layer depths. The contours of the mixing layer top slope downward toward the coast with the exception of the feature near Corona (COR) which is probably associated with the divergent wind pattern indicated in Fig. VI-48.

Figure VI-51 gives $b_{scat}$ integrations in the mixing layer at midday. Peak values occur near Pomona (POC) and Ontario (ONT) with a second maximum near Fullerton (FUL). Surface trajectories (Fig. VI-43) indicate that the material at Pomona-Ontario may not have originated in the Los Angeles area in the early morning and might be a result of local sources contributing to the already existing pollution in the area. For Fullerton, the indicated source region for the large midday values of $b_{scat}$ is the Long Beach (LGB) vicinity.

Figure VI-52 shows CO peak values in the mixing layer at midday. Largest values appear in the San Bernardino (SBD) and Pomona (POC) areas. Relatively low values occur at Riverside (RIV). Oxidant peaks (Fig. VI-53) show largest values along a line from

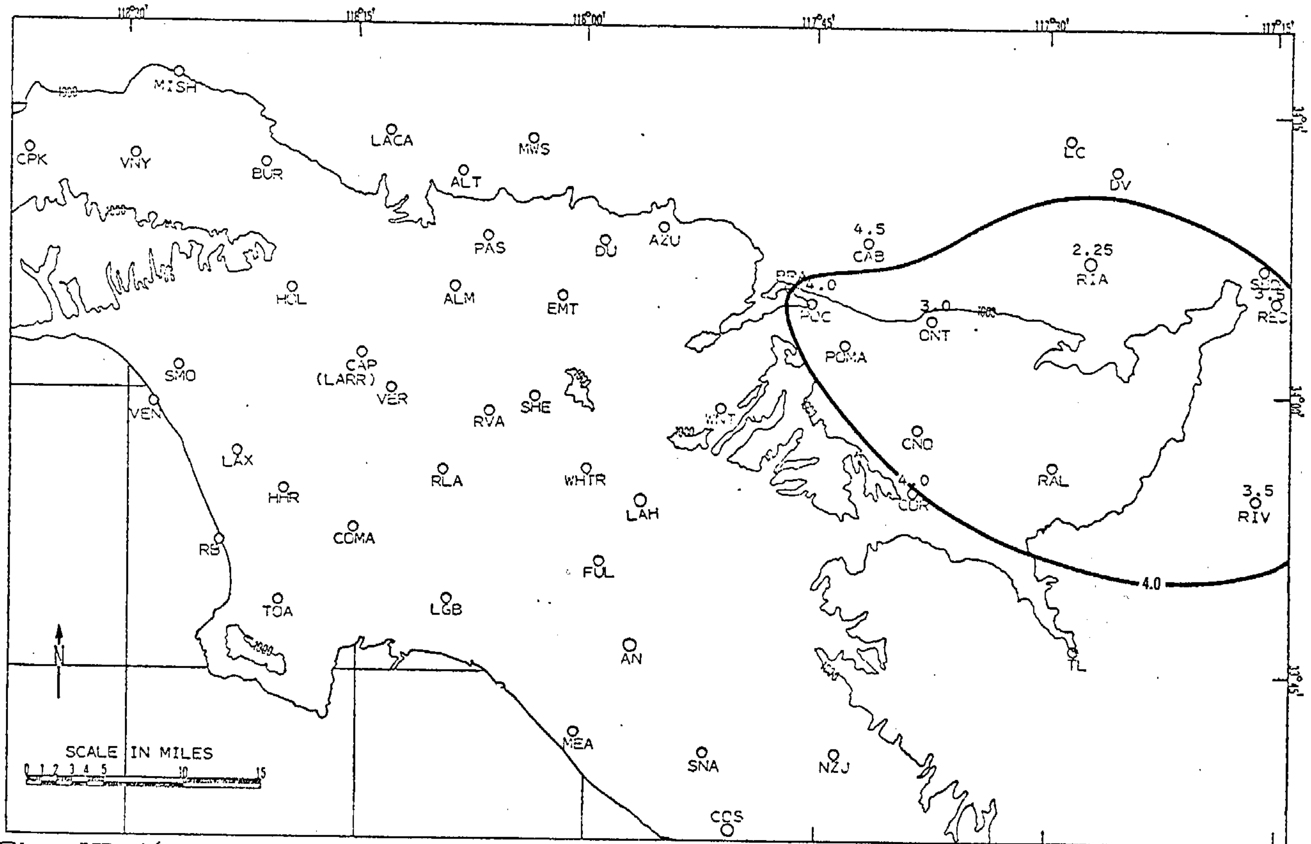


Fig. VI-46. PEAK CARBON MONOXIDE CONCENTRATIONS (ppm) WITHIN MIXING LAYER - MORNING, OCTOBER 24, 1972

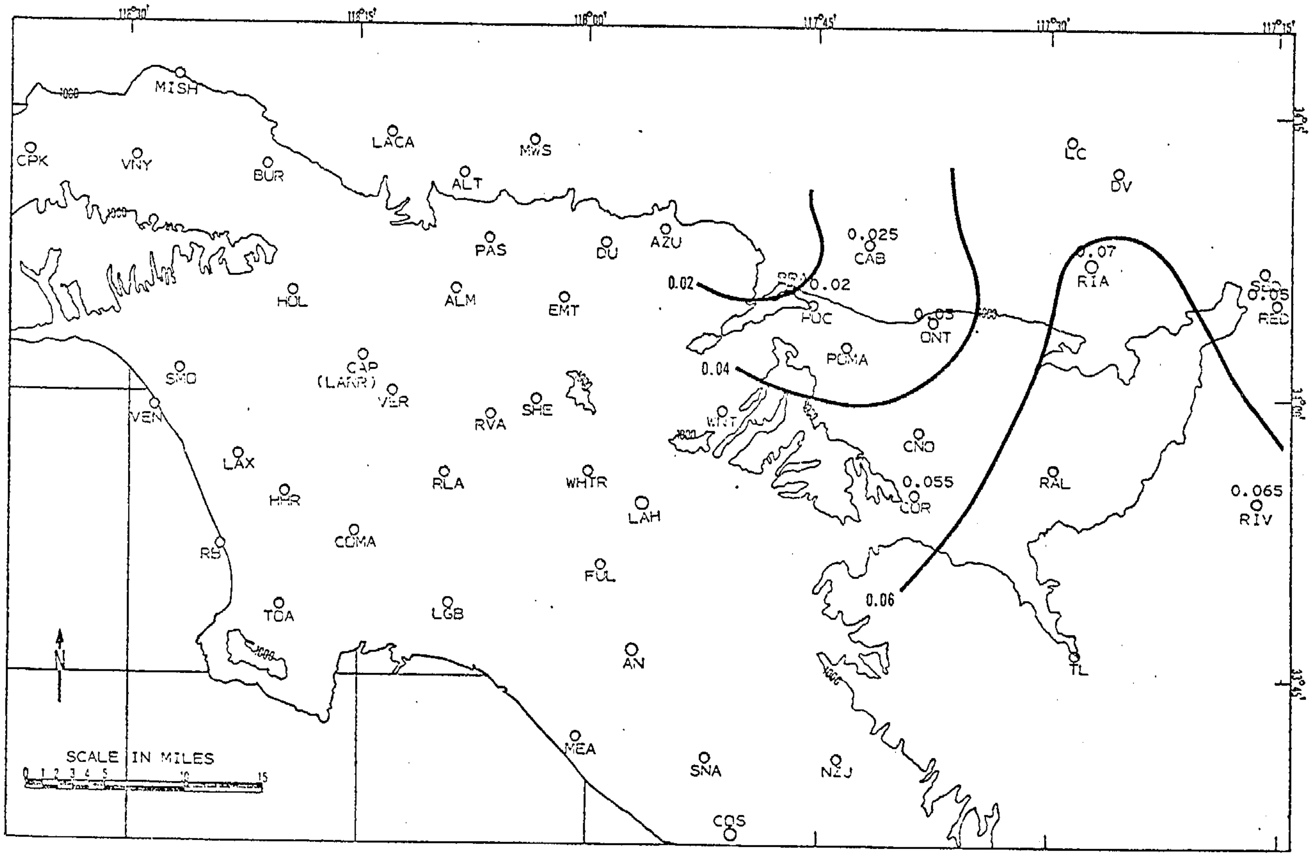


Fig. VI-47. PEAK OZONE CONCENTRATIONS (ppm) WITHIN MIXING LAYER - MORNING, OCTOBER 24, 1972

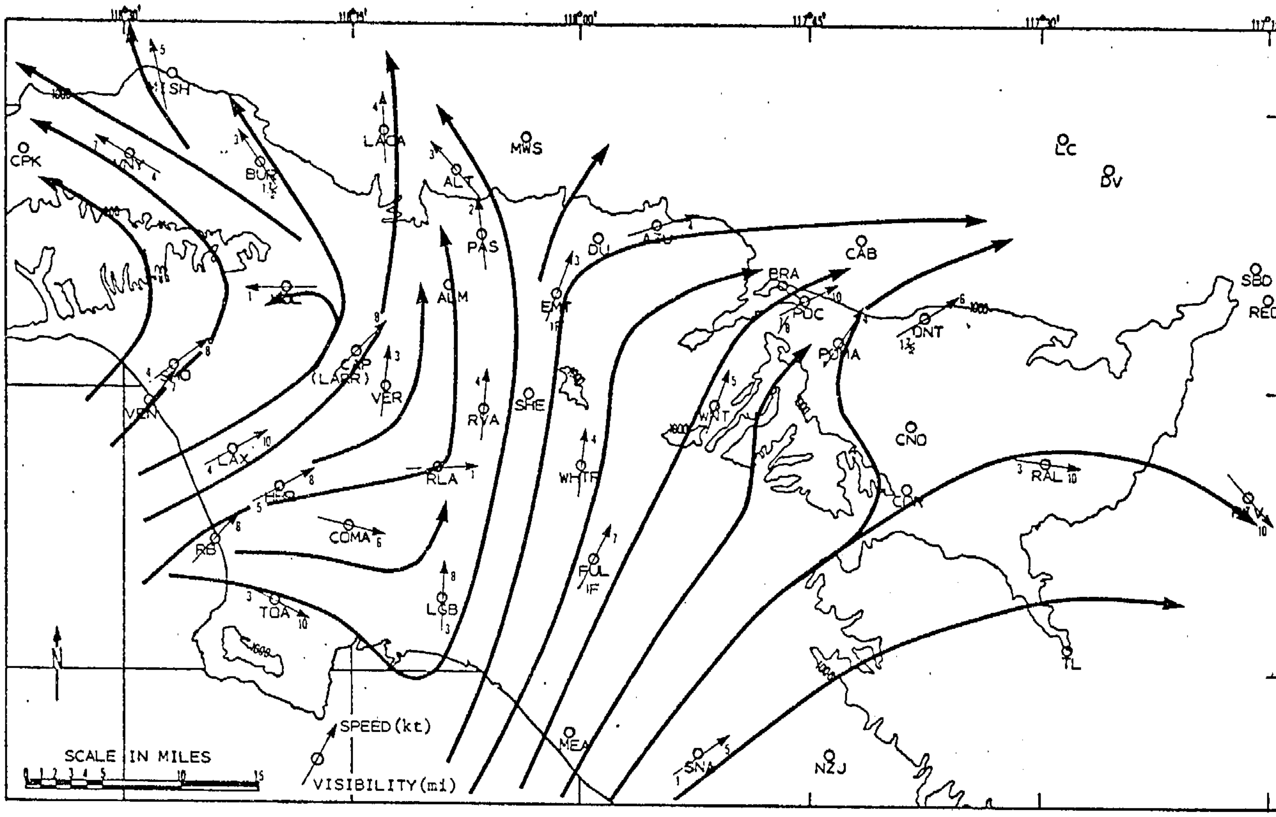


Fig. VI-48. STREAMLINE ANALYSIS - 1300 PDT, OCTOBER 24, 1972

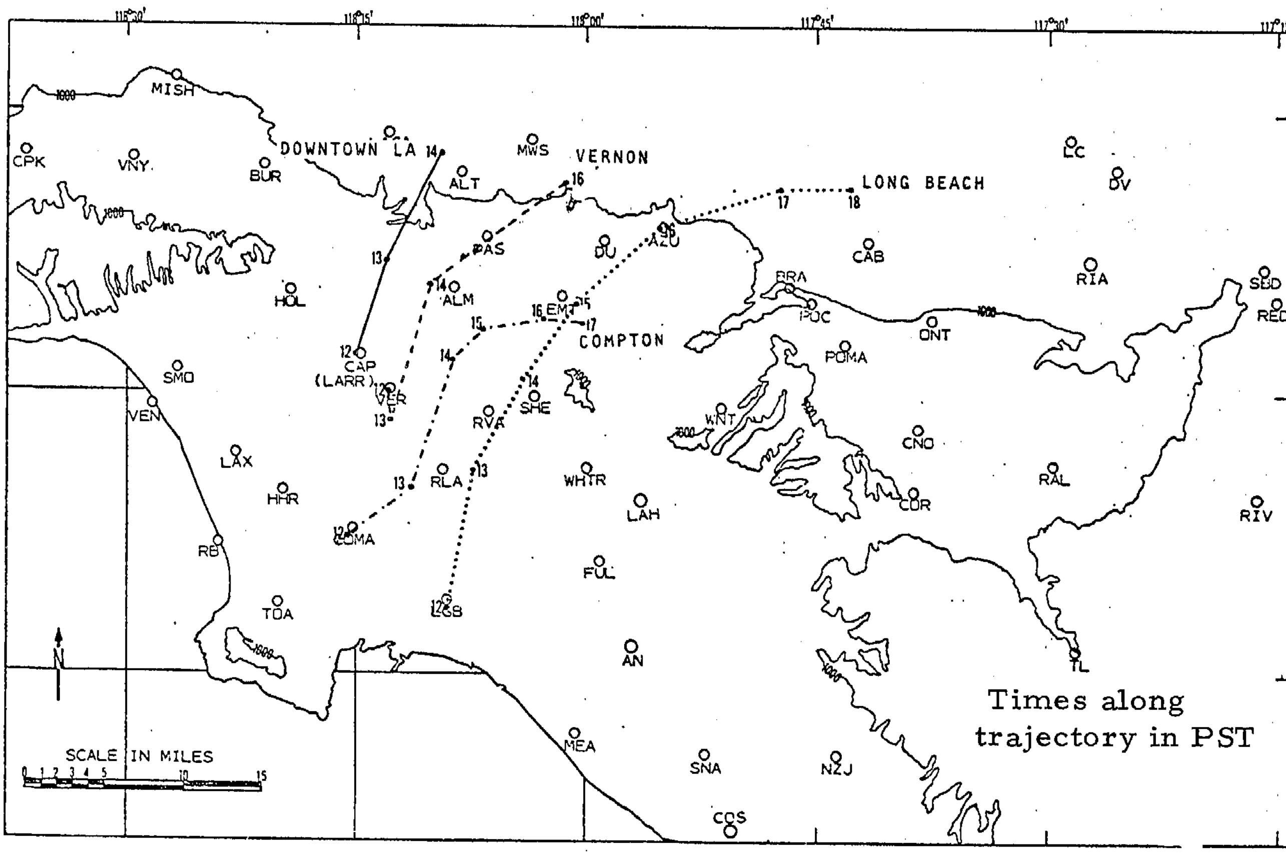


Fig. VI-49. SURFACE WIND TRAJECTORIES - BEGINNING 1200 PST (1300 PDT), OCTOBER 24, 1972

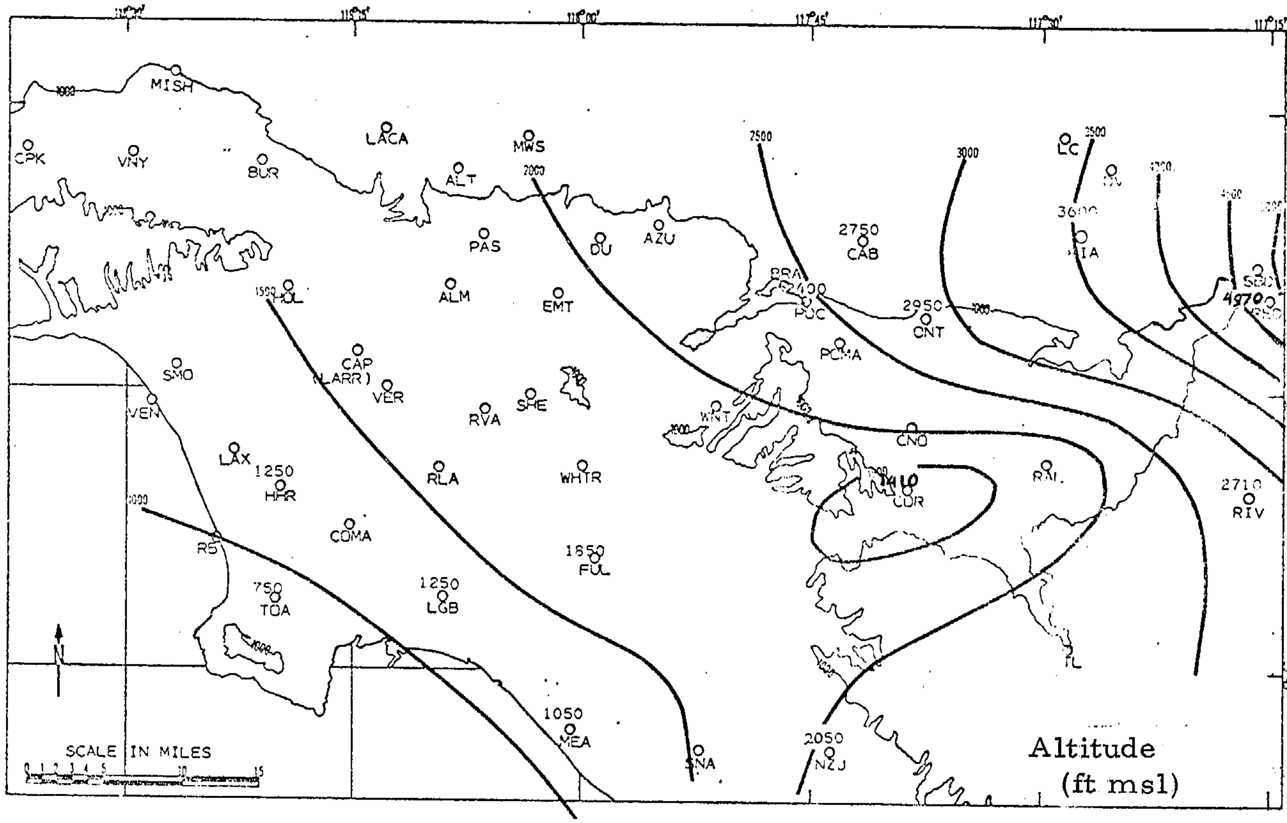


Fig. VI-50. MIXING LAYER HEIGHTS - MIDDAY, OCTOBER 24, 1972

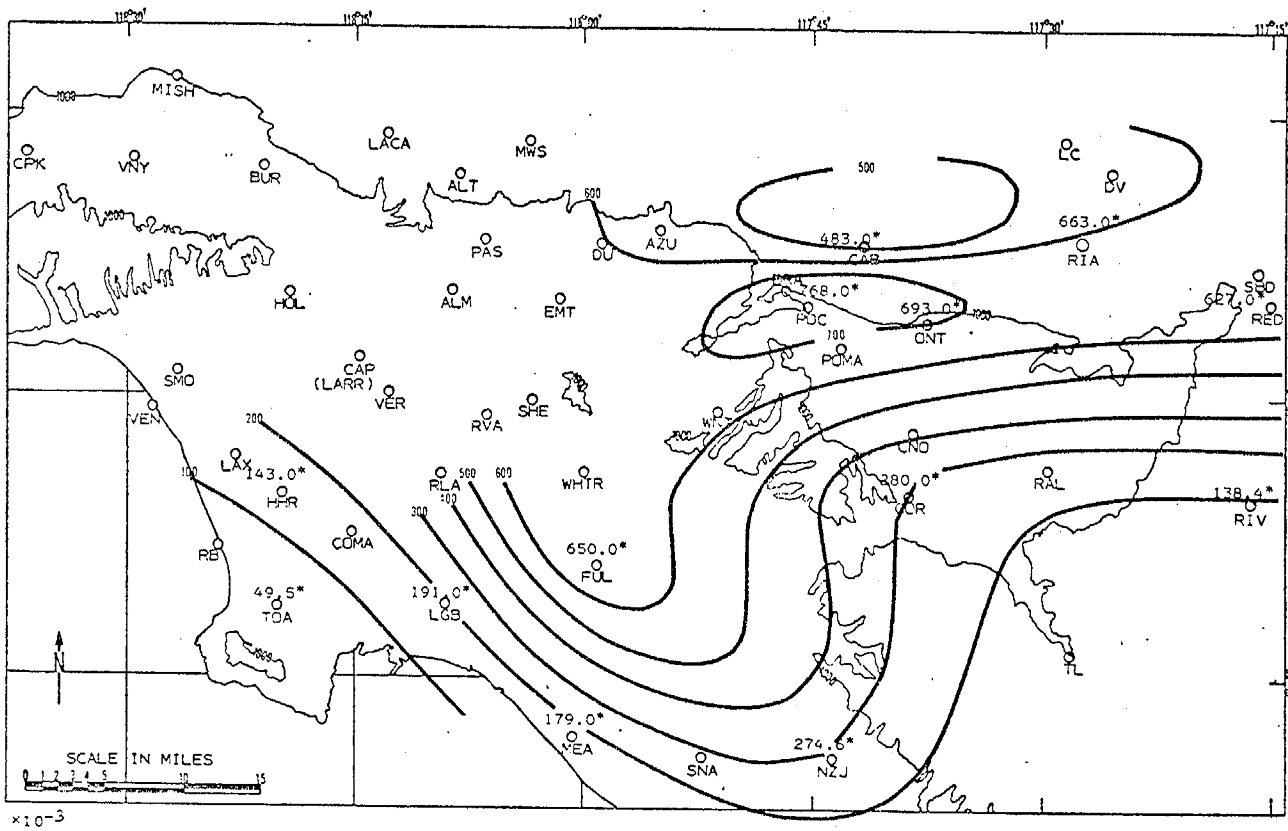


Fig. VI-51. $b_{scat}$ INTEGRATIONS - MIDDAY, OCTOBER 24, 1972

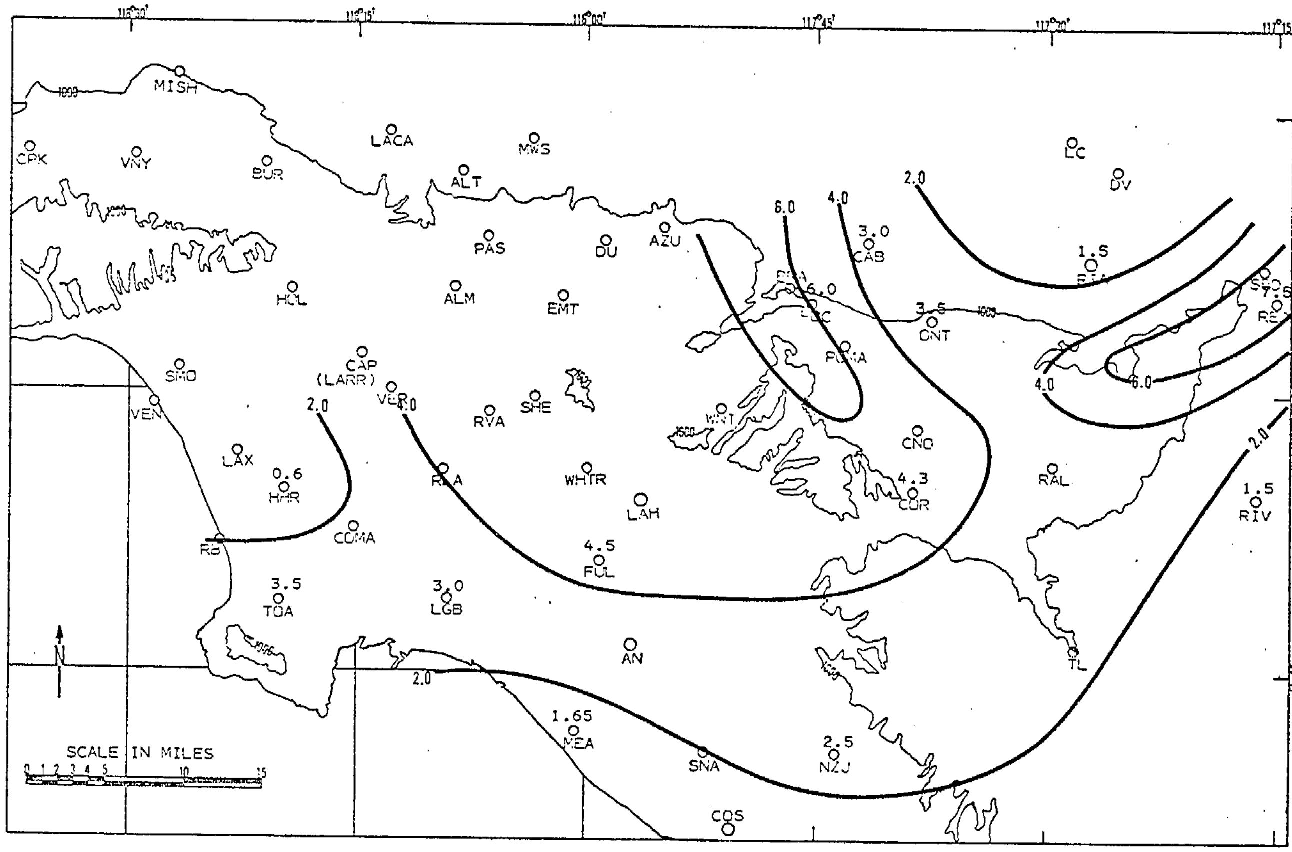


Fig. VI-52. PEAK CARBON MONOXIDE CONCENTRATIONS (ppm) WITHIN MIXING LAYER - MIDDAY, OCTOBER 24, 1972

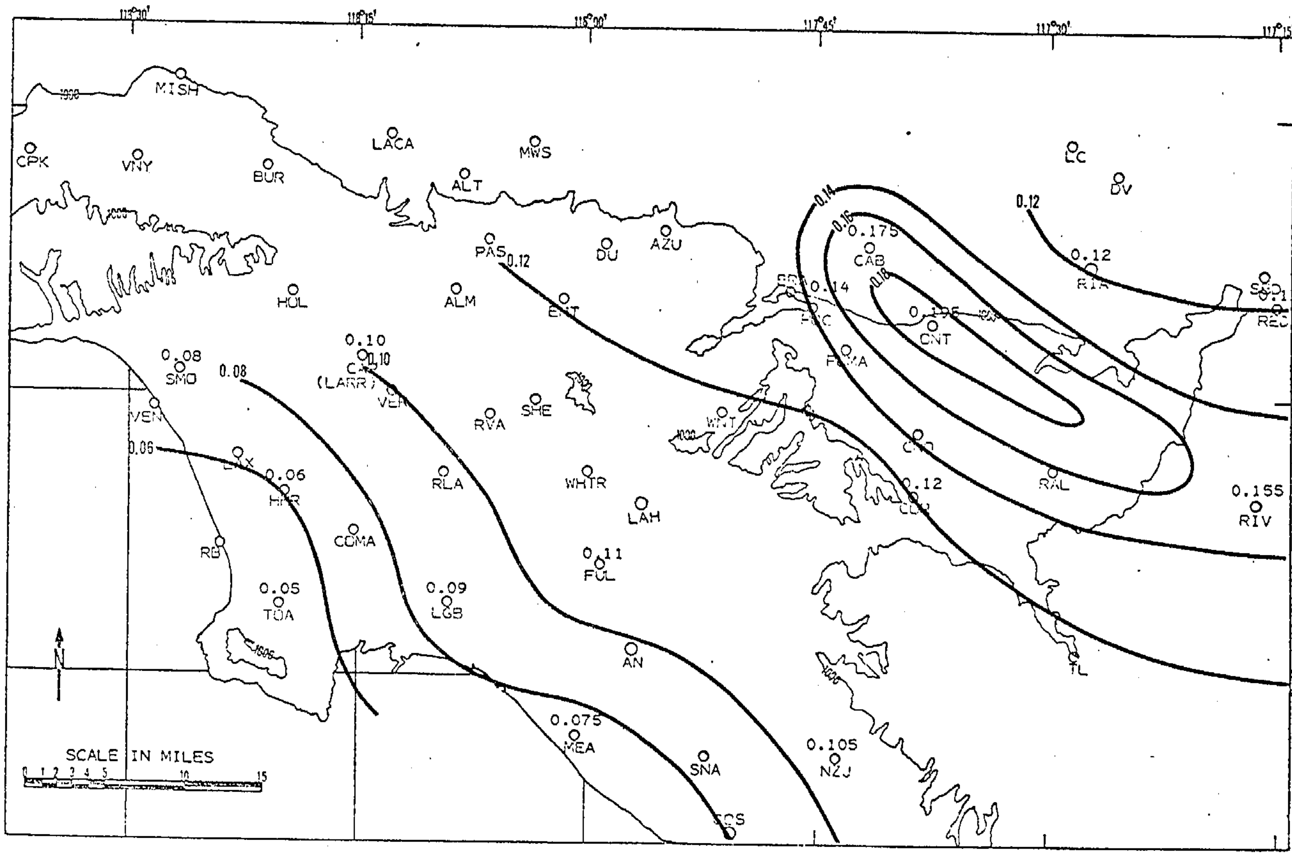


Fig. VI-53. PEAK OZONE CONCENTRATIONS (ppm) WITHIN MIXING LAYER - MIDDAY, OCTOBER 24, 1972

Ontario to Riverside, reflecting lower scavenging and stronger solar radiation.

By 1900 PDT, the streamline pattern shown in Fig. VI-54 indicated a continued sea breeze flow, but with much lighter wind speeds, particularly in the eastern sections of the basin. Evidence of a Santa Ana flow appears at San Bernardino (SBD) and the two Riverside stations (RAL, RIV) where moderate winds and good visibilities are shown. The streamline pattern suggests that a convergence zone must exist between Corona (COR) and Riverside (RIV) at the junction of the sea breeze and Santa Ana winds.

Mixing layer heights in Fig. VI-55 show the effects of the inland heating and this convergence zone. Contours slope upward rapidly from the Corona (COR) area eastward and northward. The mixing layer heights of over 4000 feet along the mountain slopes and near Riverside (RIV) represent excellent mechanisms for the escape of pollutants from the basin. Elsewhere, over the rest of the basin, the mixing layer heights are similar to those observed at midday.

Integrated $b_{scat}$ contours in Fig. VI-56 exhibit a complex pattern over the basin influenced by the following factors:

1. Low integrated $b_{scat}$ values near Redlands (RED) in the desert air accompanying the Santa Ana.

2. Large values near Riverside (RIV) in spite of the large mixing depth (Fig. VI-55). This is the result of a deep layer of pollutants in the process of escaping upward from the basin.

3. Large values along the slopes of the San Gabriel Mountains near Cable Airport (CAB). Again, these occur in deep mixing layers and indicate the escape of pollutants up the mountain slopes.

4. Low values in the coastal areas and as far east as Corona (COR) in the cleaner sea breeze air.

CO and oxidant peaks in the afternoon (Figs. VI-57 and VI-58) continue to show large values along a line between Pomona (POC) and Riverside (RIV). In this case, these patterns bear more resemblence to the $b_{scat}$ contours than was the case at midday.

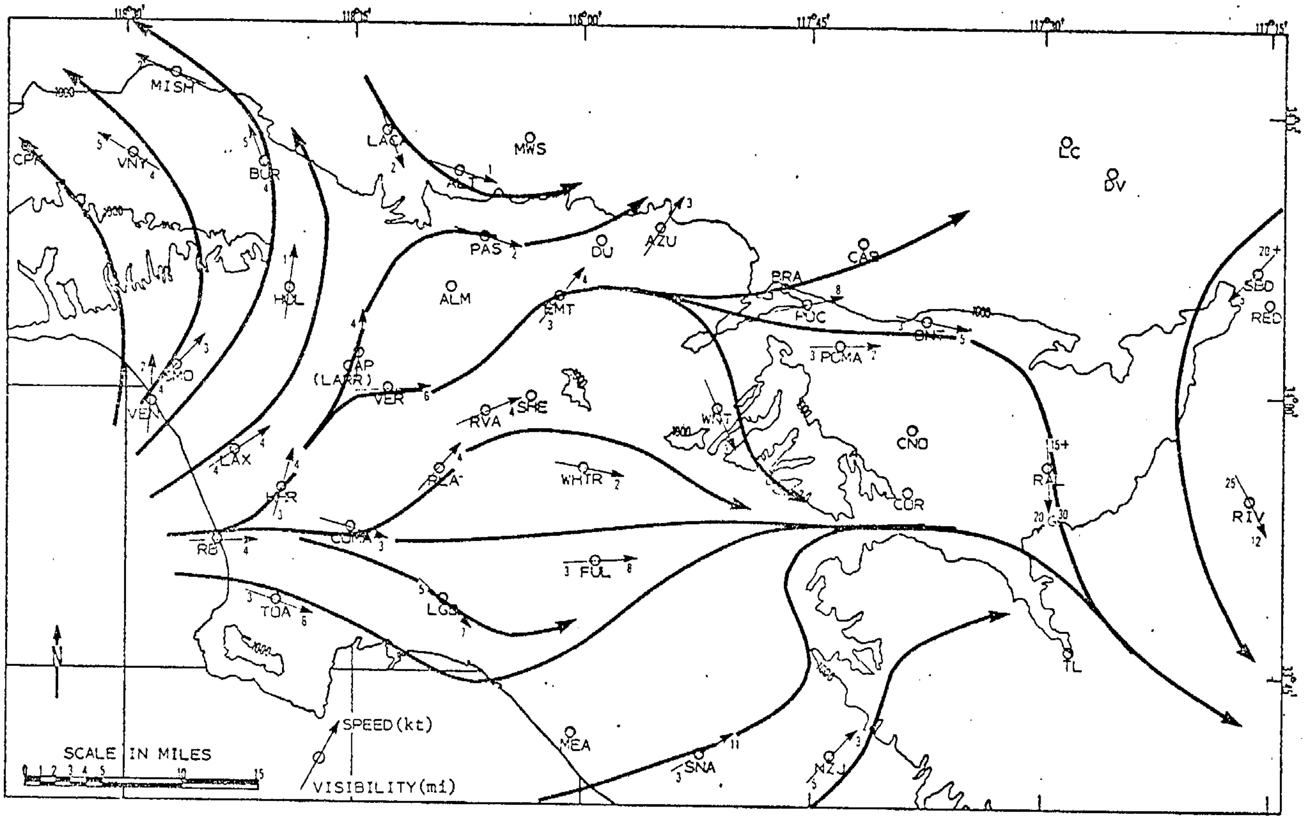


Fig. VI-54. STREAMLINE ANALYSIS - 1800 PST, OCTOBER 24, 1972

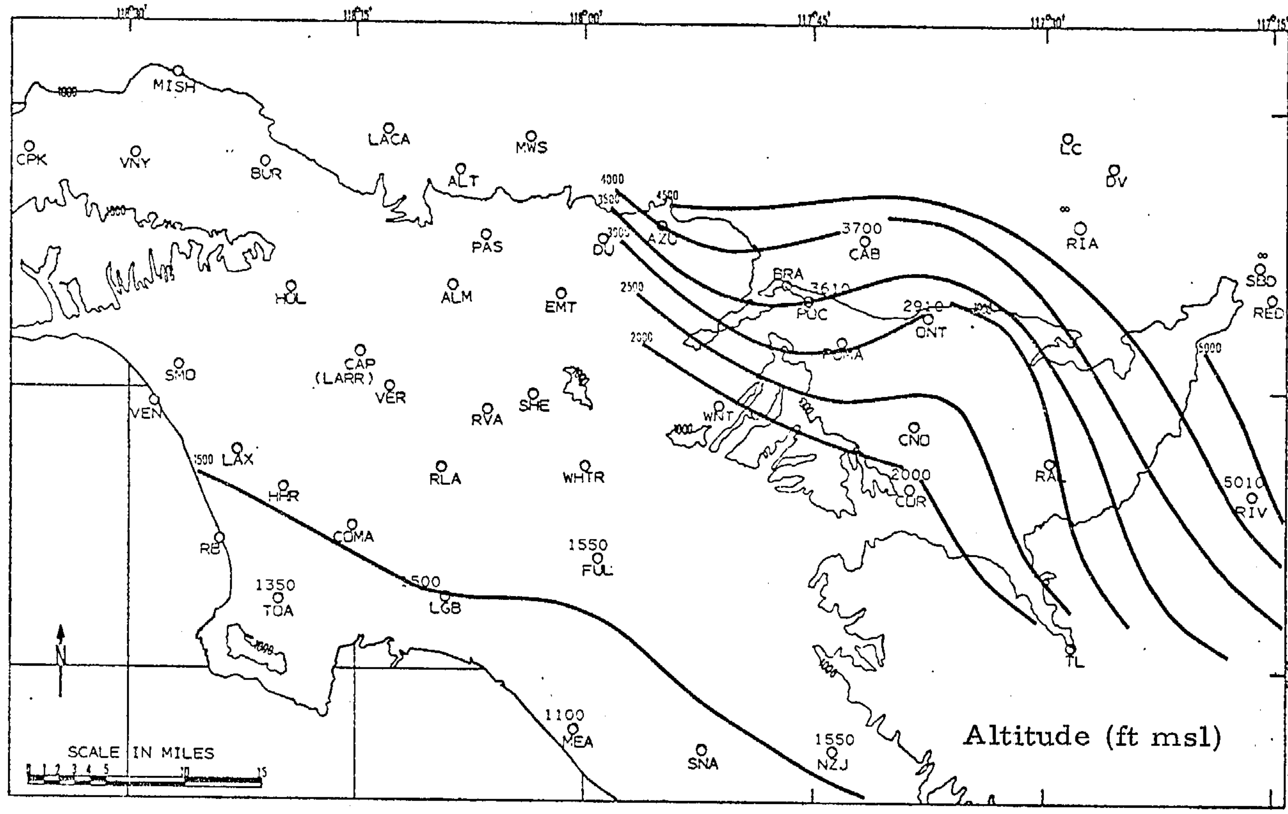


Fig. VI-55. MIXING LAYER HEIGHTS - AFTERNOON, OCTOBER 24, 1972

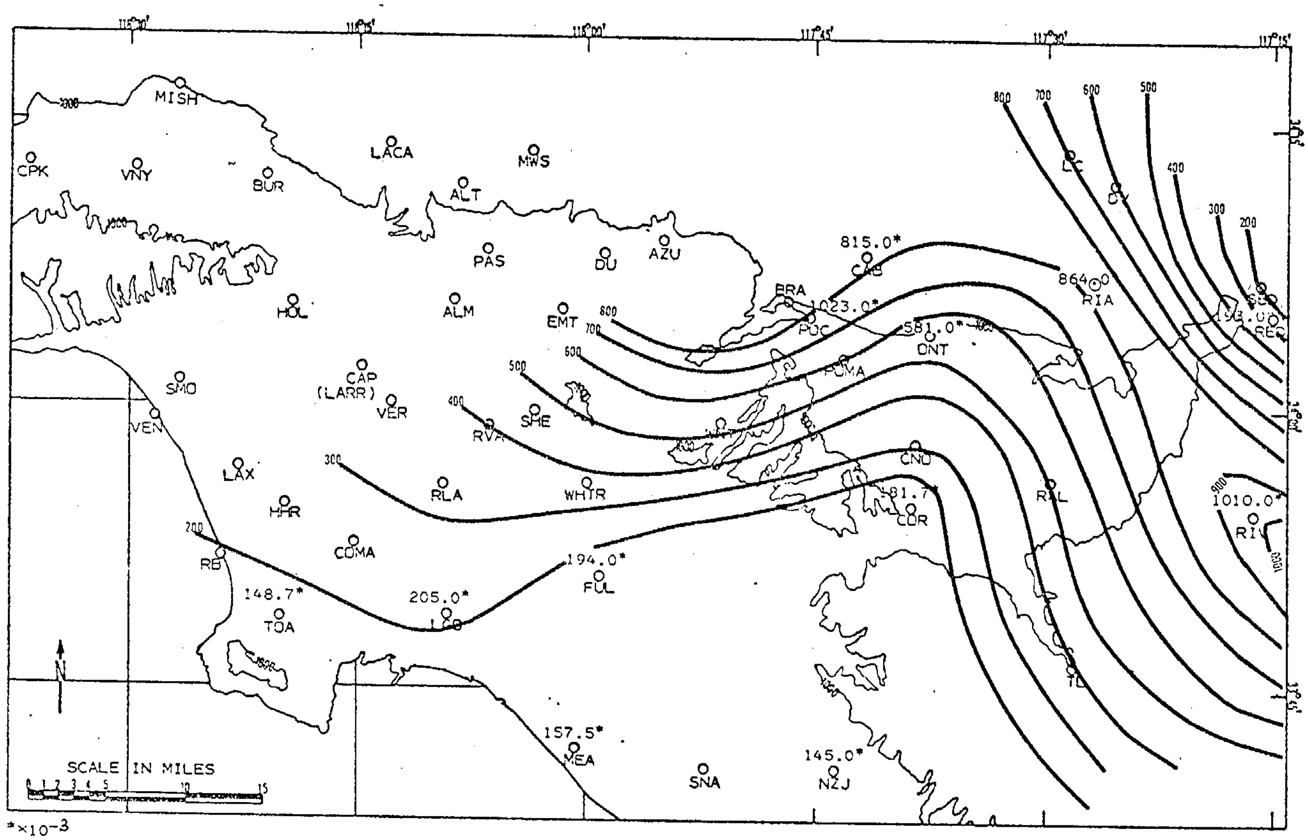


Fig. VI-56. $b_{scat}$ INTEGRATIONS - AFTERNOON, OCTOBER 24, 1972

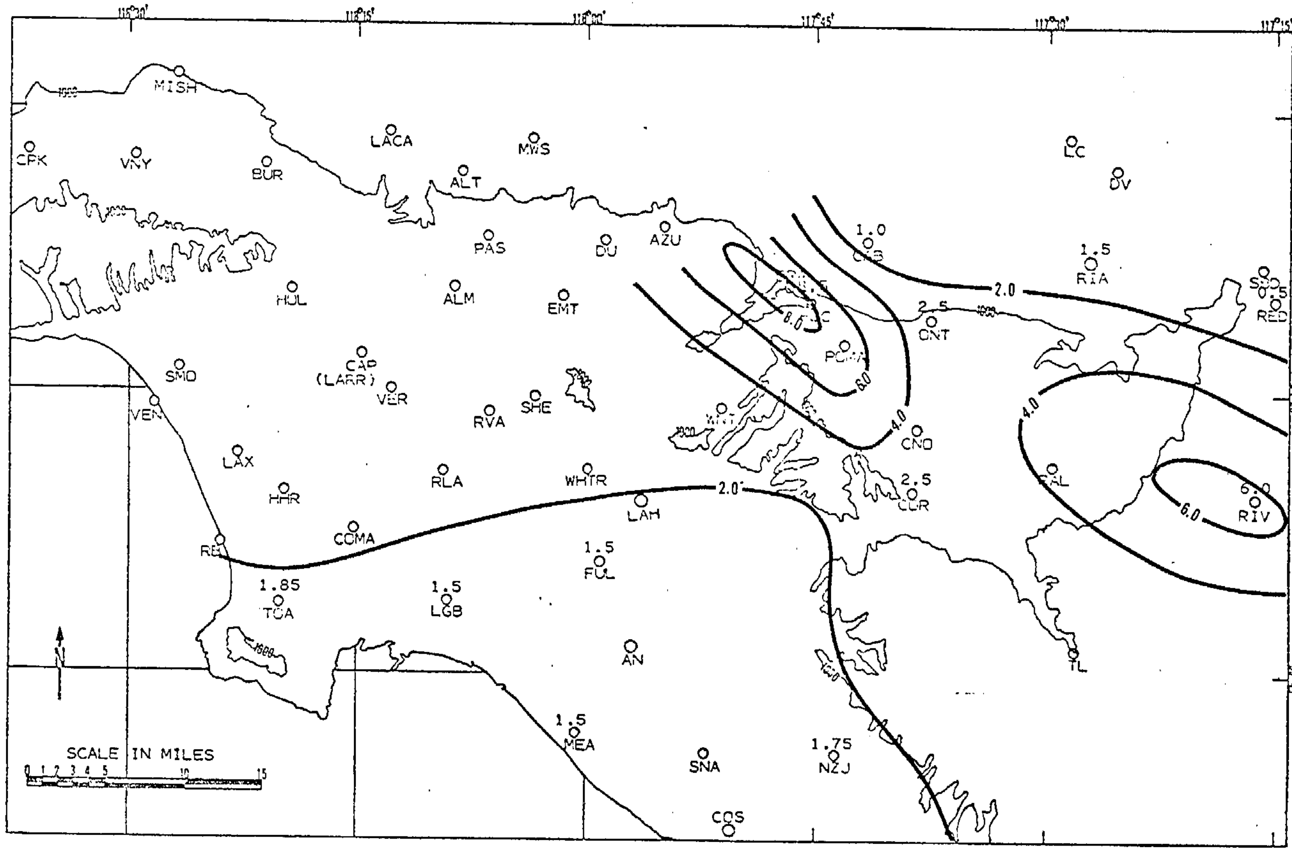


Fig. VI-57. PEAK CARBON MONOXIDE CONCENTRATIONS (ppm) WITHIN MIXING LAYER - AFTERNOON, OCTOBER 24, 1972

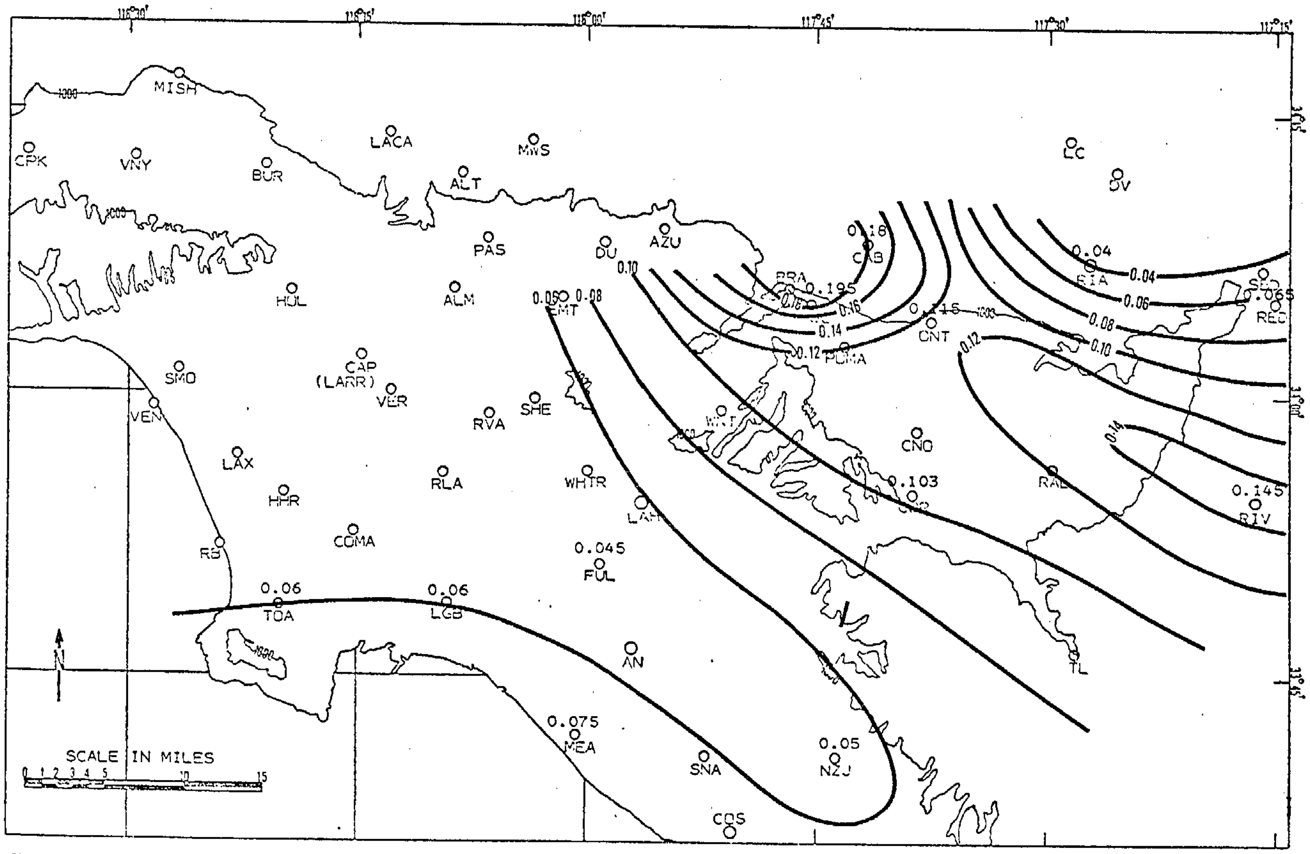


Fig. VI-58. PEAK OZONE CONCENTRATIONS (ppm) WITHIN MIXING LAYER - AFTERNOON, OCTOBER 24, 1972

Figure VI-59 shows vertical cross-sections of $b_{scat}$ along a line from Torrance (TOA) through Fullerton (FUL) to Redlands (RED). Cross-sections are shown for midday and afternoon. These cross-sections are oriented approximately along the wind. The major pollutant area in the coastal section (centered near Fullerton at midday) extends upward to about 2500 feet and eastward to Corona. In the Redlands area, the effect of the approaching Santa Ana is shown in the marked vertical growth of the $b_{scat}$ contours. By late afternoon, the pollutant material from the coastal sections has moved into the Corona-Riverside (RAL) area and is involved in the Santa Ana convergence zone which has intruded farther into the basin. Considerable material is present in the convergence zone and, at levels above 4000 feet, some of this material is carried westward over the coastal sections by the easterly winds at these levels.

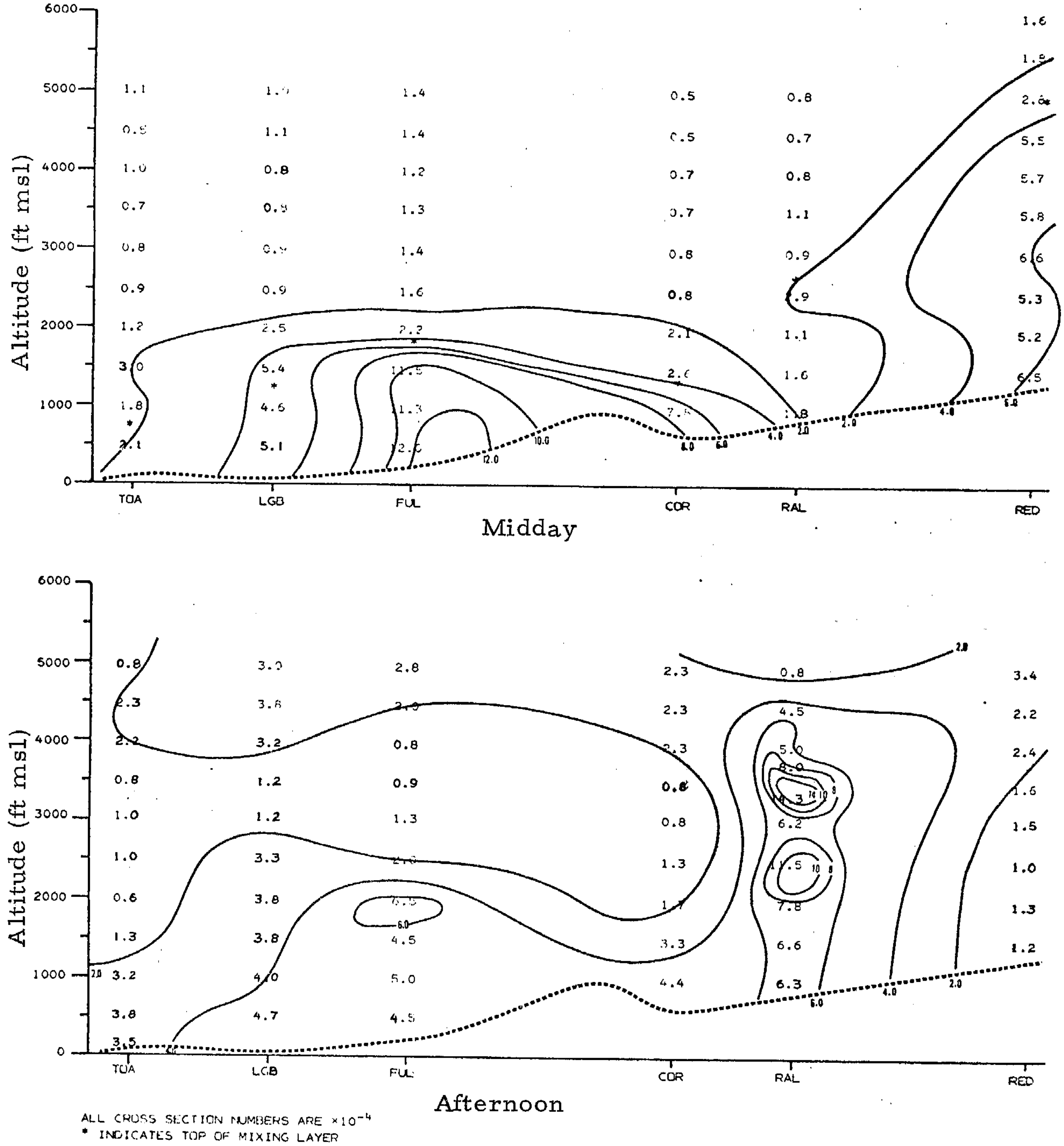


Fig. VI-59. VERTICAL CROSS-SECTION OF $b_{scat}$ MIDDAY AND AFTERNOON, OCTOBER 24, 1972